UNIVERSITA' DEGLI STUDI DI PADOVA

FACOLTA' DI INGEGNERIA

CORSO DI LAUREA IN INGEGNERIA ELETTRICA

Electric Machine with Permanent Magnets and External Rotor with Concentrated Windings: Analysis and Study on its Magnetic Circuit

Laureando: Federico Baldo

Relatore: Prof. Silverio Bolognani

INDEX

1. INTRODUCTION

The work is about the project of an electric machine, with which is possible to make an energetic exchange through an electric form. In this particular case, the machine makes possible an electromechanical conversion, i.e. the conversion from one energetic form to another with the connection given by the electromagnetic field. These converters can be divided in two categories, that is to say: motors, when electric power is converted to mechanical, generators, when the conversion goes to the opposite direction.
There are different types of electric machine, with different feeding current shapes, or different materials, or geometry.
This thesis is about an important kind of machine, called “Brushless Synchronous Electric Machine”, characterized by the fact that the exciting magnetomotive force is given by the permanent magnets mounted on the internal side of the rotor of the machine; in this a way is possible to get several good effects: first of all, there is no need of brushes, giving the machine freedom of movement and less mechanical resistance, and most of all, the efficiency of the system is considerately higher, because of the elimination of the exciting current – and of all the losses due to this current, such as Joule-effect losses.
The machine is called “synchronous” because the period of rotation is synchronized with the frequency of the feeding current, which can be mono-phase or three-phase.
Permanent magnets are the characterizing element of the machine, and the behaviour and the cost of the machine are depending by them. In fact, the disadvantage of this kind of device is the higher cost with respect to a traditional synchronous machine.

Brushless synchronous machines can have many ways of application, from the little electronic and optical devices such as CD players to the high power electric generators for the great distribution. The kind of machine which is object of the thesis can be easily adopted for low cost generation, with small home-serving eolic generators, and also as motors for fluidodynamic applications, such as ventilators and small pumps.
This kind of machine has already a lower volume than other solutions in the field of electromechanical converters, but it is still possible to reduce it, making an inversion of the two parts of the machine: in fact, while traditionally the rotating part of the machine is the internal one, and the fixed part is the external one, in the design of the machine which is the object of the study the stator is internal and the rotor is external.

2. MACHINE WITH 2 POLES

2.1 Model of the machine

The machine studied is a 1 pair of poles permanent magnet synchronous generator (Figure 1). It has an inner fixed stator with one concentrated coil and an outer movable rotor with two PMs fixed on it. The objective of this preliminary calculus is to study the no-load electromotive force induced at the terminals of the winding on the stator, when the rotor rotates with a certain angular speed.
To do that, it's necessary to make a simplified model of the machine, taking into account the following hypothesis to make the magnetic study:

- iron magnetic permeability infinitive
- no magnetic leakage
- thickness of the air gap significantly lower than the machine's length and P Ms width.

Geometrical parameters:

- g, thickness of the air gap
- d, thickness of PMs
- β, angle-extension of the magnets
- α, mechanical position of the rotor.

The first steps of the work is the magnetic calculus, which gives some indications about the behaviour of the machine, which is going to be verified later with the simulating process.
The analysis takes in account several parameters of the machine, in particular its geometry and the characteristics of the magnets.
The first value to calculate is the average magnetic flux density on in the air gap of the machine. To get it, it is necessary to increase the value of the thickness of the gap (only in the mathematical analysis) to consider the effects of the geometry of the caves on the magnetic distribution, by a coefficient called Carter's, which depends by the thickness and by the wideness of them. In this project, Carter's coefficient is estimate to be k_{Car}=1,2. This is kind of a high value, but it seems to fit with the shape of the machine, which have a low number of poles – and so a higher wideness of the caves compared with the whole lateral surface of the internal stator.
This way is possible to get the average magnetic flux density value:

$$B = B_R \frac{1}{1 + \frac{\mu_r g'}{d}}$$

eq. 1

The values involved are equal to:

- B_R = 0,4211 T
- μ_r = 1,43486
- g = 0,0005 m
- g' = k_{Car} g
- d = 0,005 m

In the and, the average B value is equal to 0,359 T.
The value of the flux passing through the magnetic circuit is a function of it following the equation:

$$\Phi_0 = B\,D\,\frac{l_{stk}}{p}\,,$$

eq. 2

which gives a value of the flux, when the machine is in the aligned position, of 0,0215 Wb.

With the purpose of a clear comprehension of the magnetic behaviour of the machine, the next step is the search of the time-dependance function of the flux, verifiable later with a FEMM simulation coupled with a MatLab script.
As the rotor rotates with a certain angular speed ω_r , we can write

$$\alpha_{(t)} = \omega_r t\,.$$

eq. 3

The model is reported in Figure 1; the machine is represented at the time instant when $\alpha_{(t)} = 0$, in the situation of maximum coupled flux.

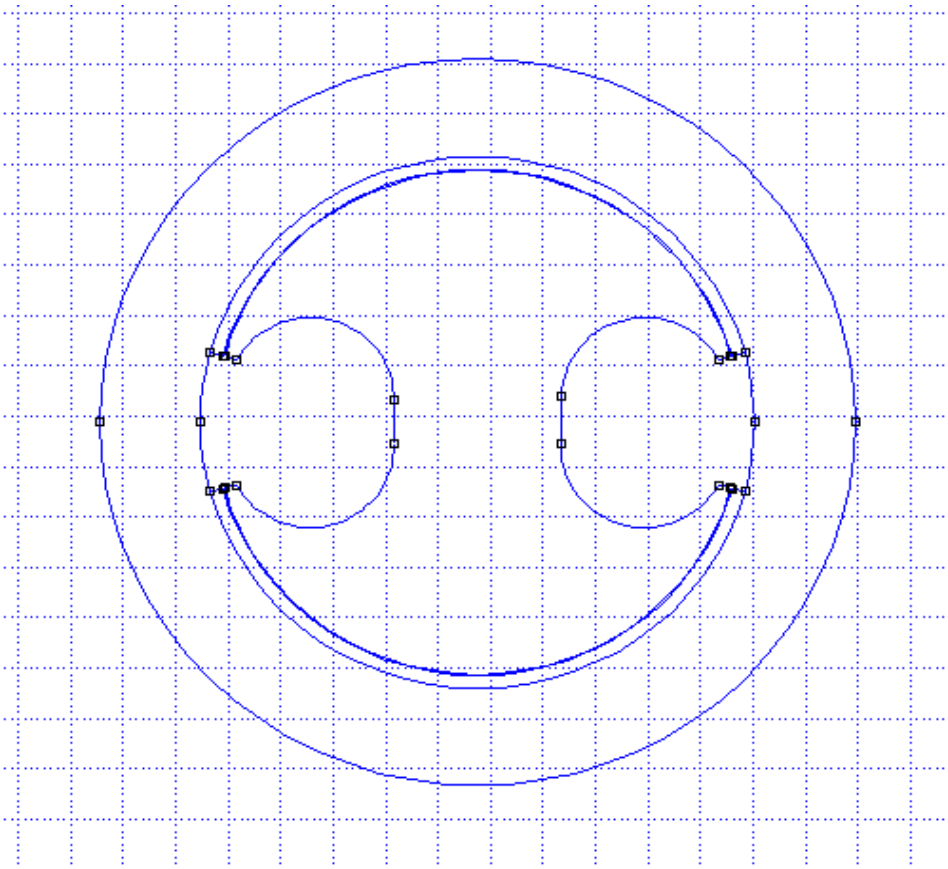

Figure 1

2.2 Analytic calculus

The polarity of the magnets is the one which produces the magnetic flux in the directions shown in Figure 1. The geometrical characteristics of the two magnets are the same, and the configuration is symmetric: it is assumed that the flux they produce is exactly the same

$$\Phi_{m1} = \Phi_{m2} = \Phi_m \, .$$

eq. 4

The value of this flux is given by the relationship

$$\Phi_m = B_m S_m \, ,$$

eq. 5

that is to say, if β is the angle covered by magnets, r an average value of radius (taken in the middle of the air gap) and l is the length of the machine in the axial direction,

$$\Phi_m = B_m r l \beta \, ;$$

eq. 6

in fact, the surface offered by the magnets to the flux is

$$S_m = rl\beta \, .$$

eq. 7

Because of the hypothesis of no flux leakage between the different parts of the machine, when the position of the rotor is the aligned one, so the flux is maximum, the flux in the inner stator and in the air gap is the same as well. This is the maximum value of the flux and its value is

$$\Phi_M = \Phi_g = \Phi_m \, .$$

eq. 8

In this way it's possible to extract the value of the magnetic induction in the magnets as a function of the inner stator magnetic flux

$$B_m = \frac{\Phi_M}{rl\beta} \, .$$

eq. 9

On the other hand, the magnets-due flux evolution in time $\Phi_{0(t)}$ is given by

$$\Phi_{0(t)} = \vartheta_{(t)} \Phi_M \, ,$$

eq. 10

where $\vartheta_{(t)}$ is the evolution of the angle for which the MMF of the magnets is coupled with the stator's arm. This angle depends on time both in absolute value both in sign, because of the alternative magnetization direction of the magnets. If the rotational speed is imposed at a value ω_r, constant, we have a dependence of ϑ by time, as shown by its evolution (Figure 2).

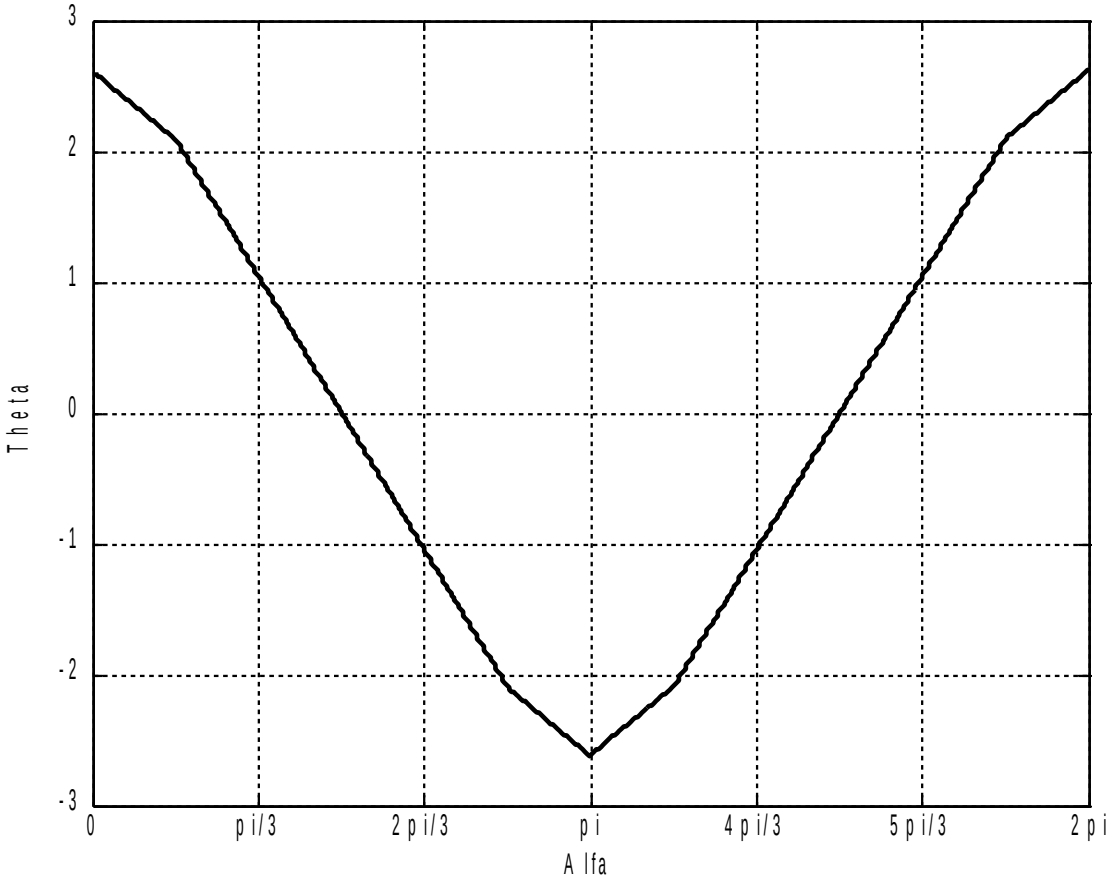

Figure 2

The graph has been obtained by imposing

$$\beta = \frac{5}{6}\pi \ .$$

eq. 11

The direct proportionality between the flux and $\vartheta_{(t)}$ is right only if we make the following hypothesis: the magnetic flux produced by the the not-faced portions of the PMs is not useful, that is to say that it doesn't get coupled with the winding on the inner stator. This means that the air gap is much smaller than the magnets width, and d and g are both much smaller than the radius of the machine.

In the brushless machines, the flux is given by the sum of two contributes: the permanent magnet due-one and the feeding current-due one.
To get the second term of the flux it is necessary to apply the Ampere law on the magnetic circuit, with the hypothesis that the magnetic permeability in the iron is infinite, which gives

$$N\, i_{(t)} = \int H\, dl = R_{TOT(t)}\, \Phi_{(t)} \ ,$$

eq. 12

where H is the magnetic field and N and i , instead, are the number of coils of and the current flowing in the winding. With the purpose to have a correct distribution of current in the caves, with a proper current density, but wanting to push the simulations towards the most stressing conditions by a magnetic point of view, a number N = 250 turns has been chosen.

Finally, we can obtain the value of the magnetic flux

$$\Phi_{(t)} = \frac{N i_{(t)}}{R_{TOT(t)}} + \Phi_{0(t)} \ .$$

eq. 13

The total reluctance of the path followed by the flux is, in the hypothesis of infinitive permeability of the iron, equal to the sum of the reluctances of the air gap and of the magnets.
Tough, the reluctance in the permanent magnet-given space is not constant, because of the insertion of a portion of air during the rotation of the system.
Hence, R is not a constant, but it depends by time. In fact, there is an angle, called $\theta_{(t)}$, which represents the angle on which we have the presence of air in the space between the gap and the iron part of the rotor. This air causes an increment of the reluctance of the magnetic circuit. In this case there is a variation in time of the absolute value of $\theta_{(t)}$, but not in sign, because the angle is used only to calculate the reluctance of the space between the stator and the iron part of the rotor, which has a thickness equal to g+d. The evolution of this reluctance, calculated only for one pole, which can be called $R_{(t)}$ and takes in account both the reluctances of the air and of the magnets, is plotted below. Analytically, the expression of the reluctance can be written:

$$R_{(t)} = \frac{g}{\mu_0 rl\beta} + \frac{d}{rl(\mu_0\theta_{(t)} + \mu_m\beta - \mu_m\theta_{(t)})} \quad .$$

eq. 14

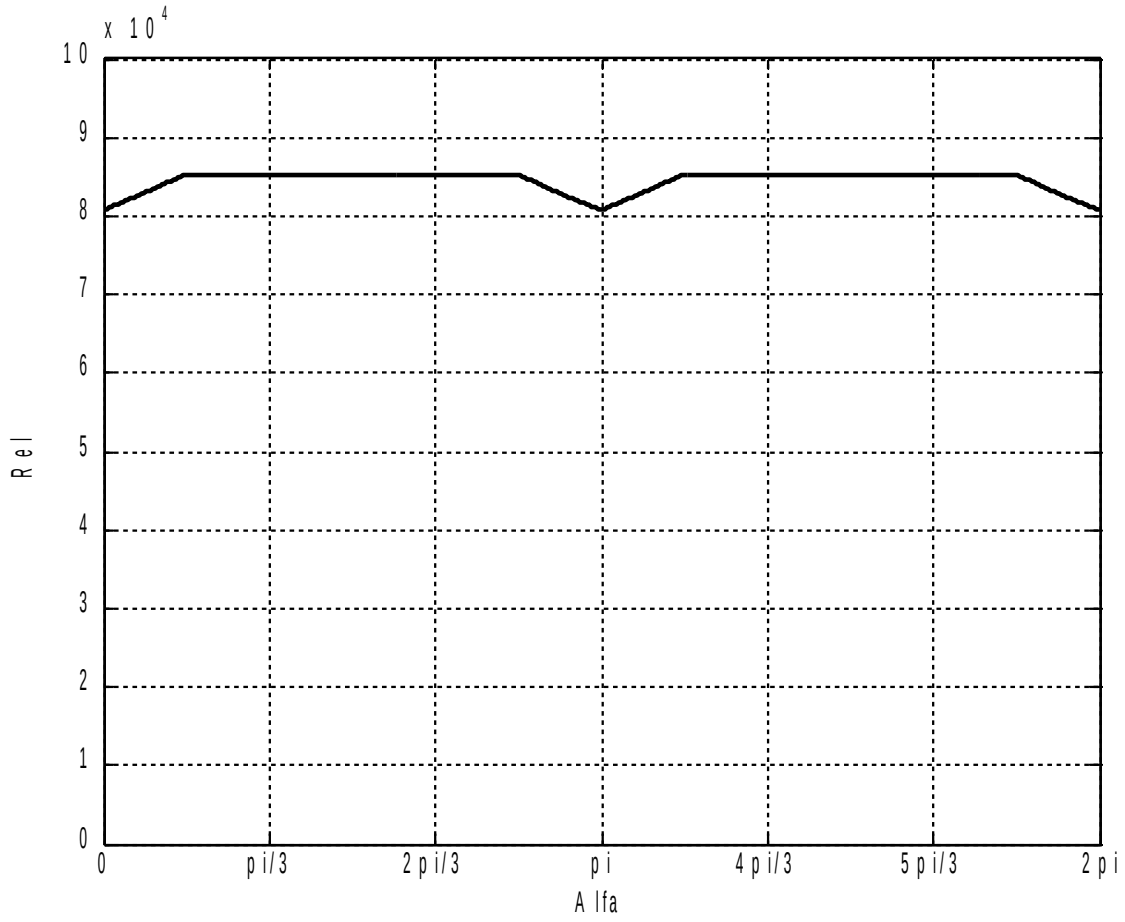

Figure 3

As a result of the magnetic analysis of the machine, the induced flux passing through the internal stator has a dependence in time due both to the different contribution given by the magnets for each angular position – taken in account with the evolution of $\vartheta_{(t)}$ – and to the behaviours of reluctance and current.
Hence, the equation of the flux in time is the following:

$$\Phi_{(t)} = \frac{N\, i_{(t)} + \vartheta_{(t)} \Phi_M}{2\, R_{(t)}}$$

eq, 15

To estimate the electromotive force at the terminal of the windings, it's necessary to calculate the magnetic flux coupled with the winding, that is to say

$$\lambda_{(t)} = N\Phi_{(t)} = \frac{N^2 i_{(t)} + N\, \vartheta_{(t)} \Phi_M}{2\, R_{(t)}} \ .$$

eq. 16

If we consider the winding as an open circuit, we will have $i = 0$, so we can write

$$\lambda_{0(t)} = N\Phi_{0(t)} = \frac{N\, \vartheta_{(t)} \Phi_M}{2\, R_{(t)}} \ .$$

eq. 17

The evolution of the flux $\Phi_{0(t)}$ as a function of α – and so of time – will be:

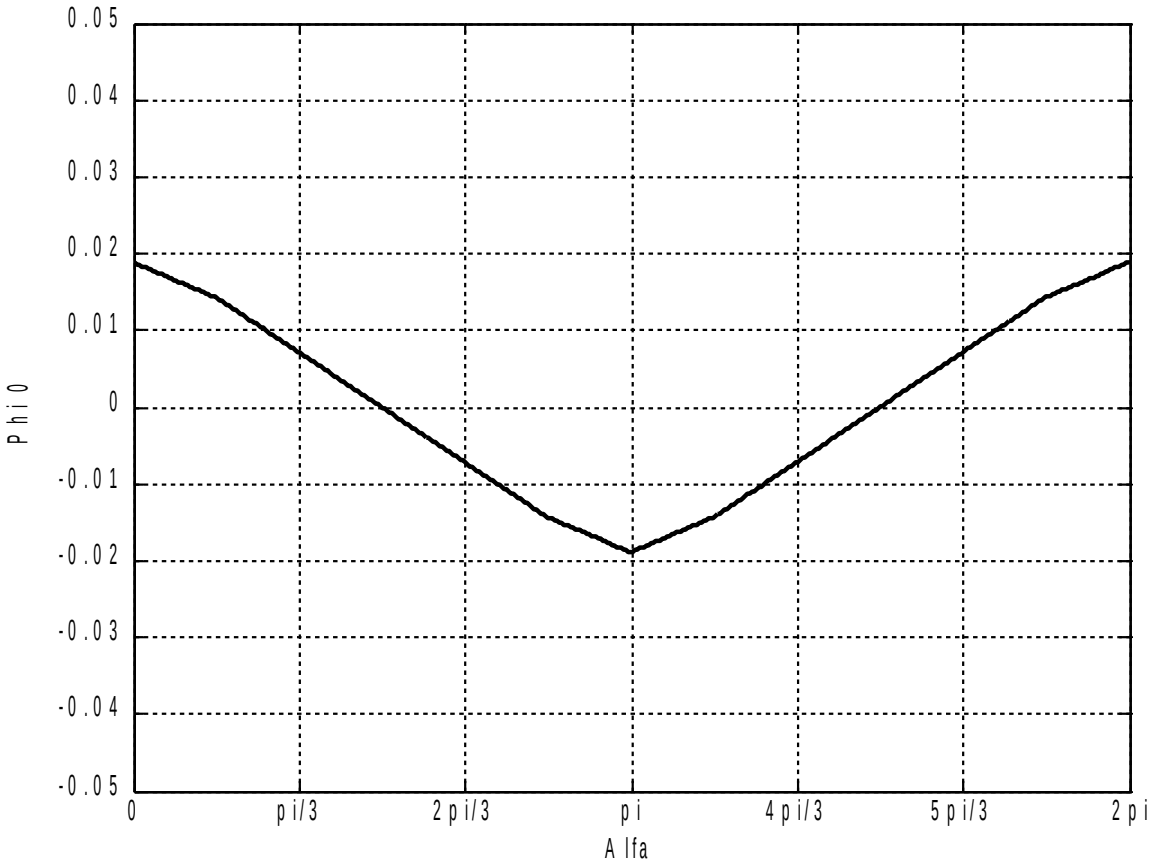

Figure 3

The evolution has been obtained for the following the geometrical and magnetic values:

$$\omega_r = 314 \ rad/s$$
$$\beta = 5\pi/6 \ rad$$
$$D = 10 \ cm$$
$$l = 30 \ cm$$
$$B_R = 0.4211 \ T$$

In order to calculate the emf per turn produced by the machine in no-load condition, it's necessary to start from the coupled-flux expression obtained from the magnetic circuit analysis. For the Faraday-Lenz law, the emf is equal to the derivative with respect to time of the coupled flux, with opposite sign. It is necessary to remember since now that this analytic calculus is valid only if it is assumed that there isn't saturation in the magnetic circuit – that is to say for low values of current. Anyway, since the value to be calculated in this chapter is the emf originated only by the magnets $e_{0(t)}$, results can be considered as sufficiently accurate.

$$e_{0(t)} = -\frac{d\lambda_{0(t)}}{dt} = -\frac{d}{dt}\left(\frac{N\,\vartheta_{(t)}\,\Phi_M}{2\,R_{(t)}}\right).$$

eq. 18

In the quantity between the parenthesis, the only time-depending terms are $\vartheta_{(t)}$ and $R_{(t)}$, so:

$$e_{0(t)} = -\frac{N\,\Phi_M}{2R_{(t)}^2}\left(\frac{d\vartheta_{(t)}}{dt}R_{(t)} - \frac{dR_{(t)}}{dt}\vartheta_{(t)}\right).$$

eq. 19

The derivative with respect to time of $R_{(t)}$ can be calculated as

$$\frac{dR_{(t)}}{dt} = \frac{d(\mu_m - \mu_0)}{rl\left(\mu_0\theta_{(t)} + \mu_m\beta - \mu_m\theta_{(t)}\right)^2}\frac{d\theta}{dt};$$

eq. 20

the derivative of $\theta_{(t)}$ with respect to the angle of rotation is discontinuous, and so will be the one of the reluctance "seen" by the magnetic flux.

For a better visualization of the electromotive force induced in the winding, it can be useful to report the evolution of the emf at the terminal of the windings, when they are open, divided for the number of the turns, so as to get the plot of the emf per turn due to the magnets.
The graph of $e_{0(t)}$ per turn, in these conditions, is

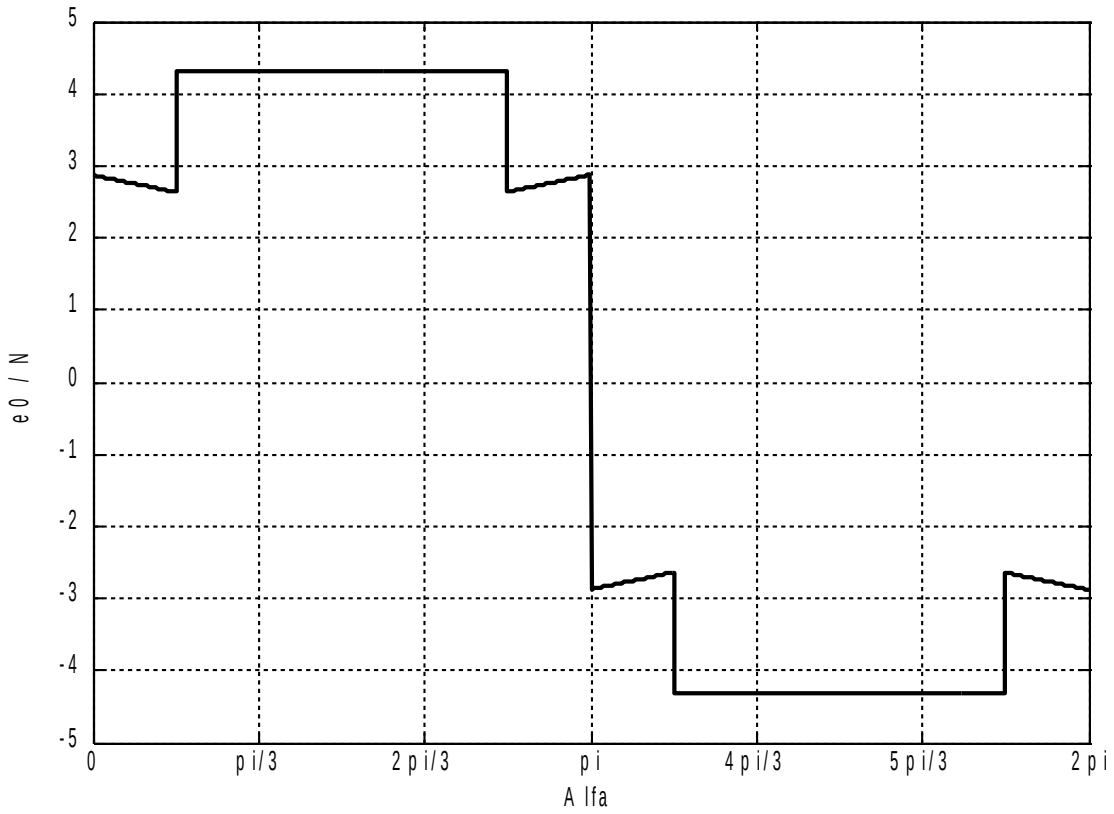

Figure 5

The formulation of the electromagnetic torque can be obtained as the partial derivative with respect to the angular position of the magnetic coenergy, according with the energy conservation principle. The torque expression is

$$T=\frac{\partial W'_m}{\partial \alpha}.$$

eq. 21

For the magnetic coenergy calculus, it is necessary to make an integral, considering as the starting status the zero point in the (H,B) plane. Because of the normal magnetization of the machine due to the permanent magnets, it's necessary to de-magnetize the system.
This can be obtained if in the winding flows a fictitious current i_0 : the Ampere law applied to the simplified magnetic circuit of the machine could be written as (eq. 15)

So, with the imposition of $\Phi=0$, we can find the value i_0

$$i_0=\frac{-\Phi_M R}{N}.$$

eq. 22

The expression of the magnetic coenergy is

$$W'_m = \int_{i_0}^{i} \lambda di = \int_{i_0}^{i} (L\, i_{(t)} + \lambda_0)\, di$$

eq. 23

The result of the integral, to be clear, cannot be computed in an analytical way, because of the not-linear nature of the magnetic characteristic of the iron/steel.

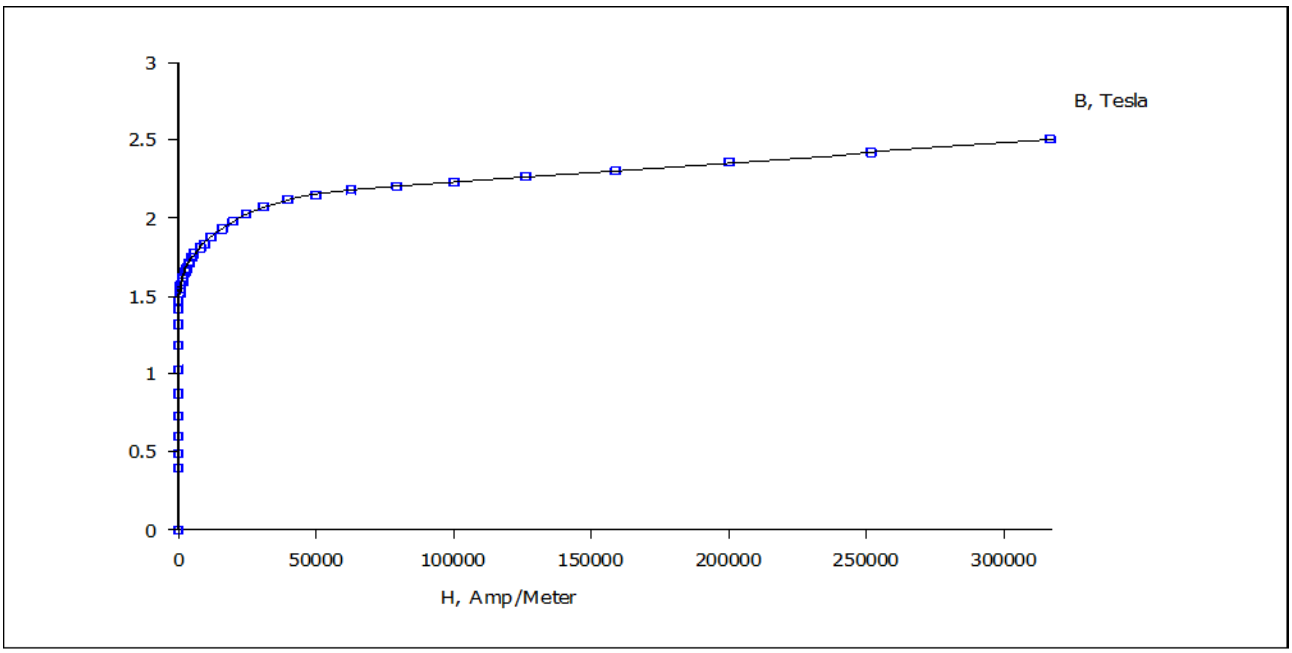

Figure 5

2.3 Femm Simulations

To have a reconstruction of the magnetic behaviour of the machine it is necessary to build a simulation of it with a Finite Element software, such as FEMM.
Writing a program with MatLab, it is possible to make the simulation run for different values of the angular position of the rotor, with no current flowing in the windings, so as to obtain the no-load characteristic of the machine, in terms of flux and electromagnetic torque. This torque is the cogging torque, typical of the machines equipped with permanent magnets, due to the disturbing effect to the rotation of the rotor made from the interaction between the magnetic flux produced by the magnets and the shape of the inner stator.
The model used for the simulations is the following:

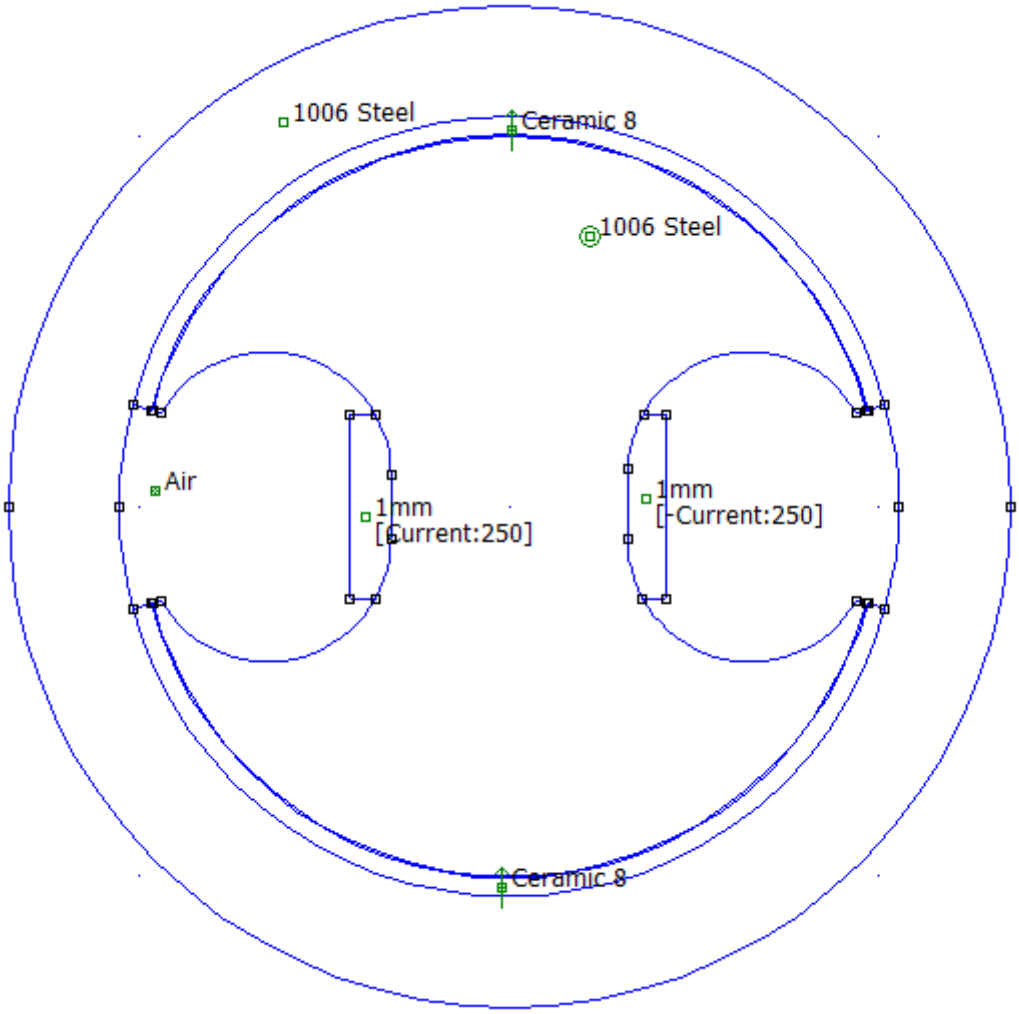

Figure 6

The representation of the flux and of the cogging torque are below:

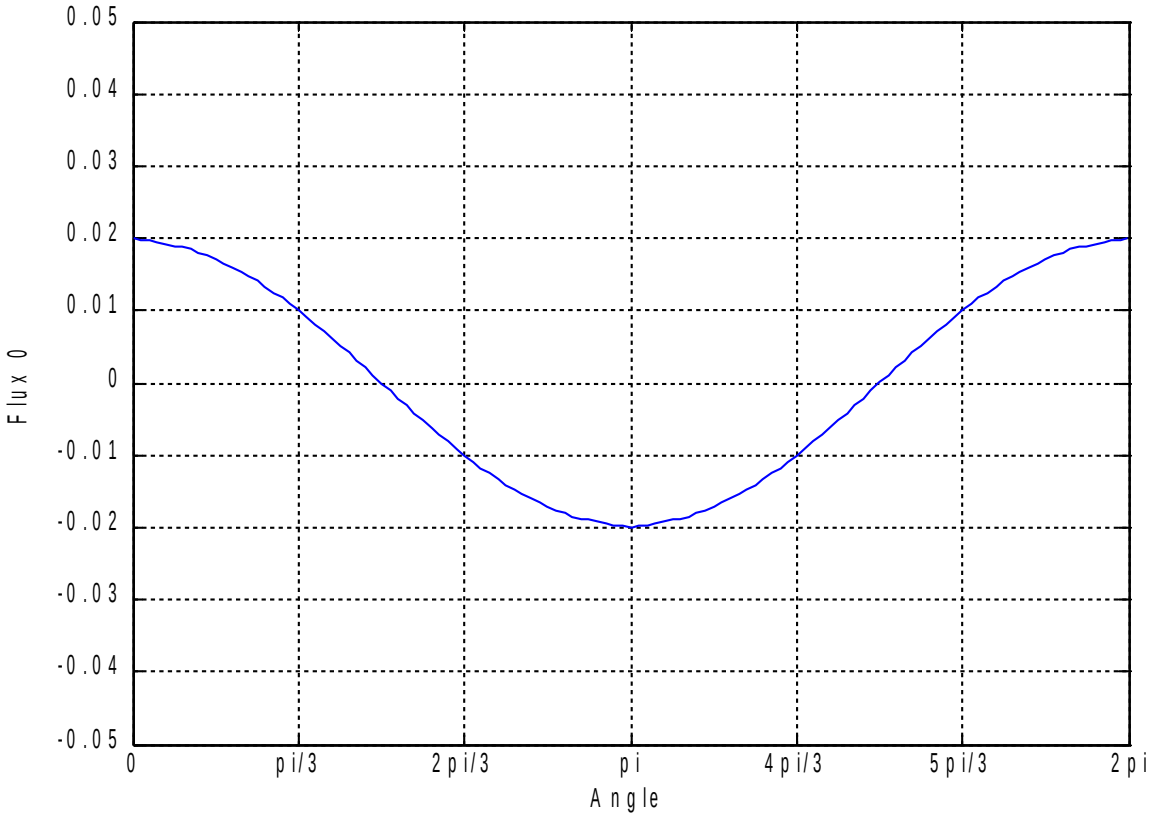

Figure 7

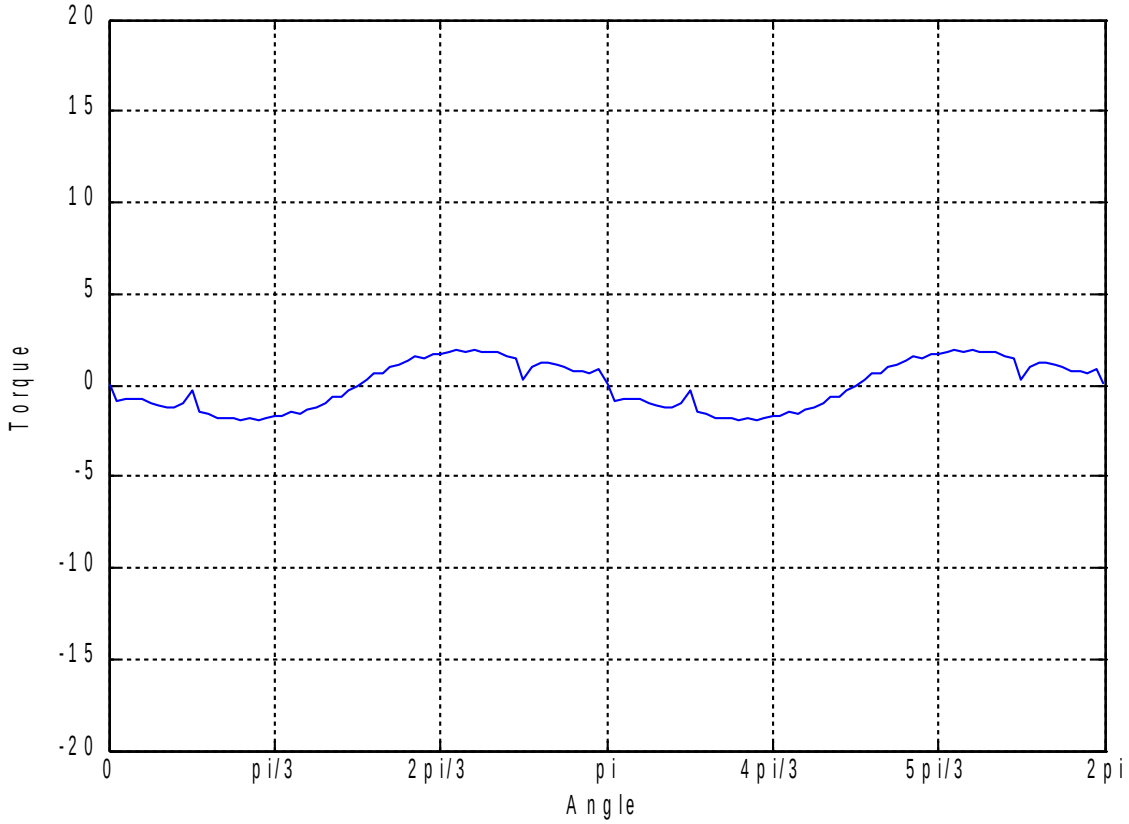

Figure 8

It is now possible to get the evolutions of the electromechanical parameters of the machine when it's fed by a sinusoidal current.
Hence, from now on, evolutions will be plotted for different values of feeding current, $i_{(t)}$, which follows the cosinusoidal behaviour:

$$i_{(t)} = I_M \cos(2\omega t + \varphi)$$

eq. 24

Values changing for each simulation are both the peak value and the angular phase.
Cosinusoidal law has been chosen instead of sinusoidal one so as to have $i_{(t)}$ and $\Phi_{0(t)}$ in phase when $\varphi=0$.

MMF=1000 At, φ=0

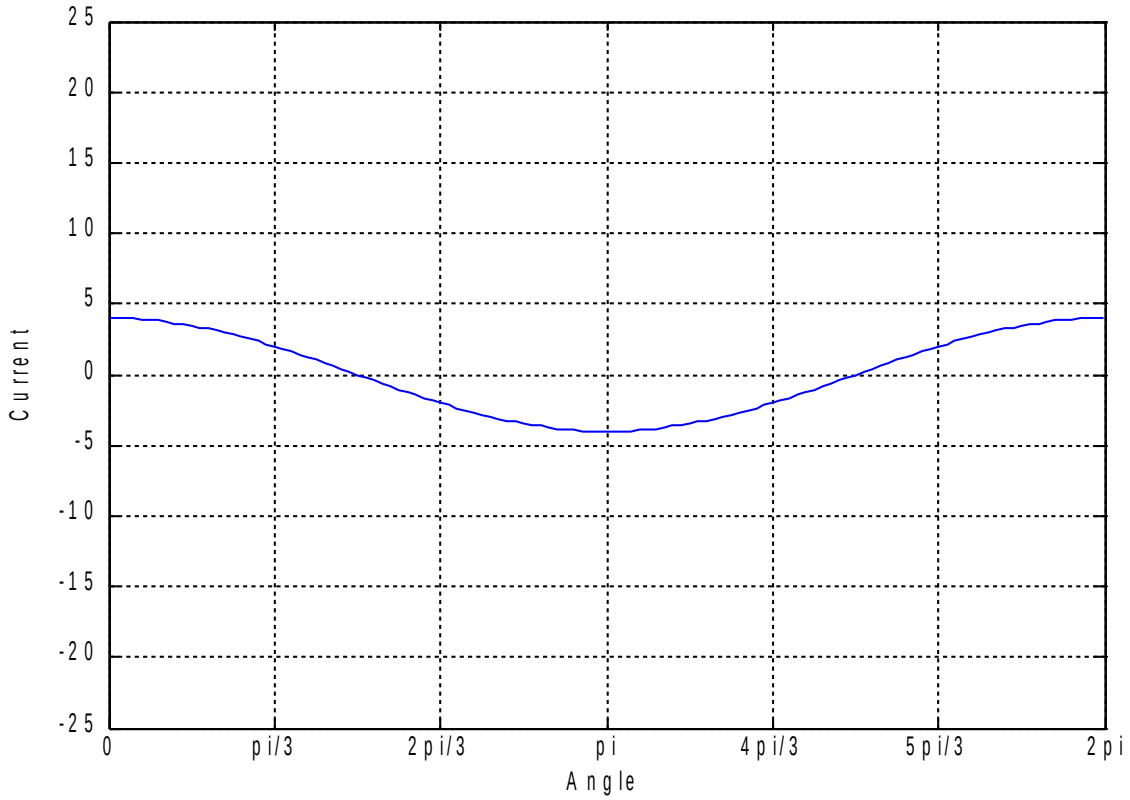

Figure 9

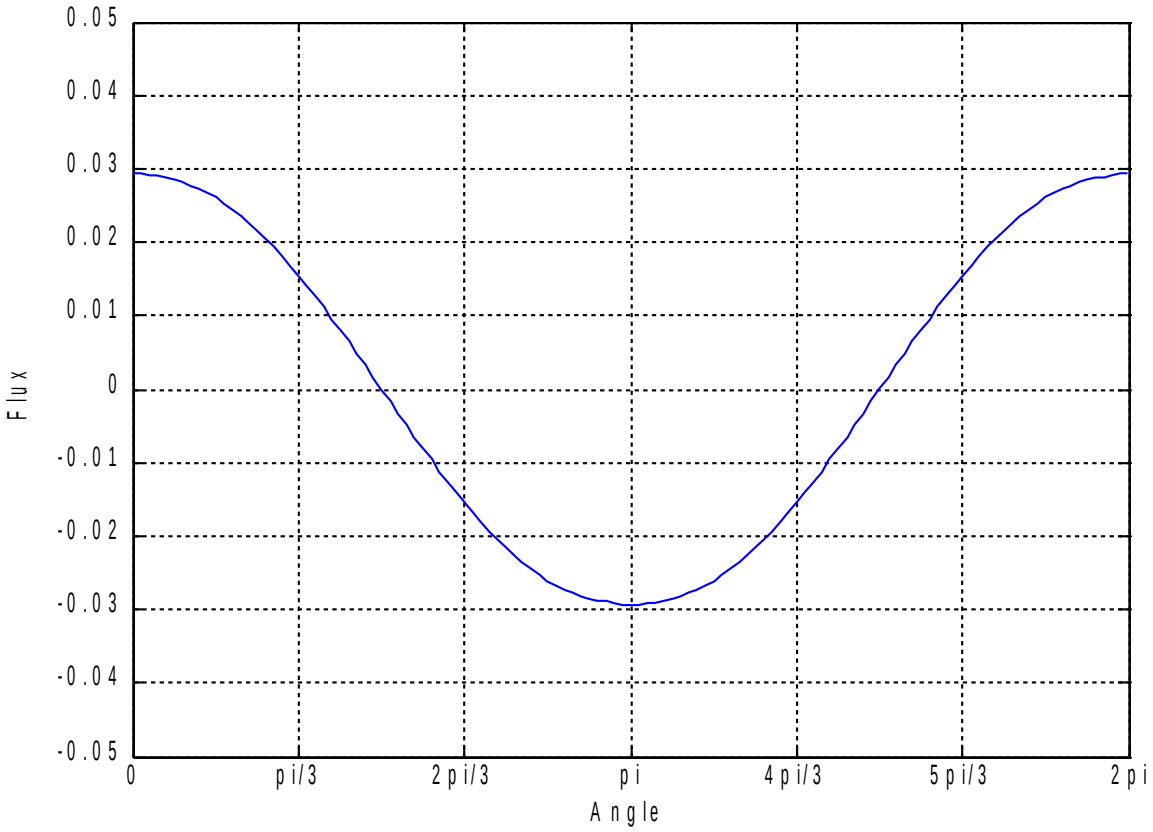

Figure 10

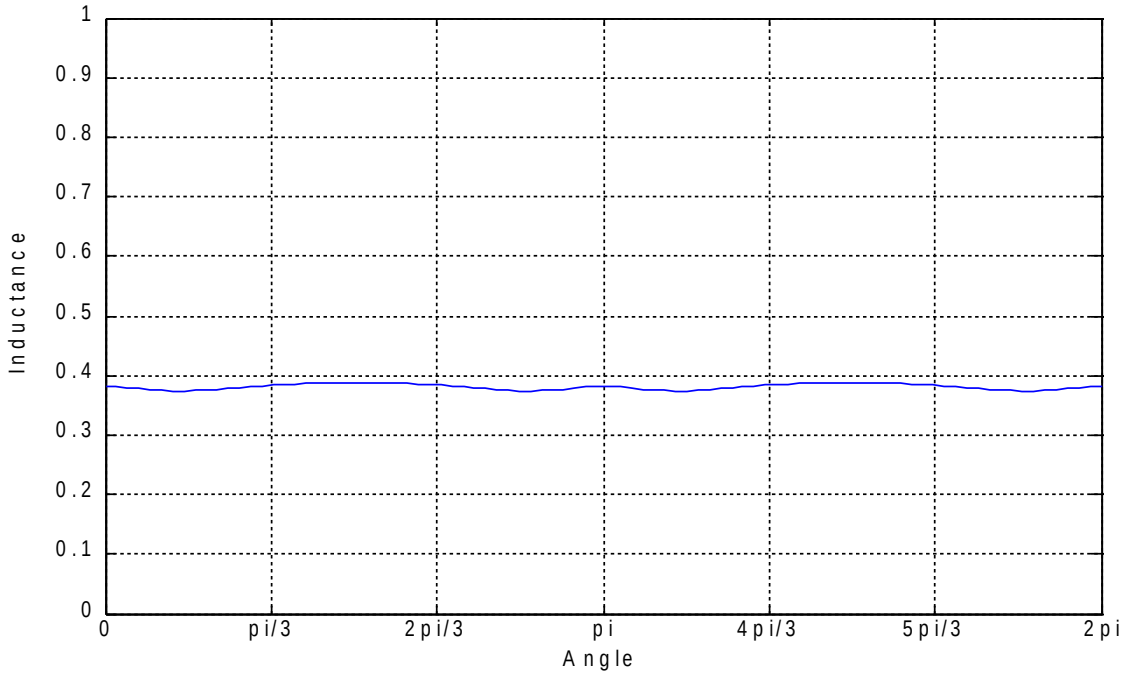

Figure 11

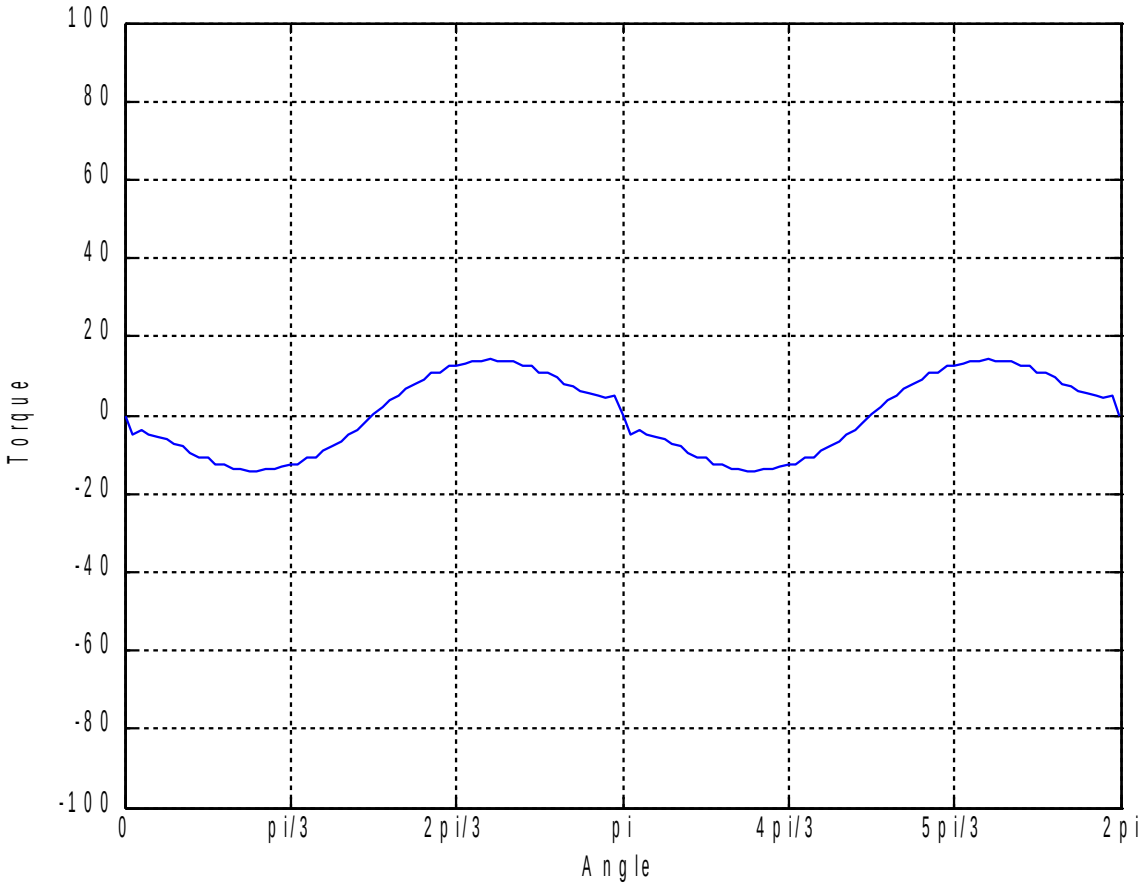

Figure 12

MMF = 1000 At, φ=30°

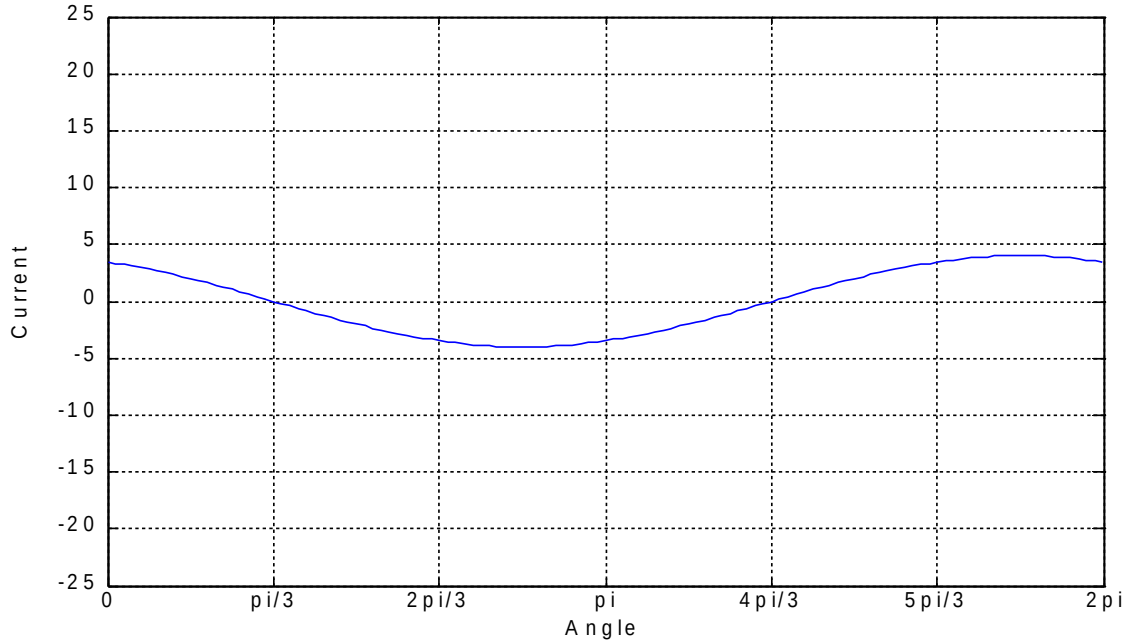

Figure 13

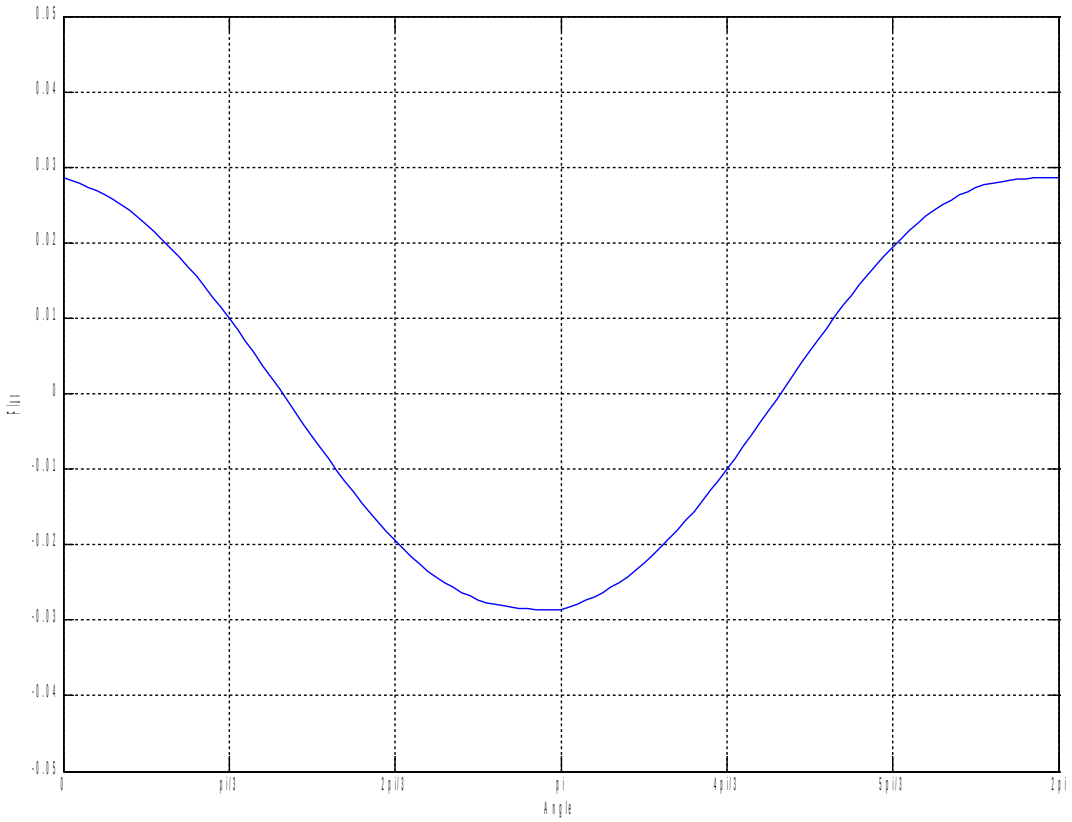

Figure 14

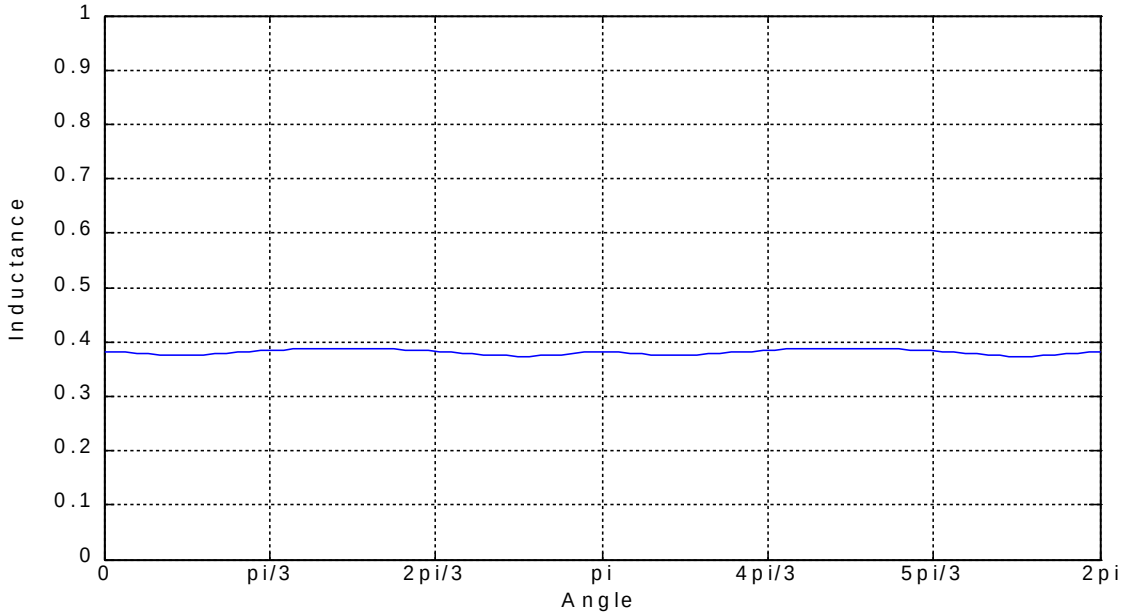

Figure 15

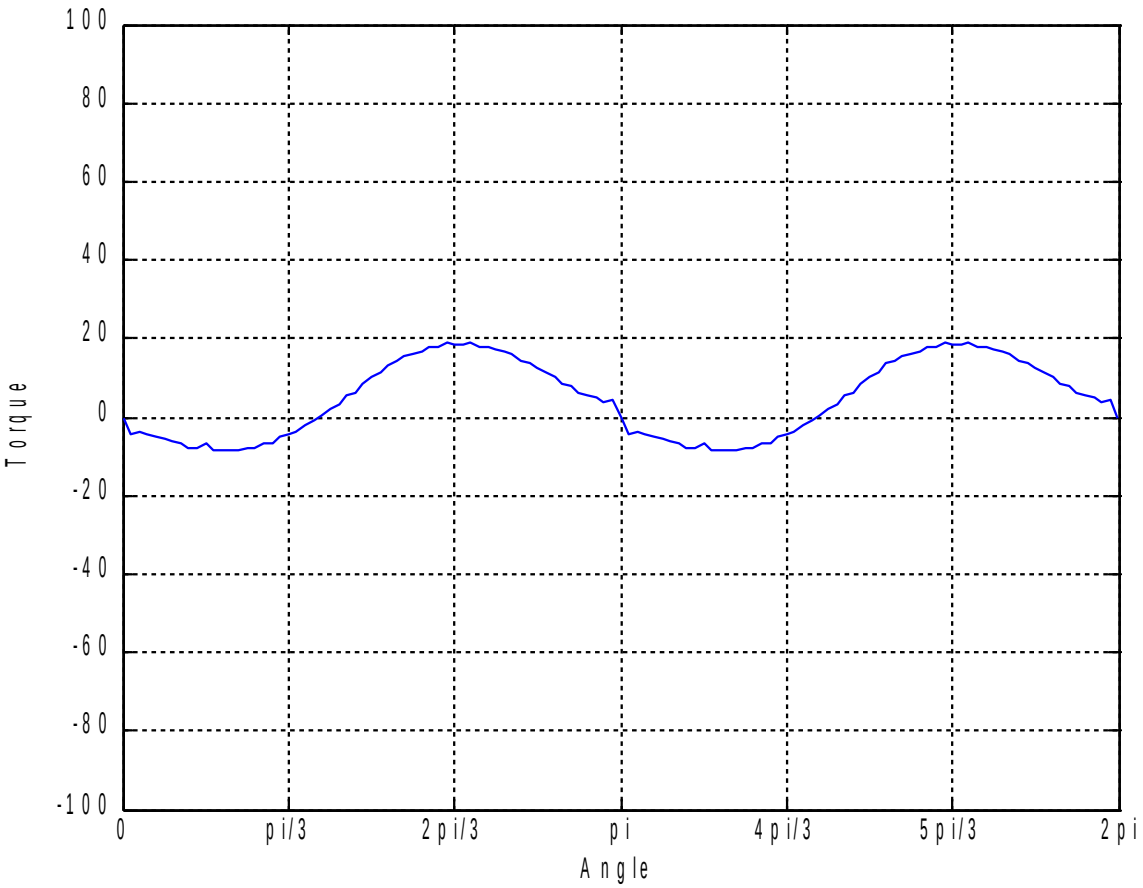

Figure 16

MMF = 1000 At, φ=60°

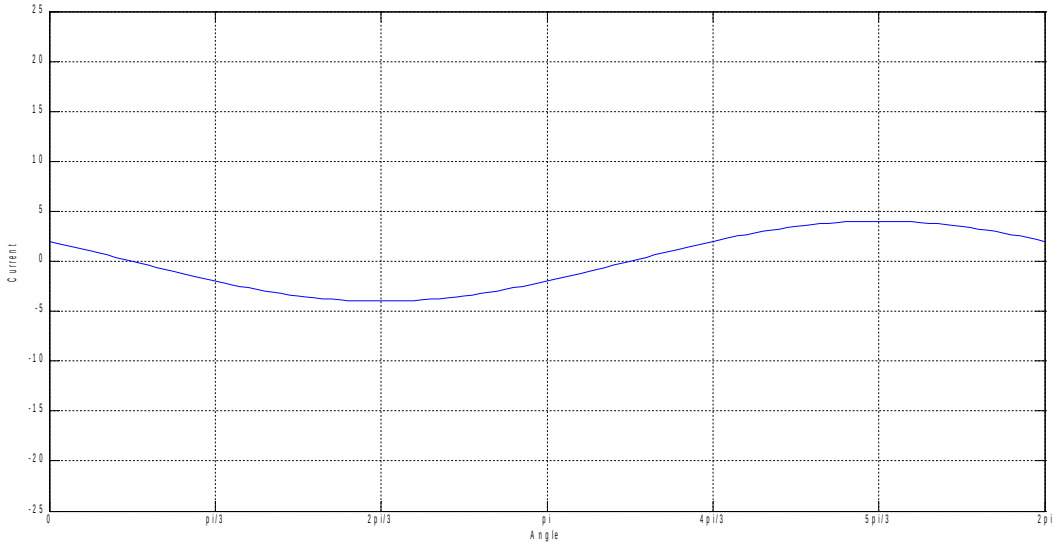

Figure 17

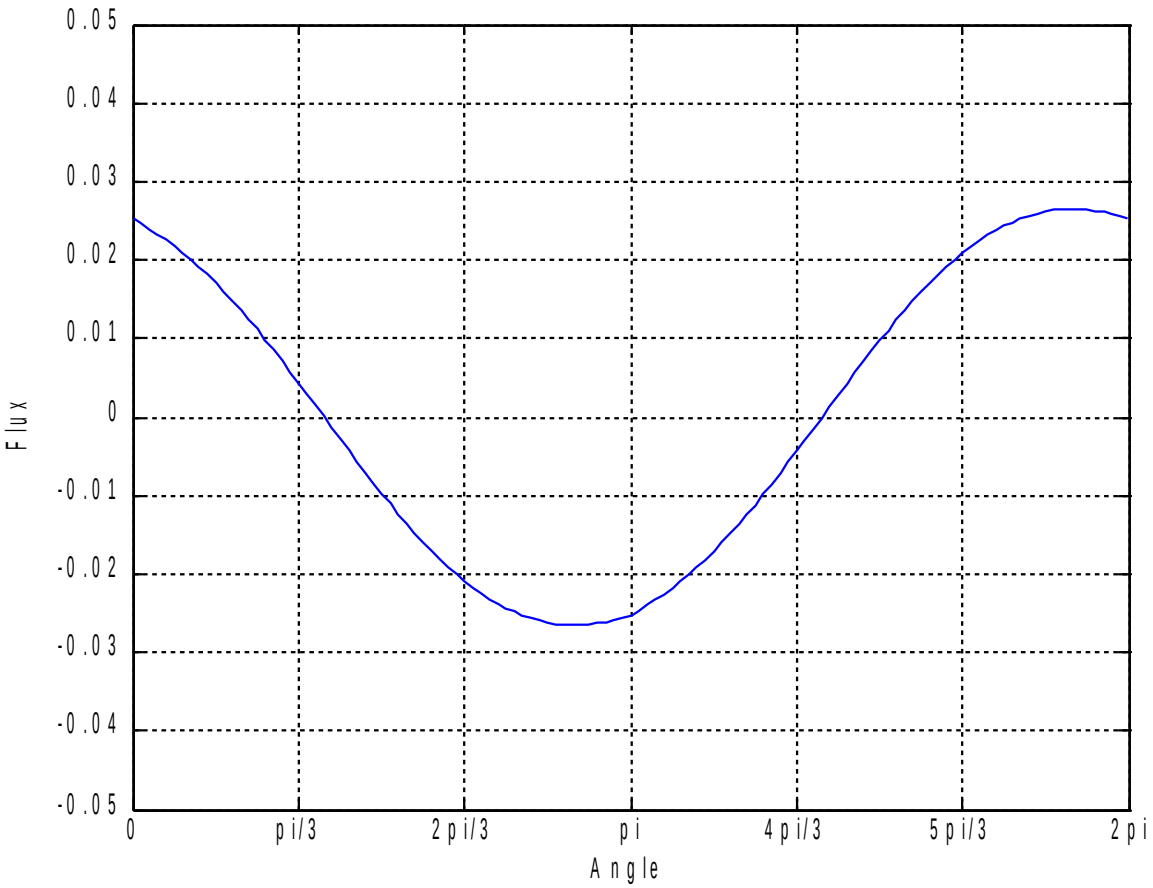

Figure 18

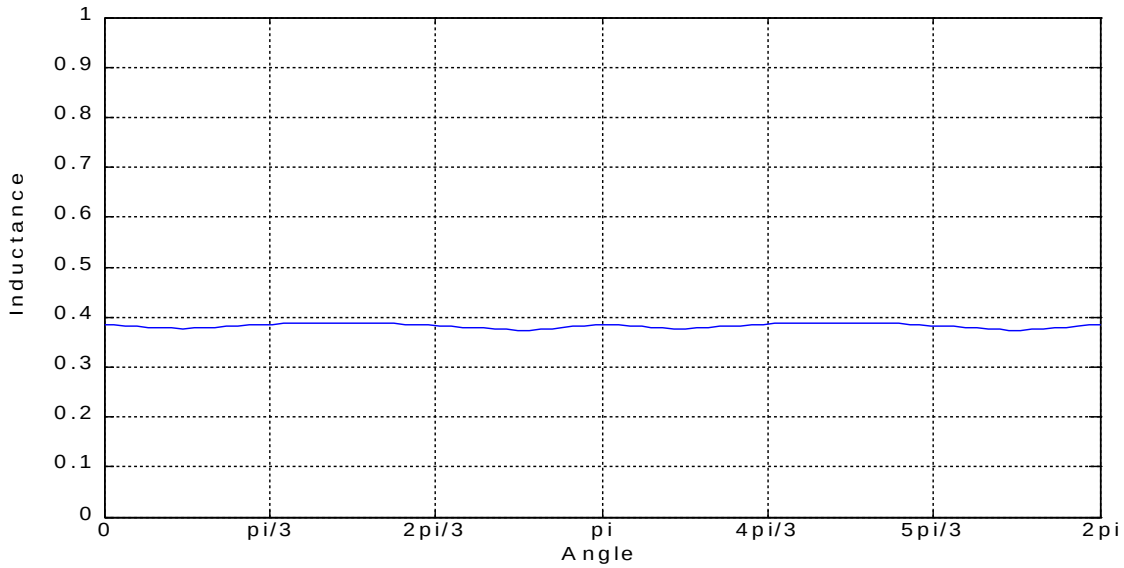

Figure 19

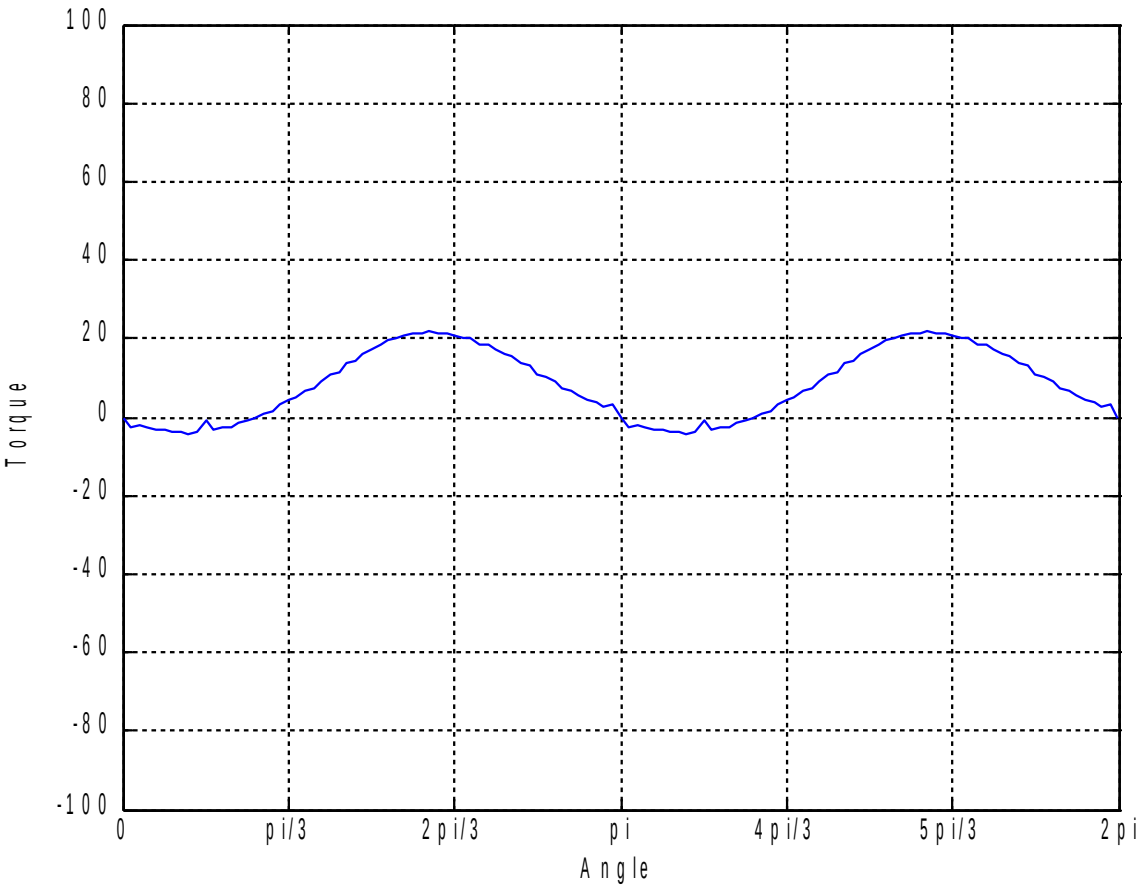

Figure 20

MMF = 1000 At, φ=90°

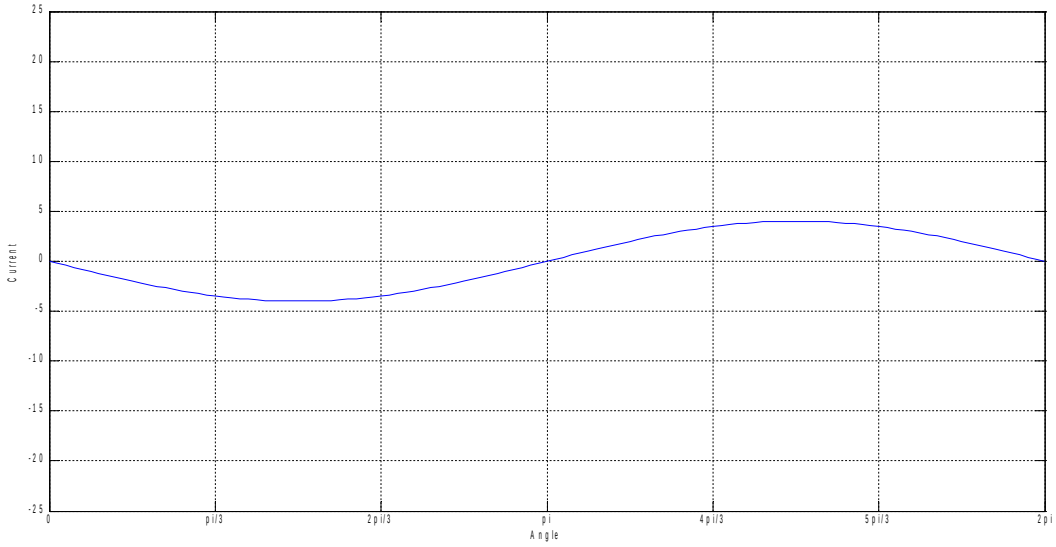

Figure 21

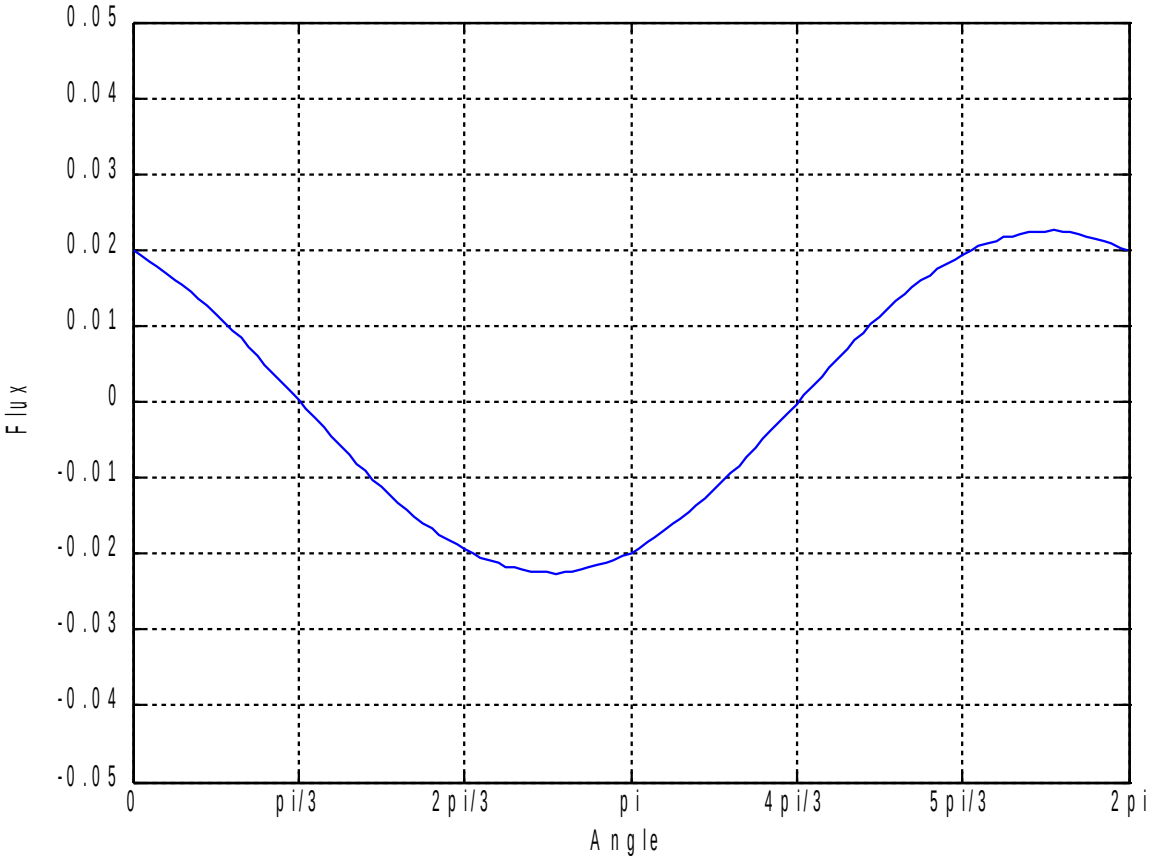

Figure 22

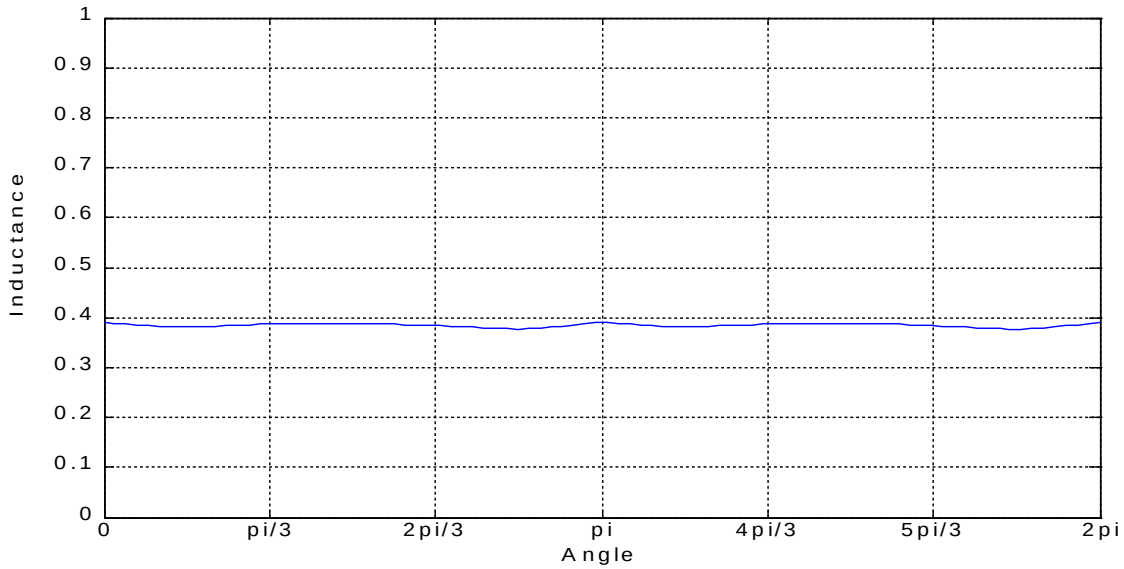

Figure 23

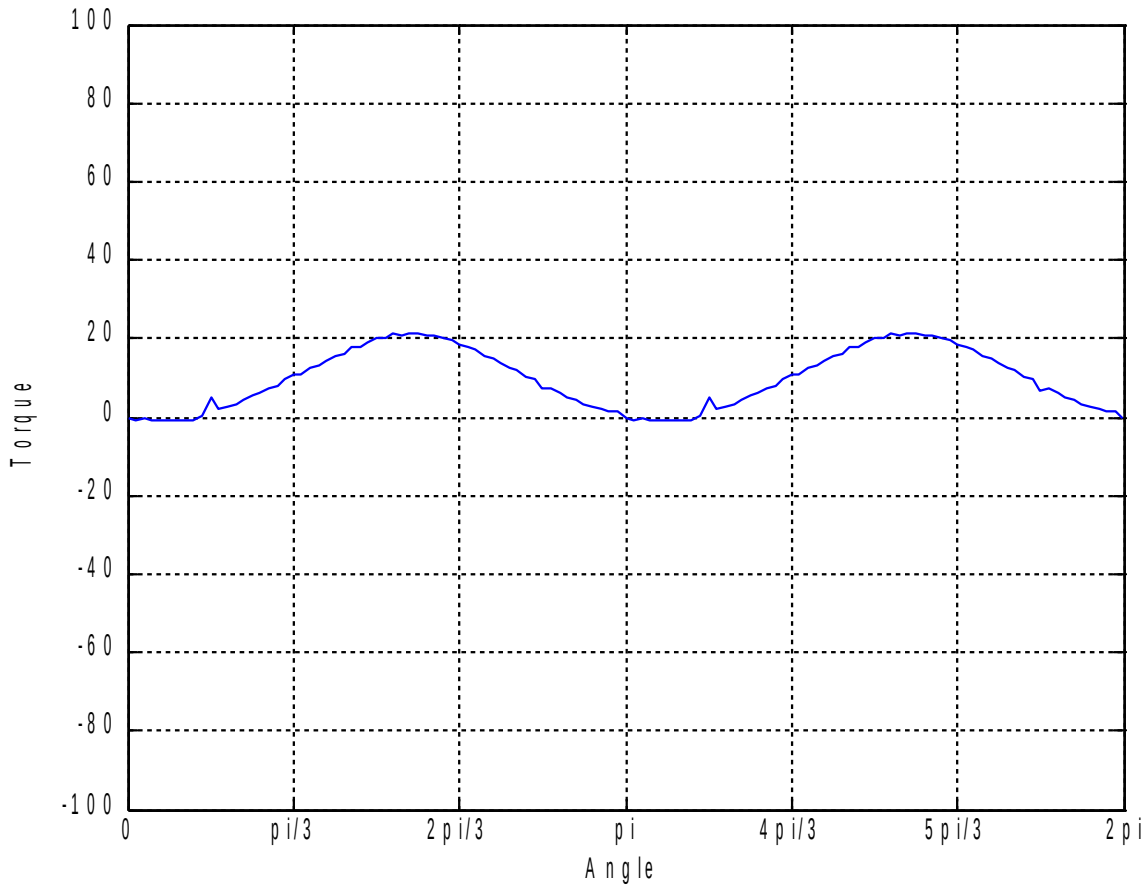

Figure 24

MMF = 2000 At, φ=0°

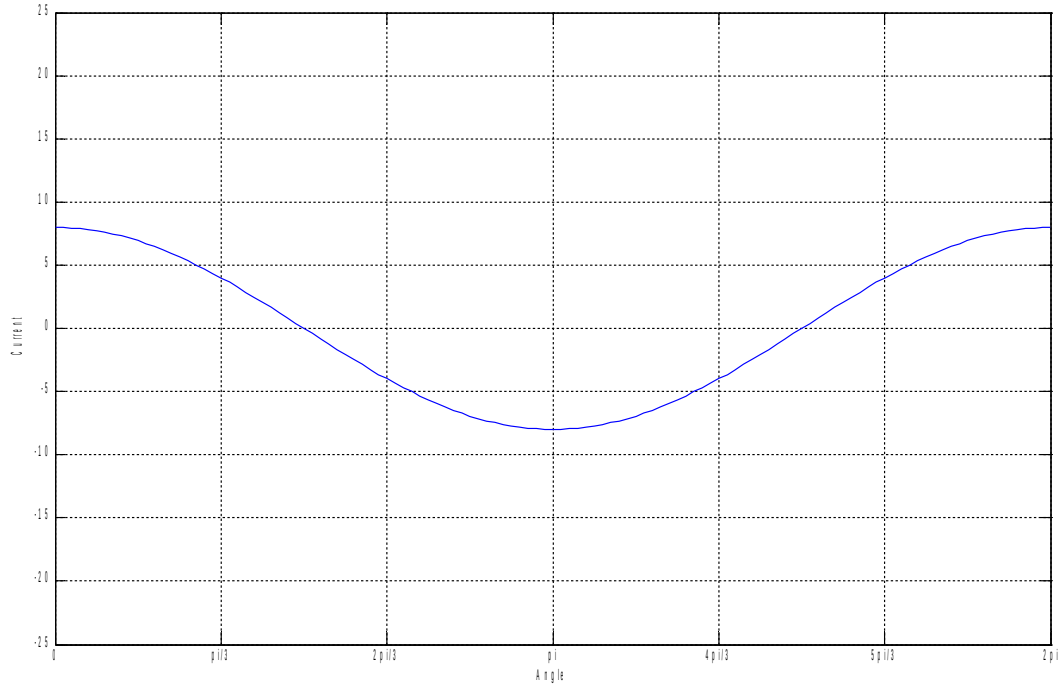

Figure 25

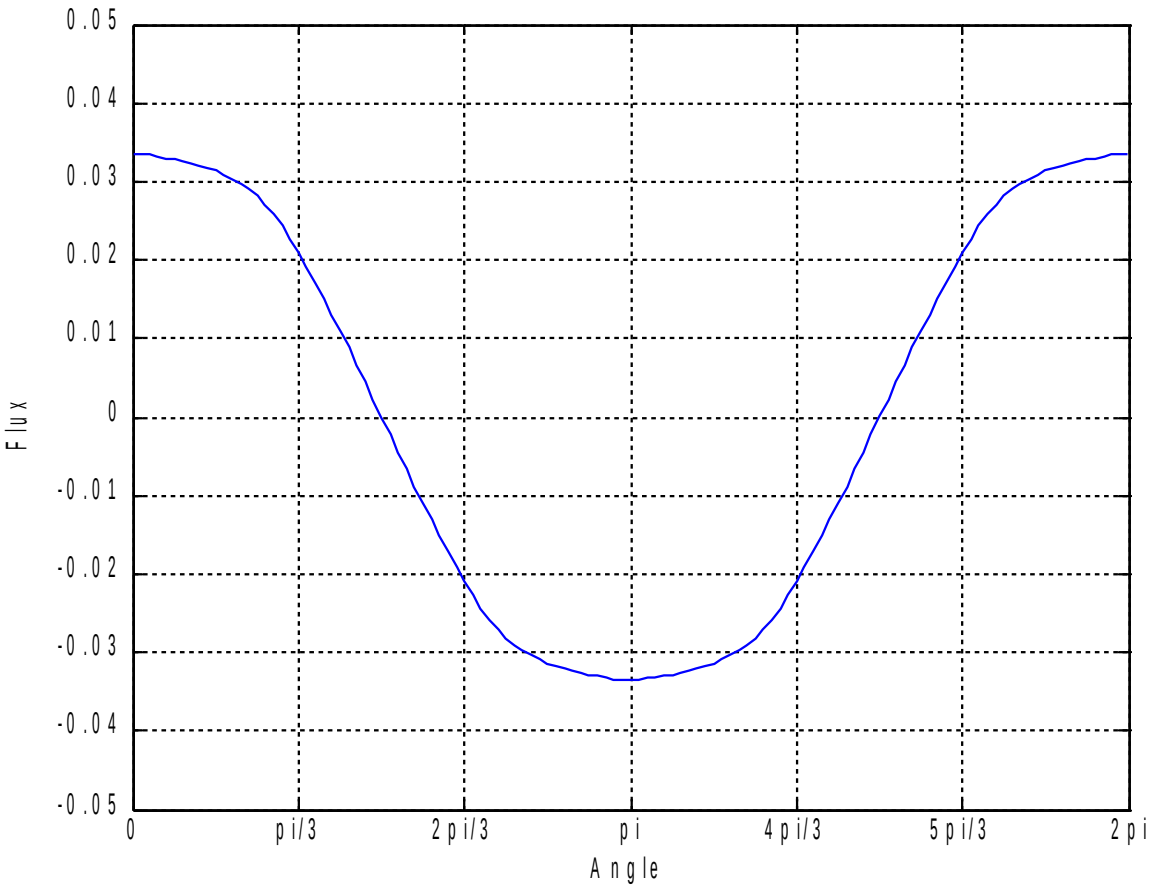

Figure 26

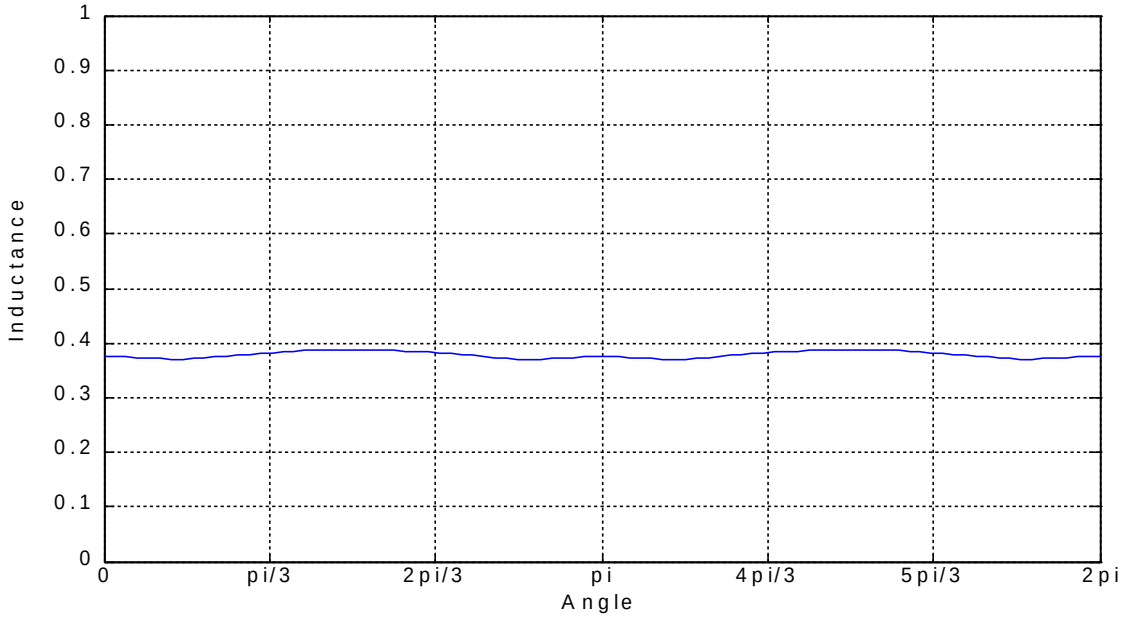

Figure 27

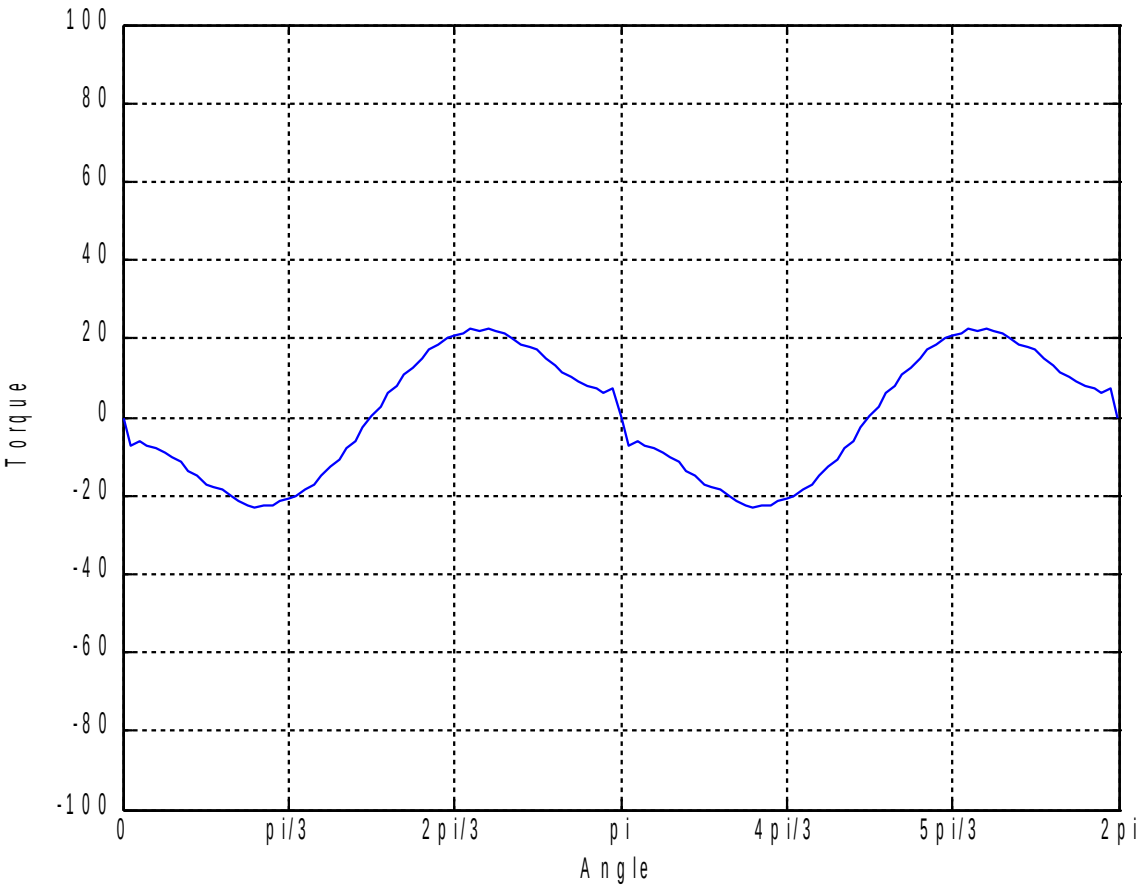

Figure 28

MMF = 2000 At, φ=30°

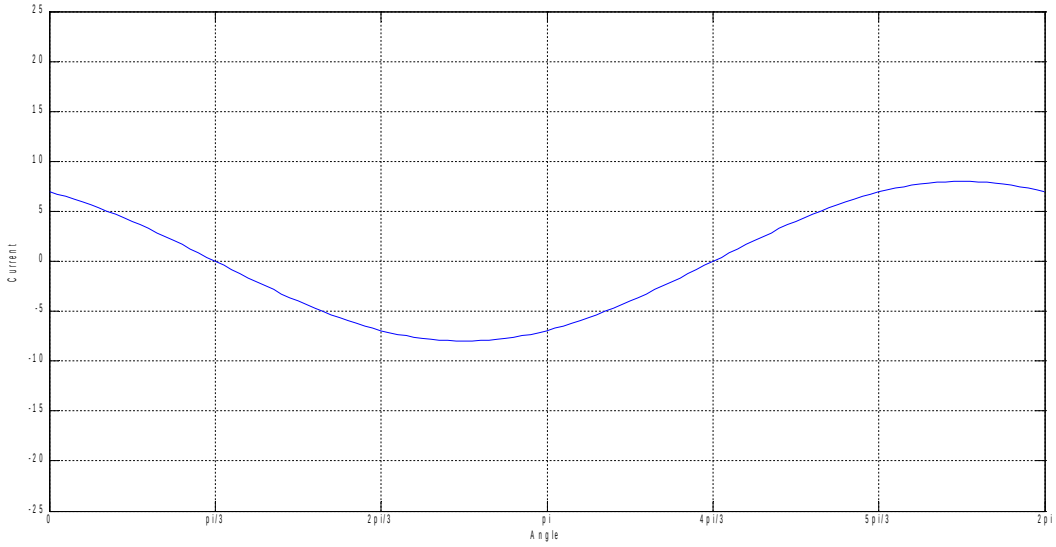

Figure 29

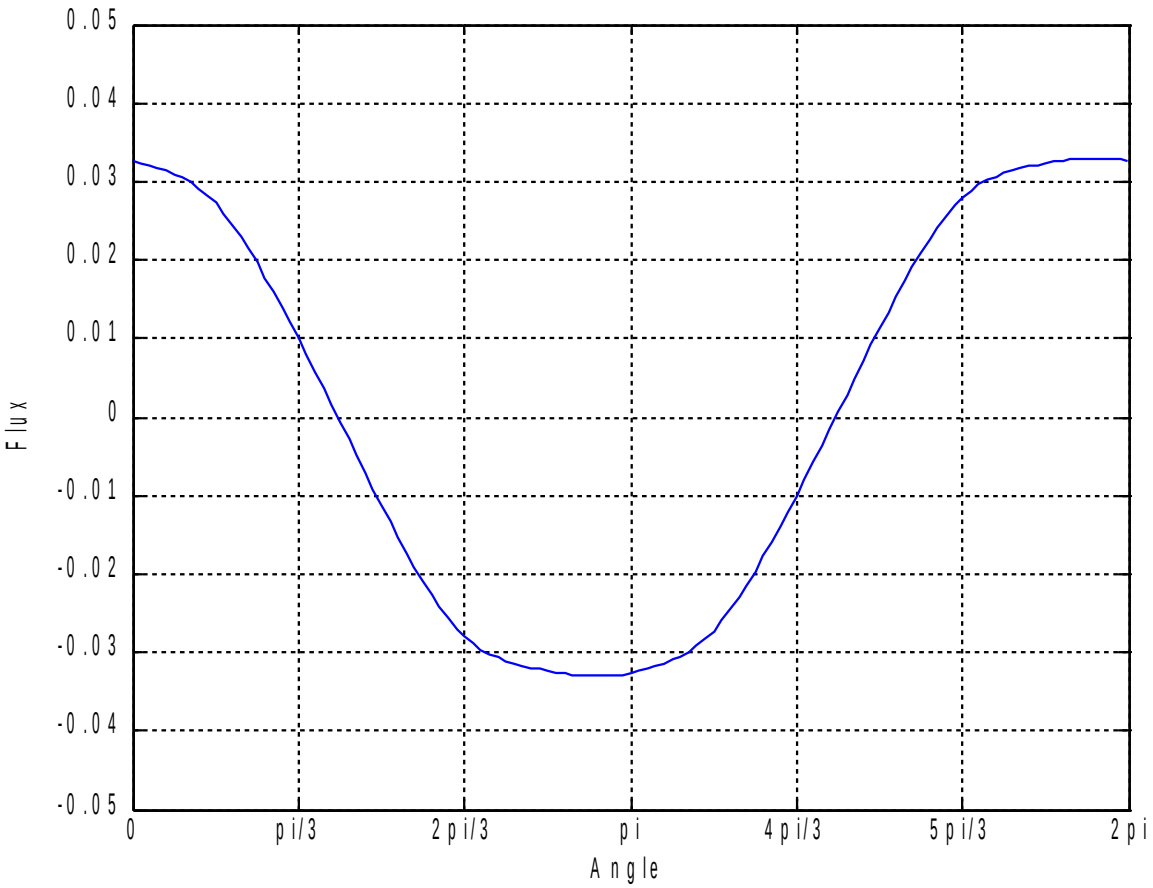

Figure 30

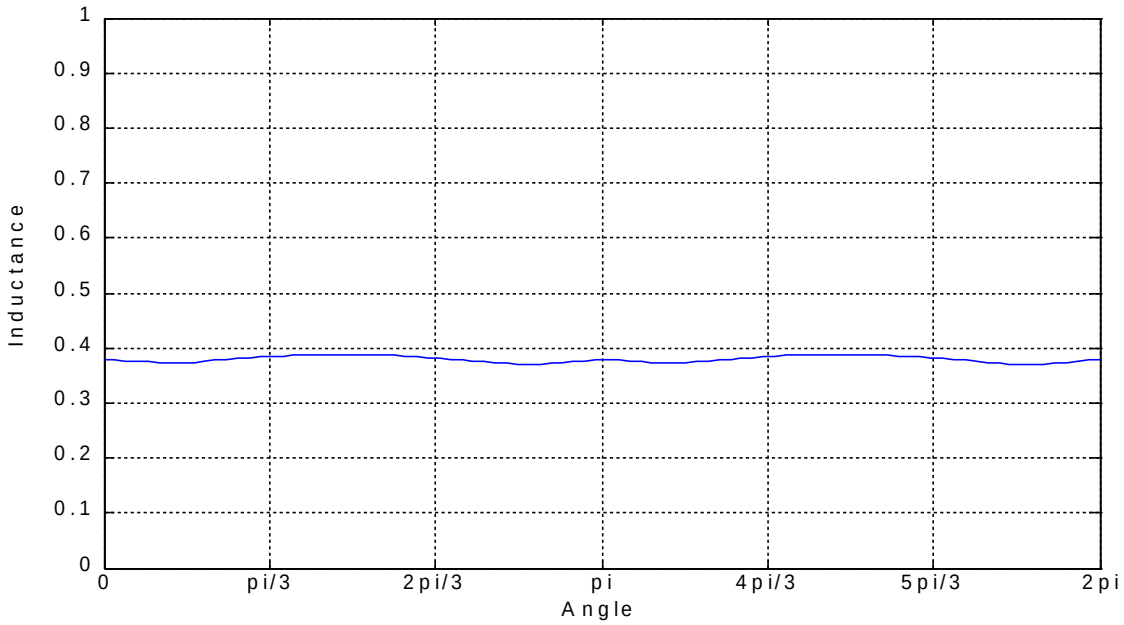

Figure 31

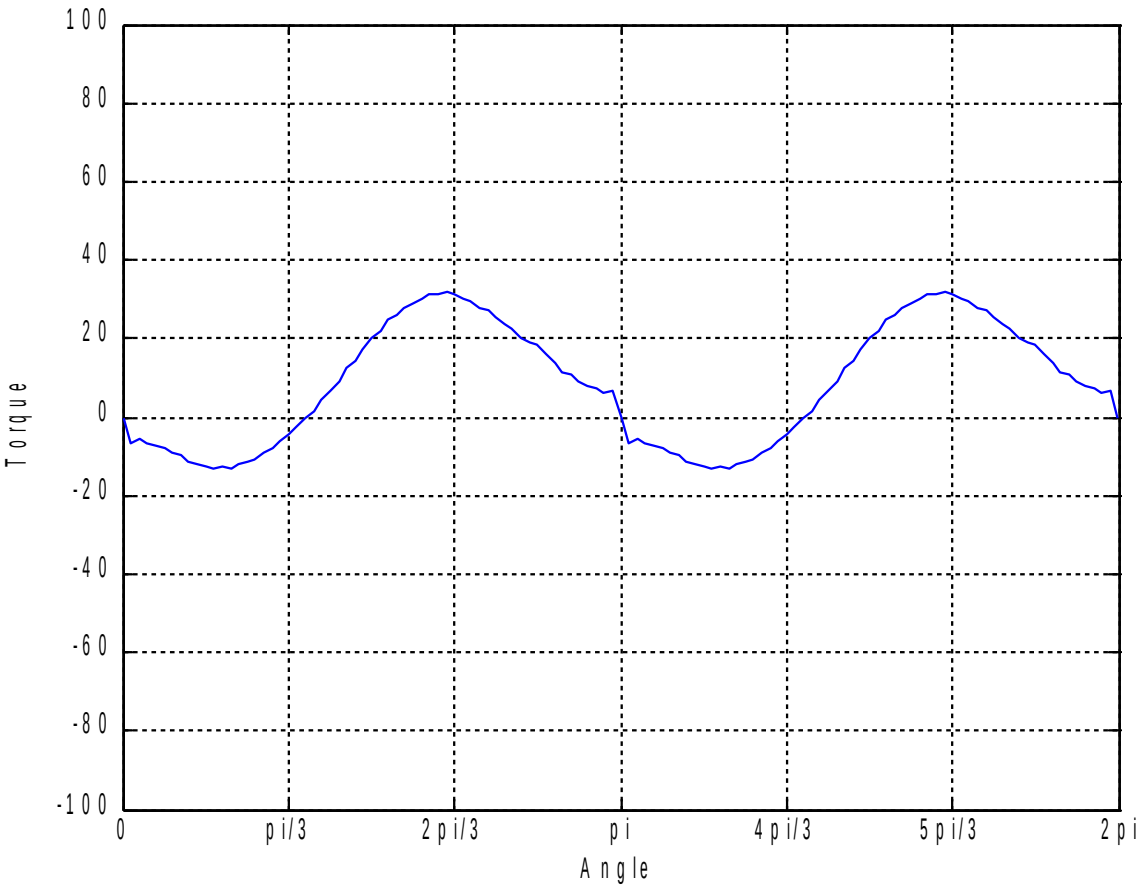

Figure 32

MMF = 2000 At, φ=60°

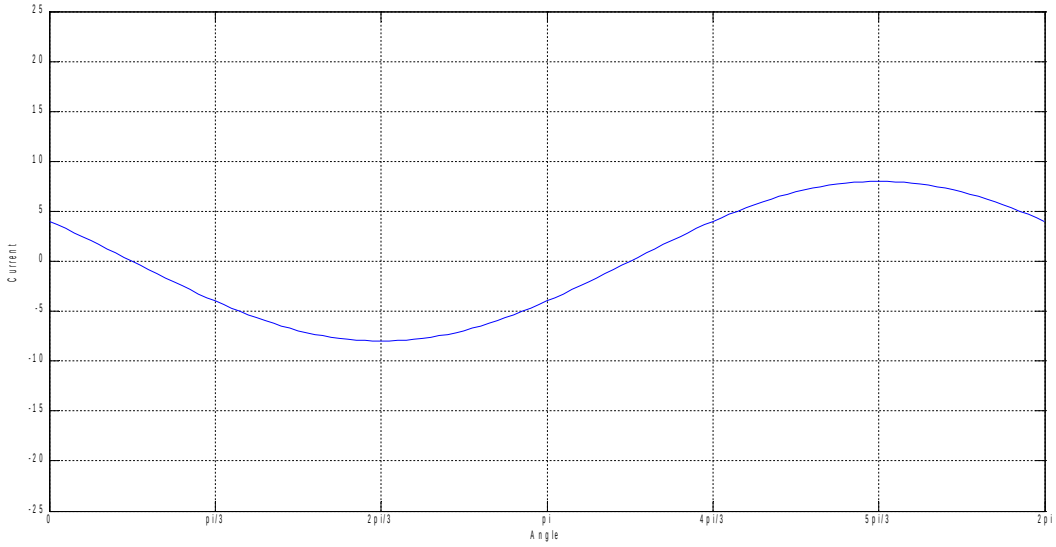

Figure 33

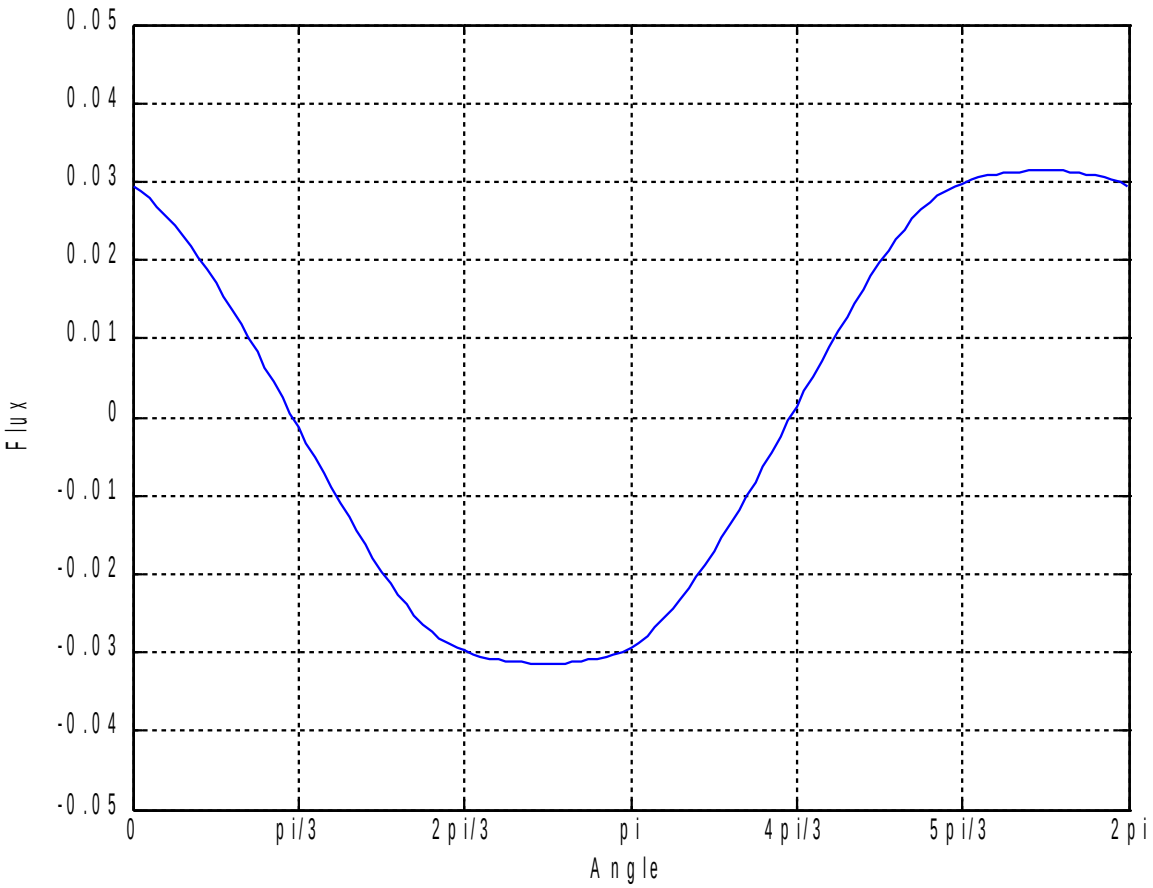

Figure 34

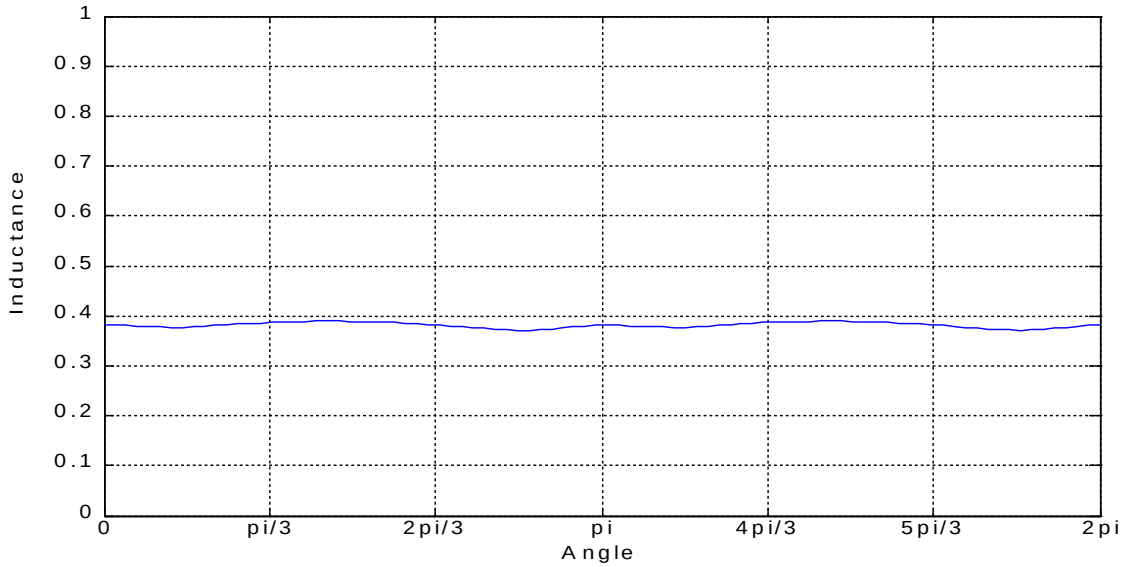

Figure 35

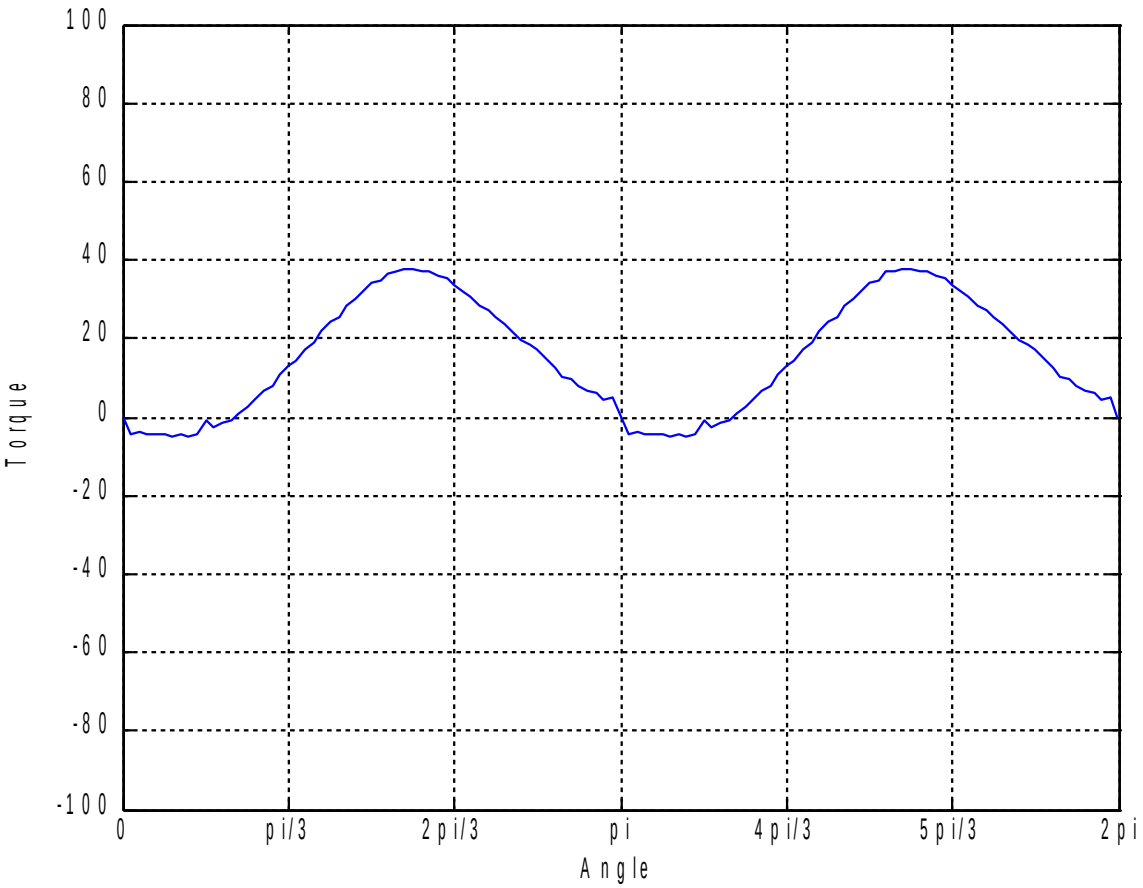

Figure 36

MMF = 2000 At, φ=90°

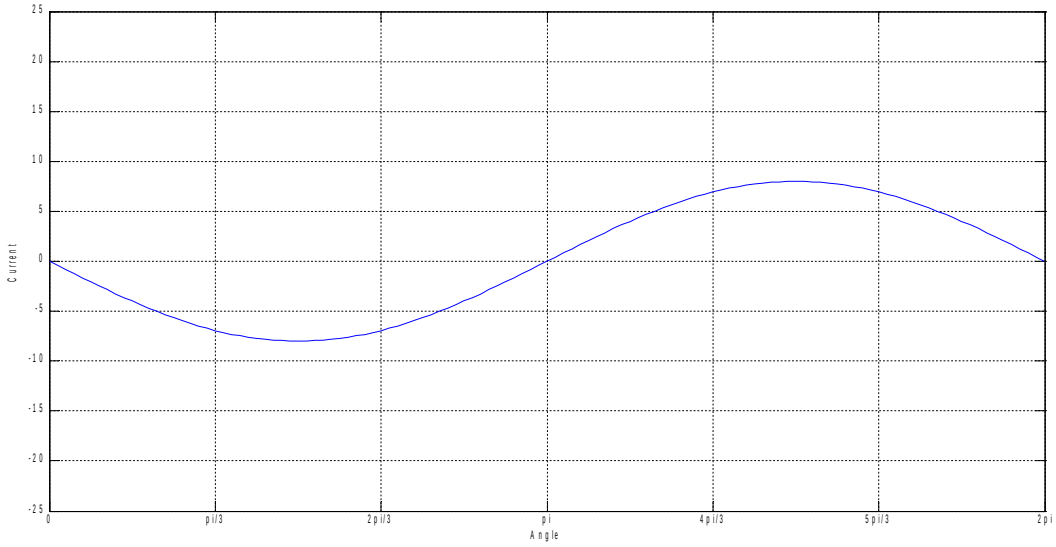

Figure 37

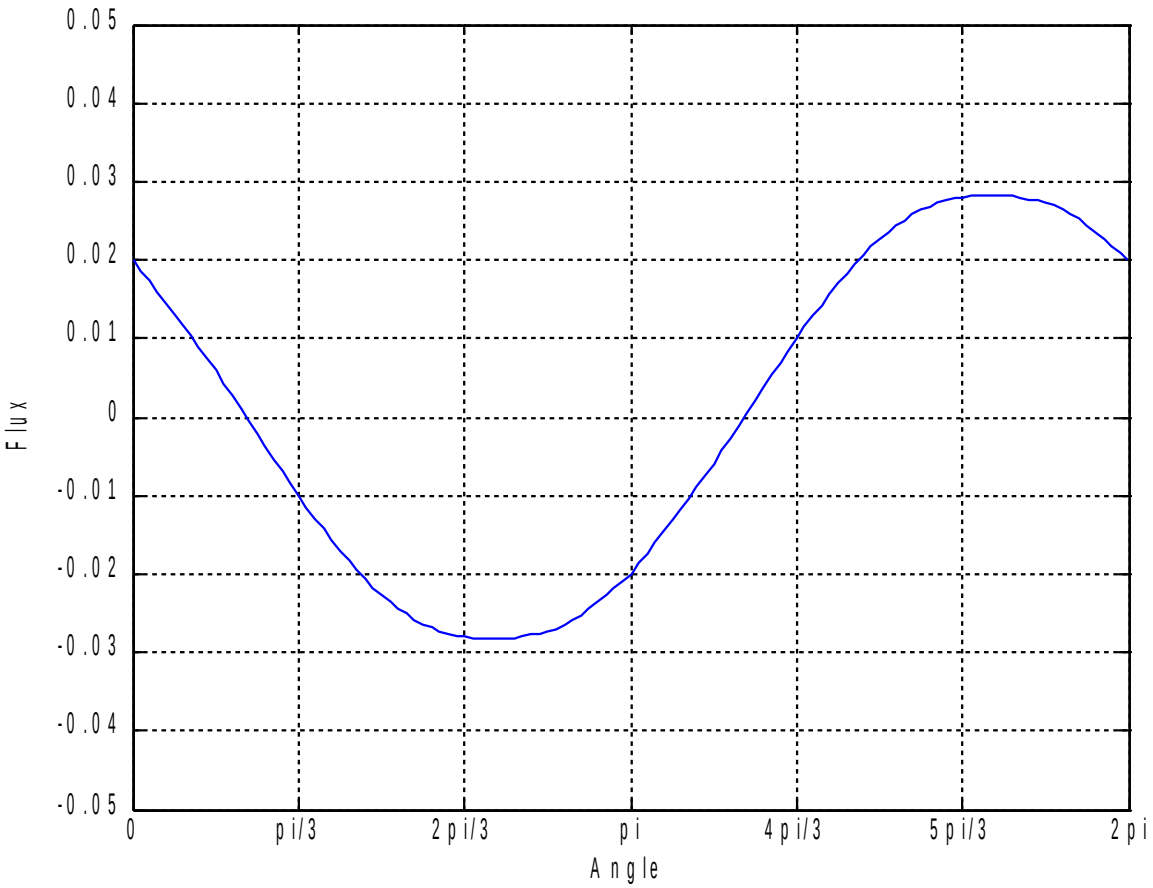

Figure 38

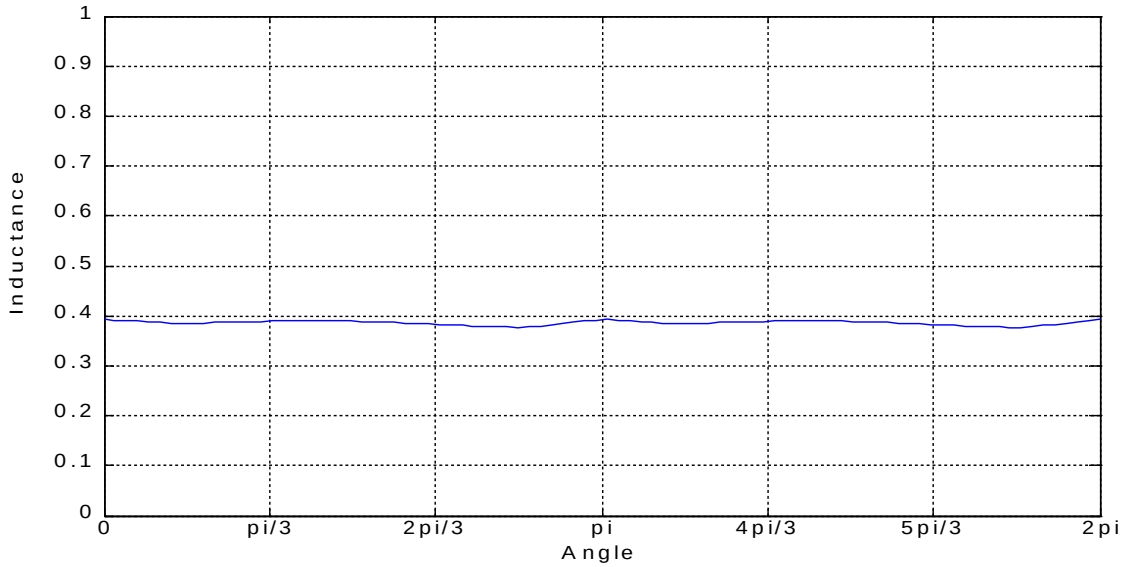

Figure 39

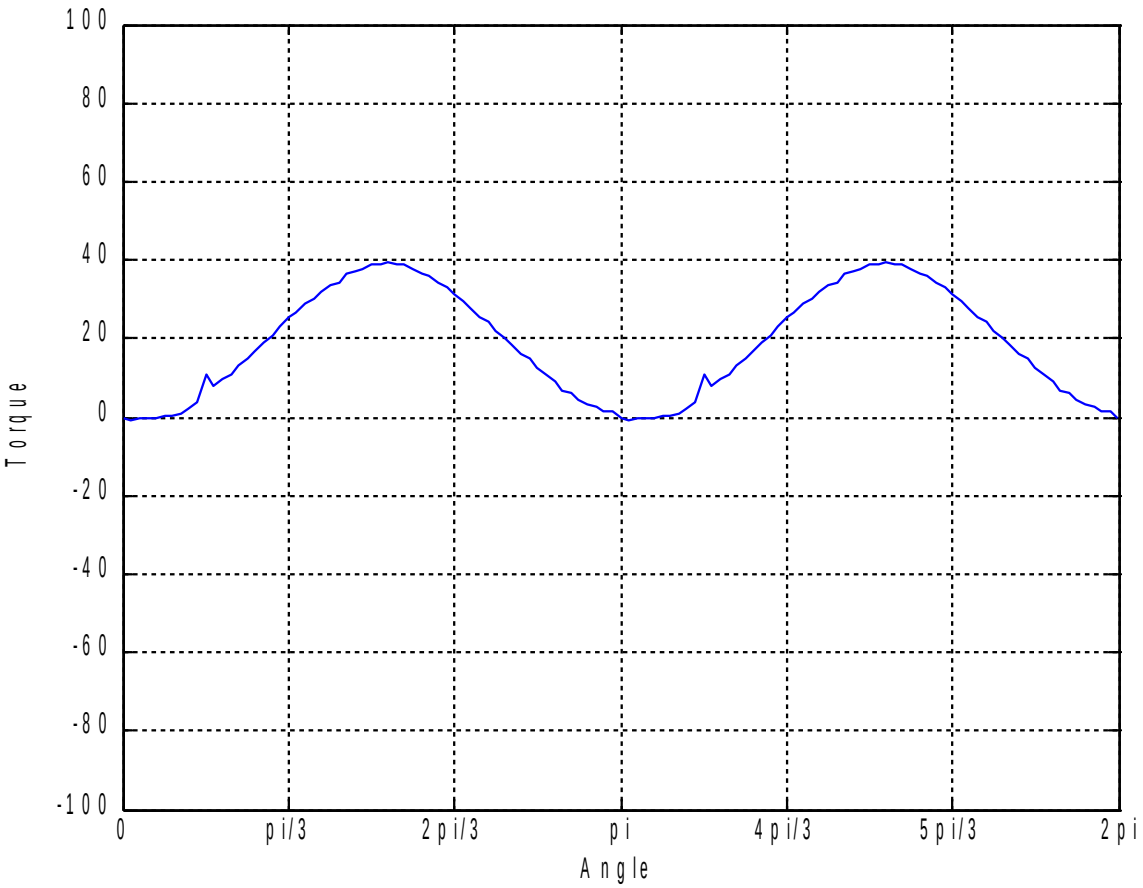

Figure 40

MMF = 3000 At, φ=0°

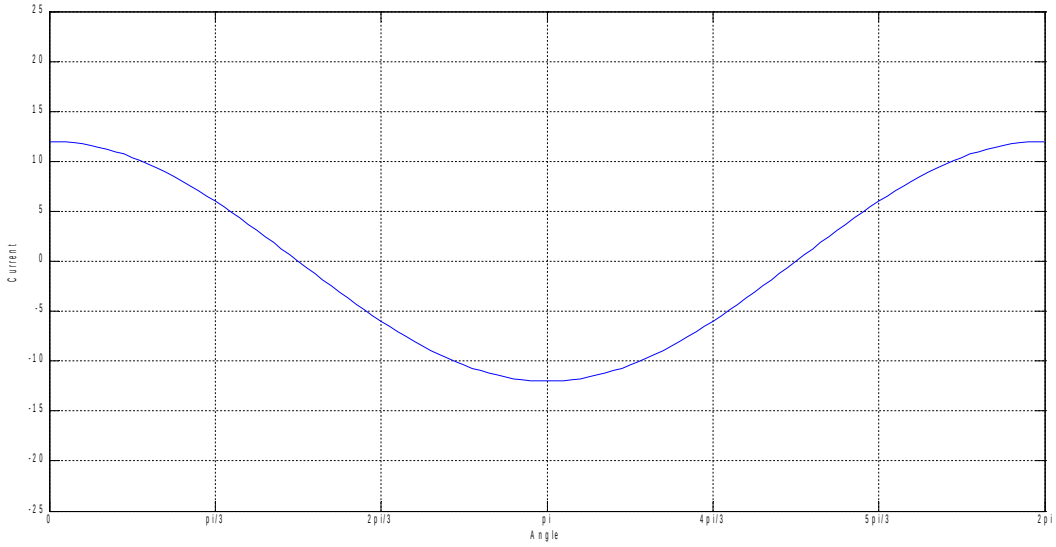

Figure 41

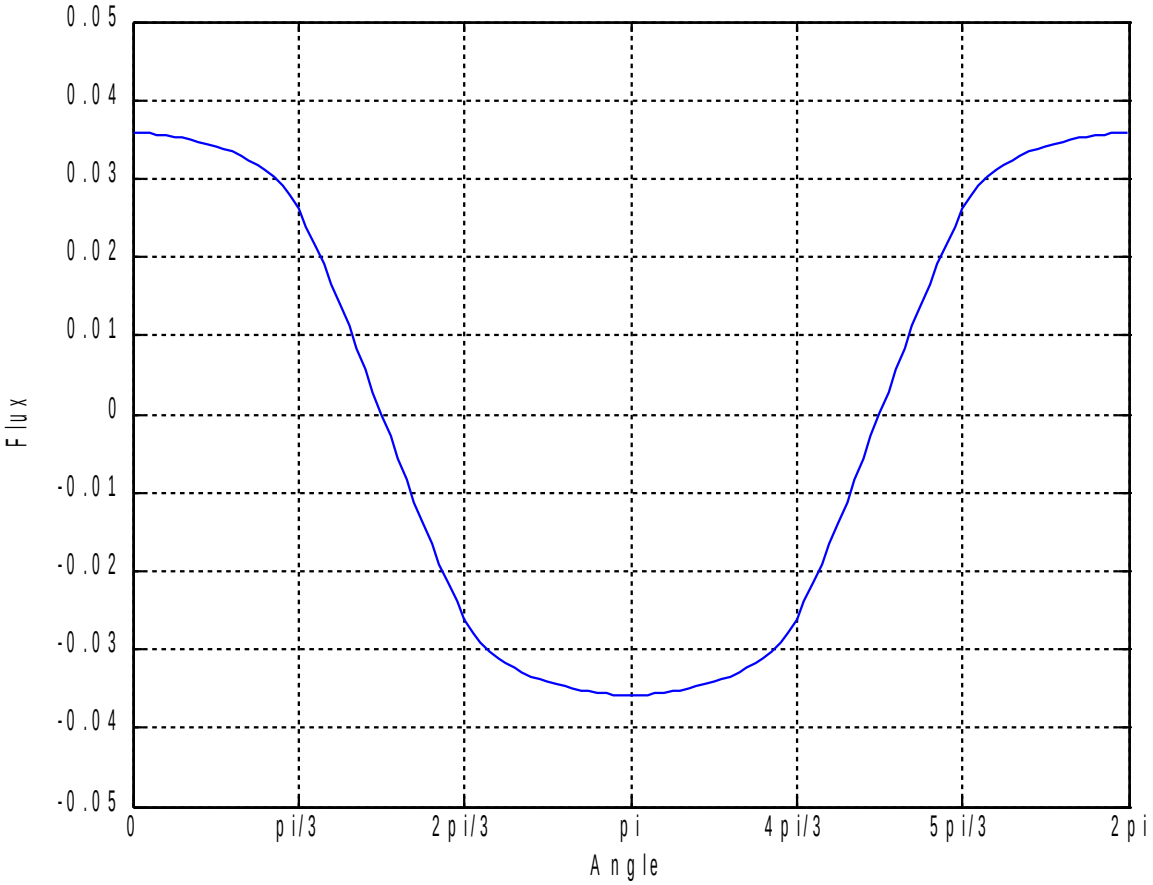

Figure 42

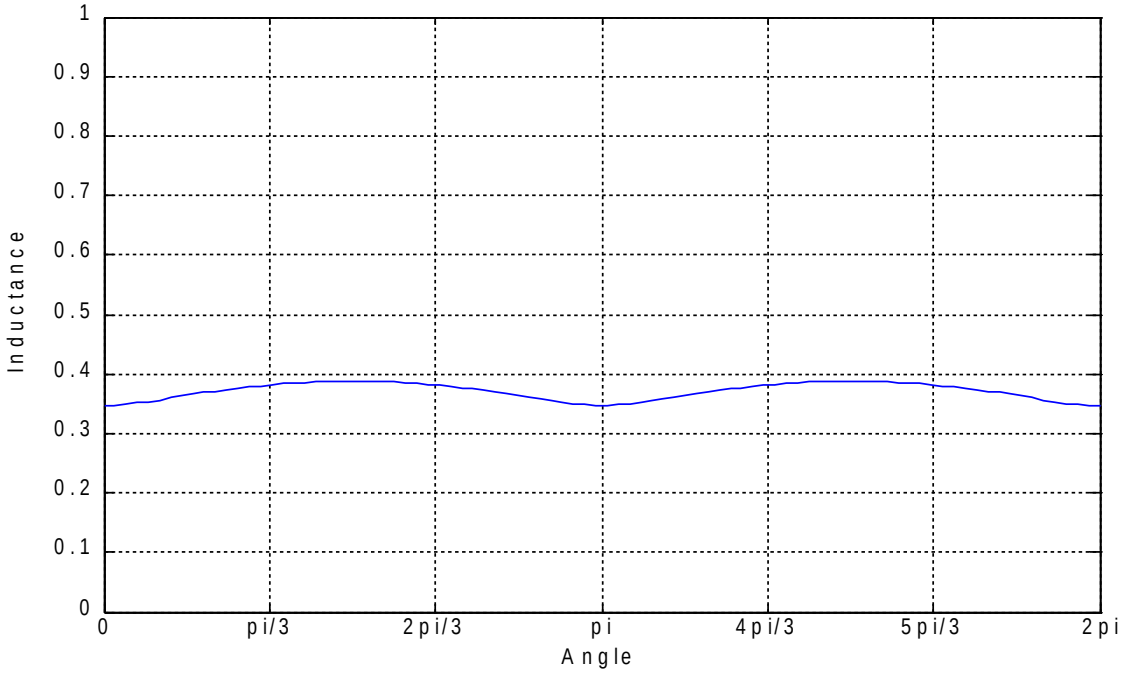

Figure 43

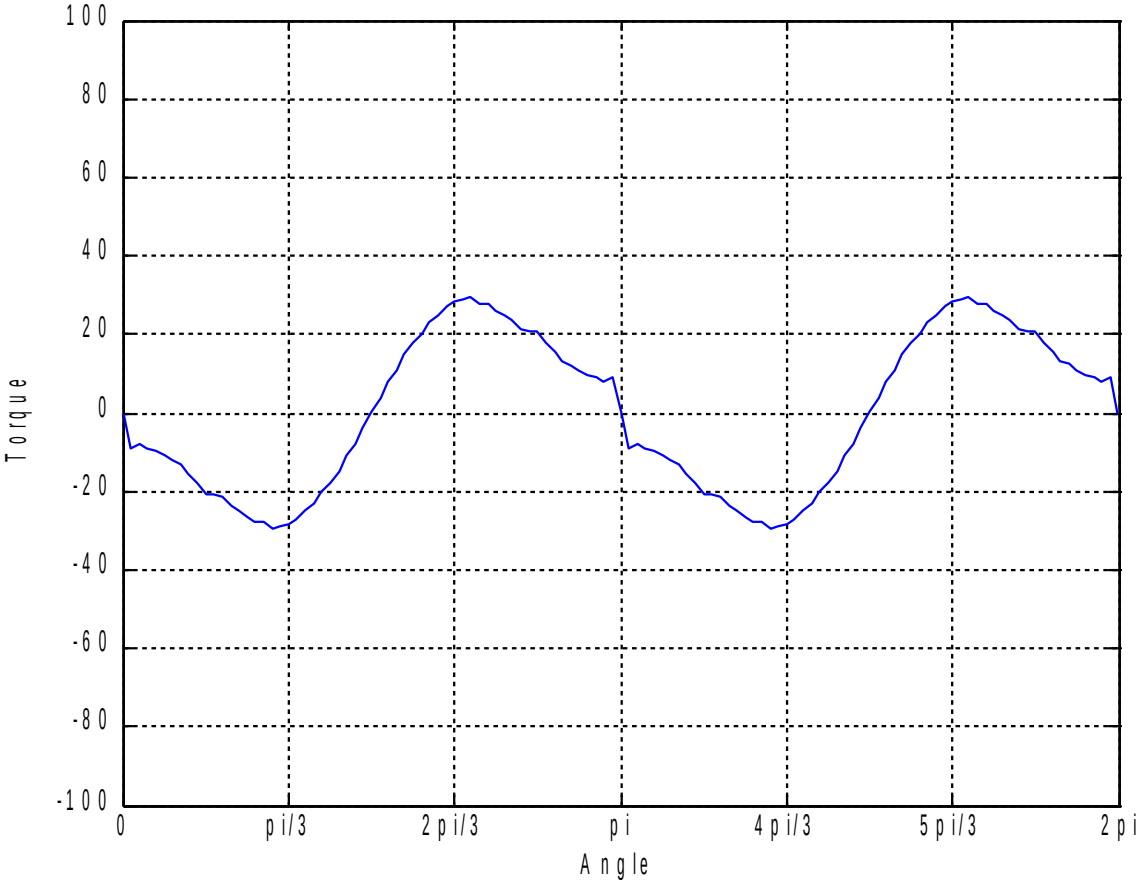

Figure 44

MMF = 3000 At, φ=30°

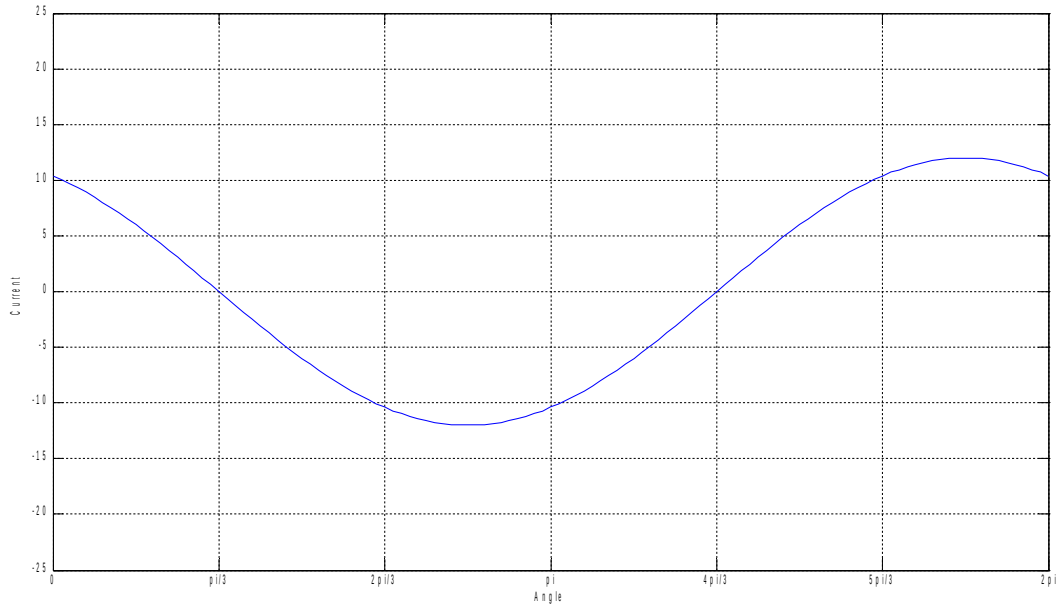

Figure 45

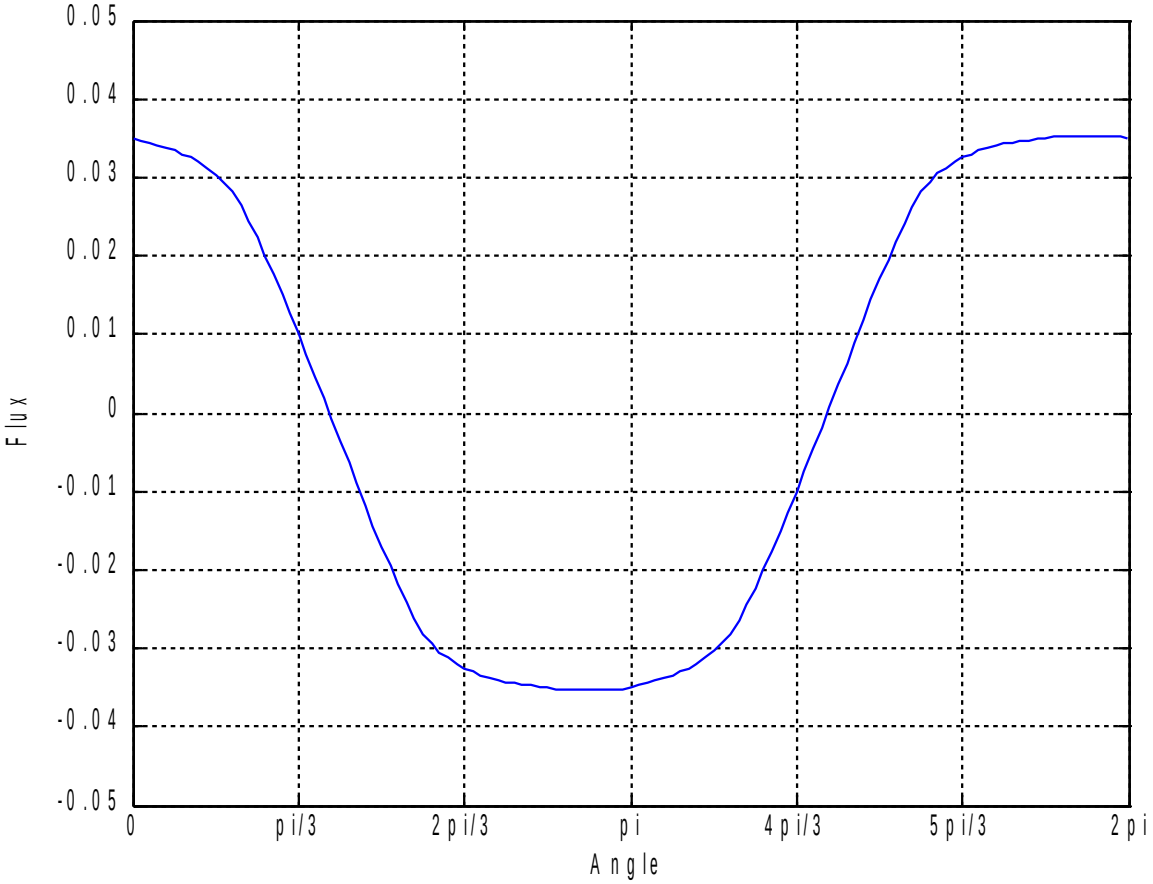

Figure 46

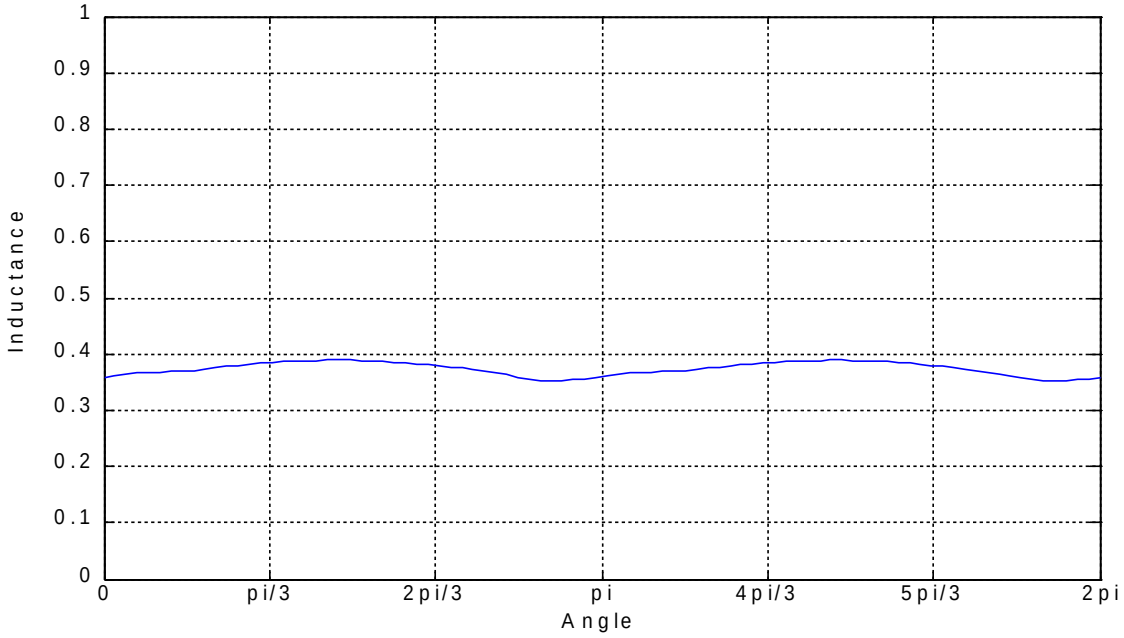

Figure 47

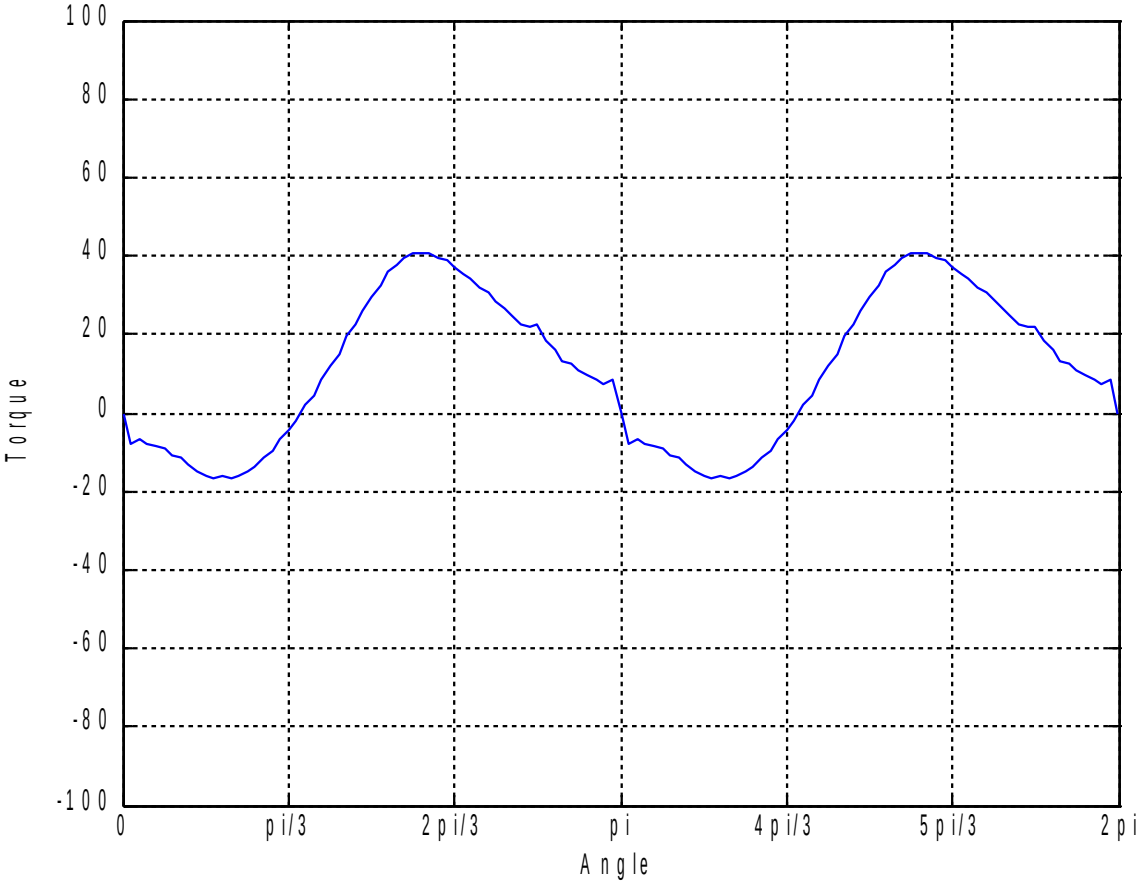

Figure 48

MMF = 3000 At, φ=60°

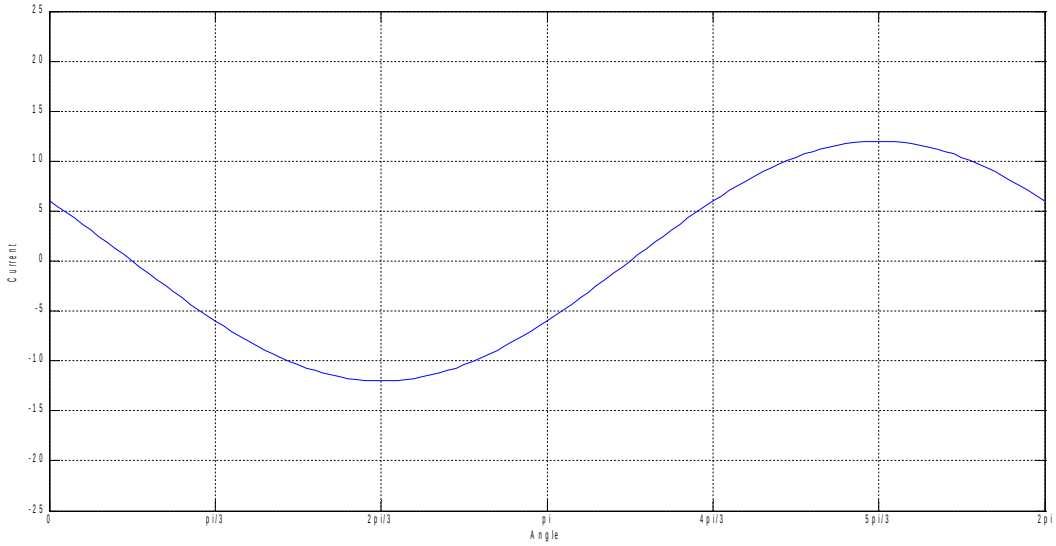

Figure 49

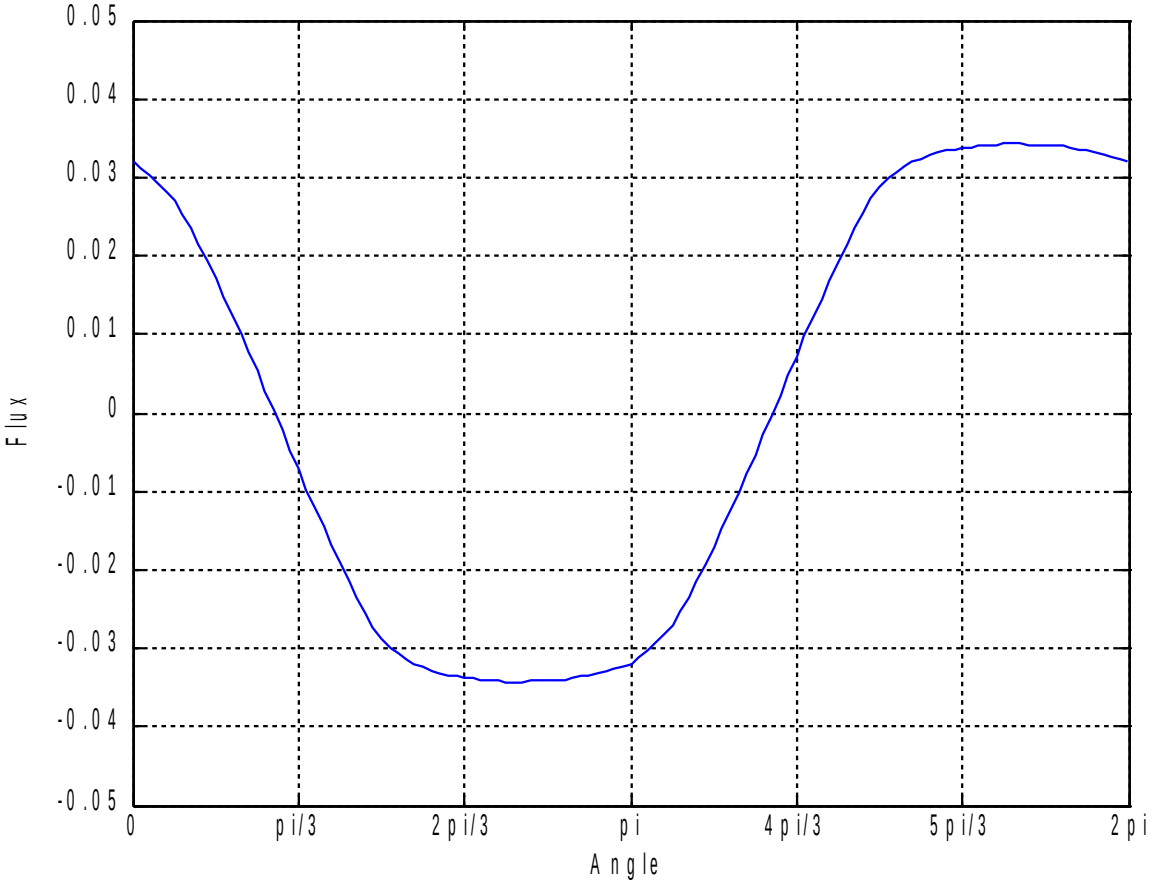

Figure 50

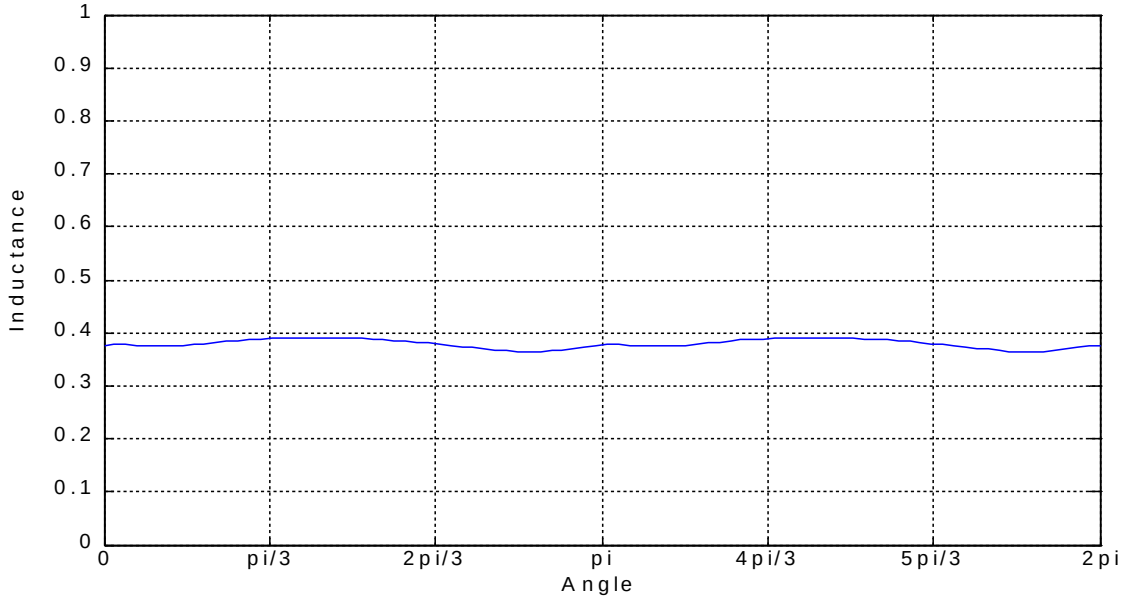

Figure 51

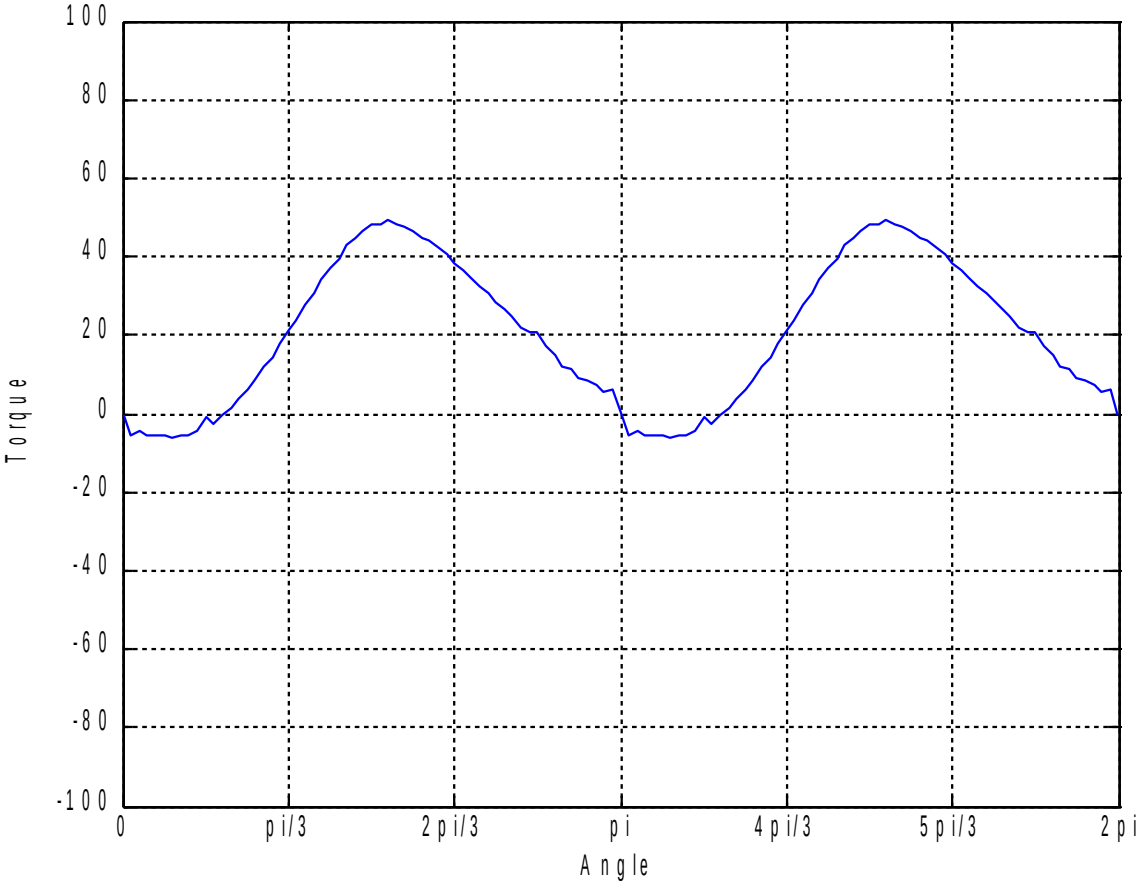

Figure 52

MMF = 3000 At, φ=90°

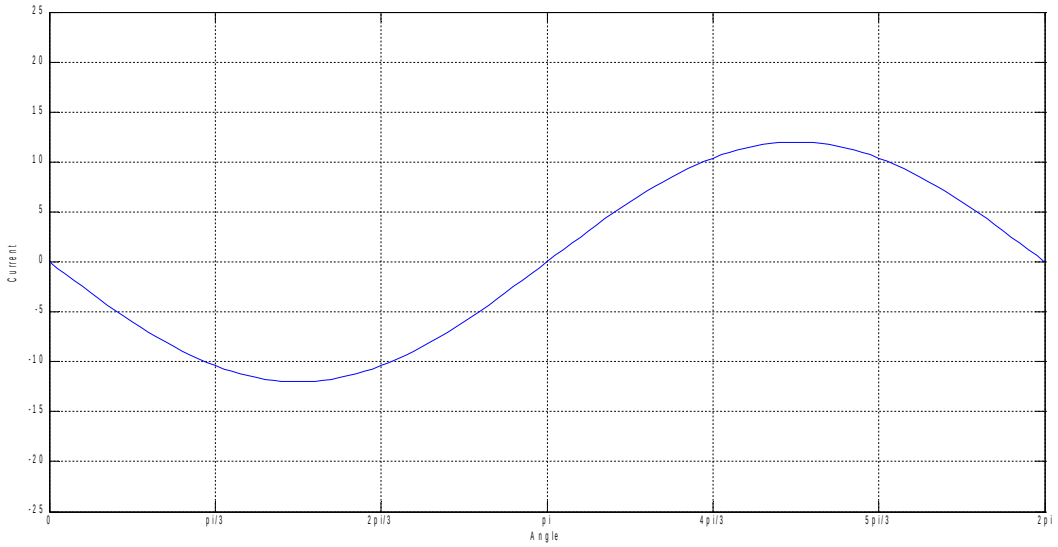

Figure 53

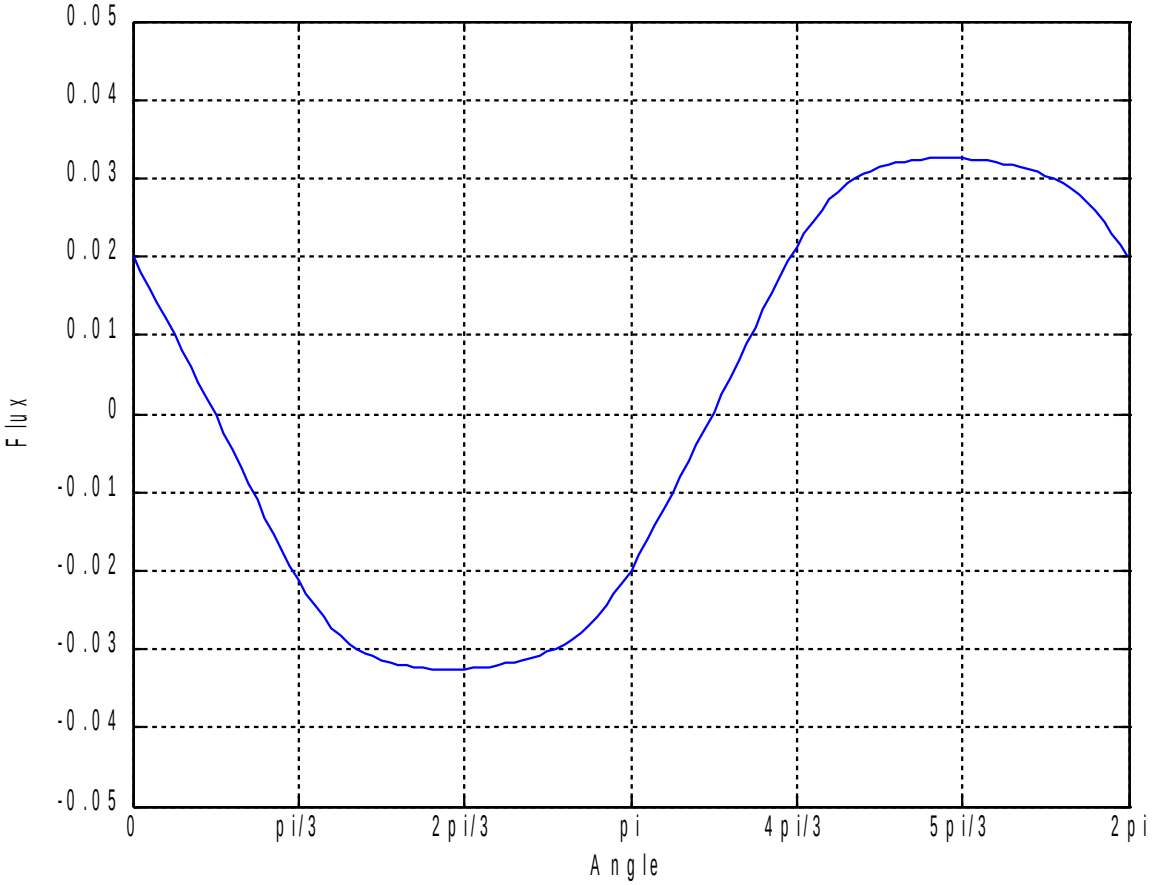

Figure 54

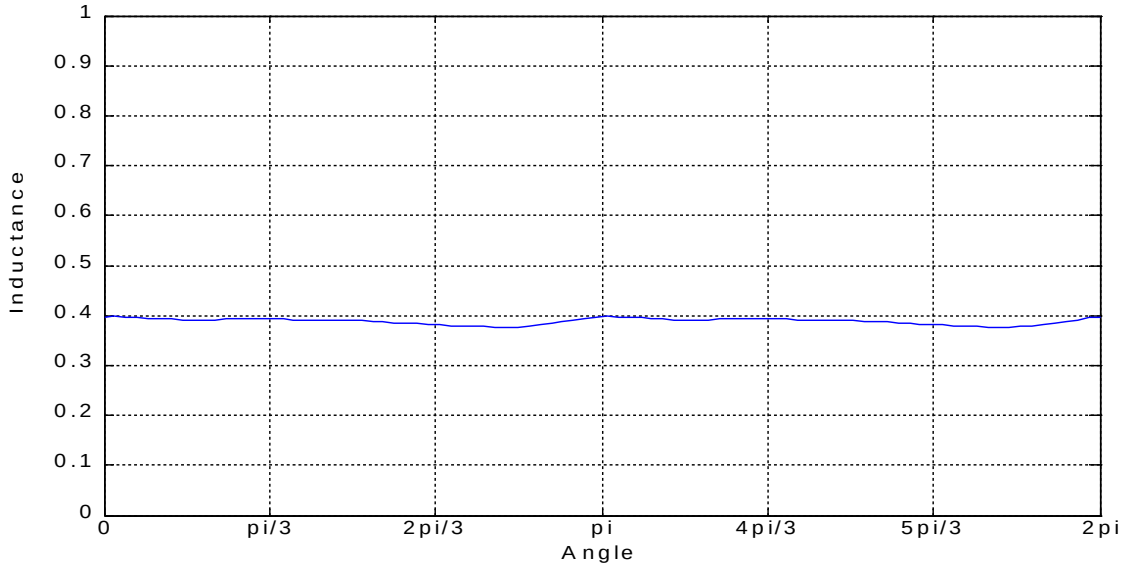

Figure 55

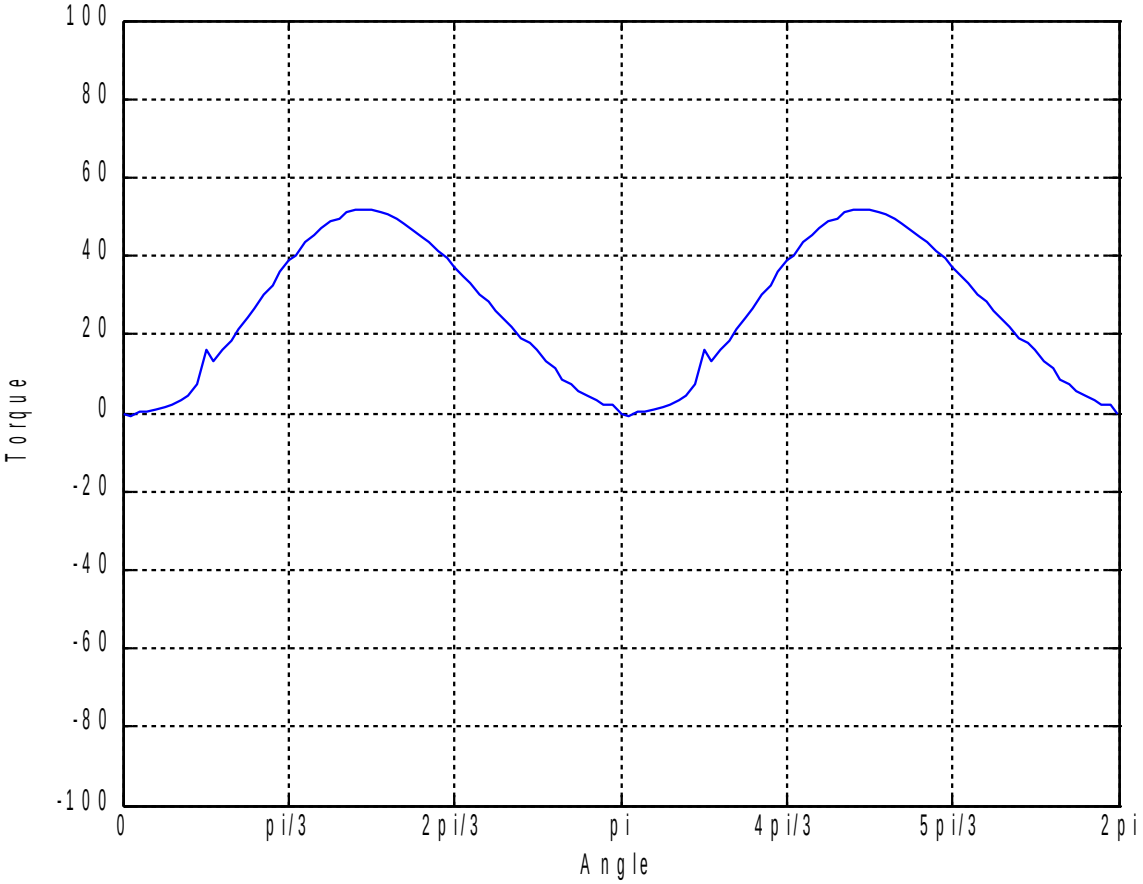

Figure 56

MMF = 4000 At, φ=0°

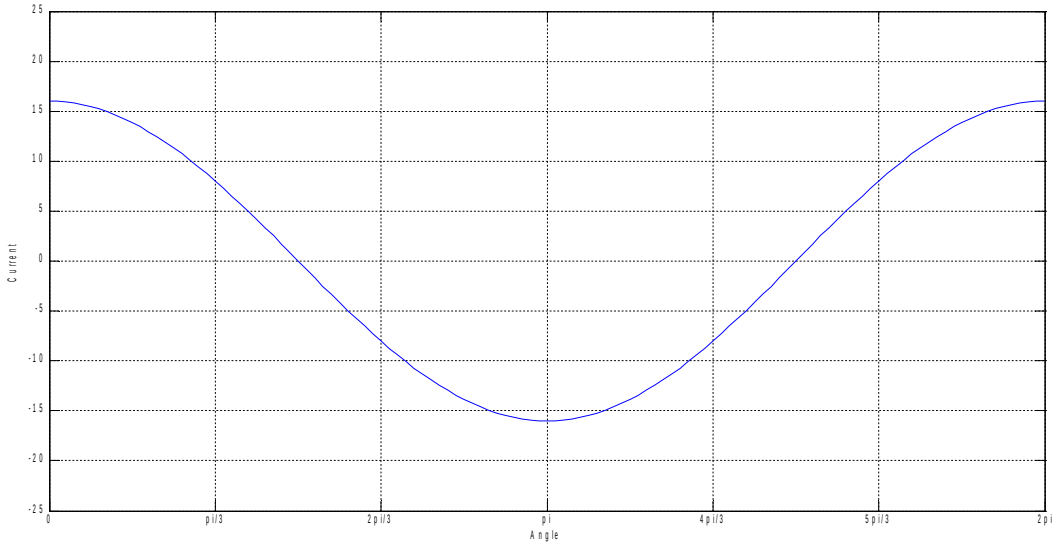

Figure 57

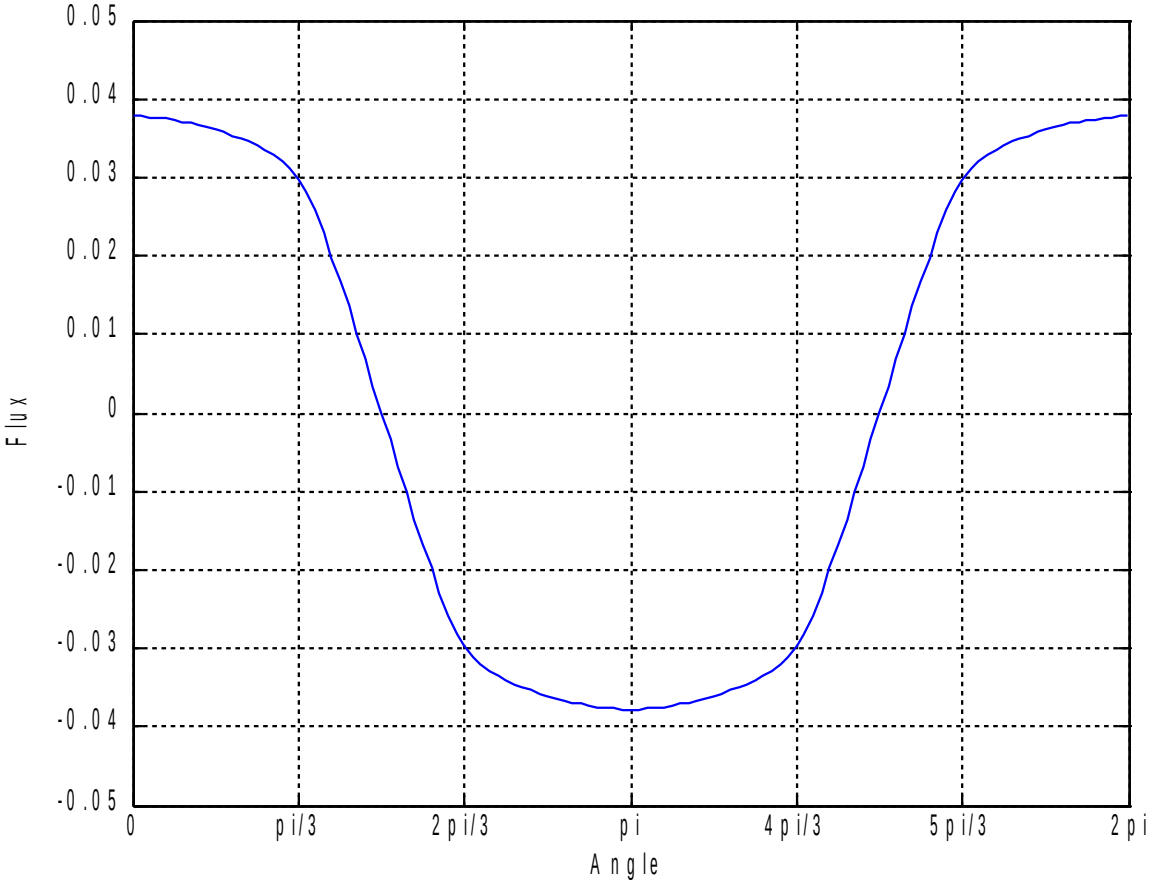

Figure 58

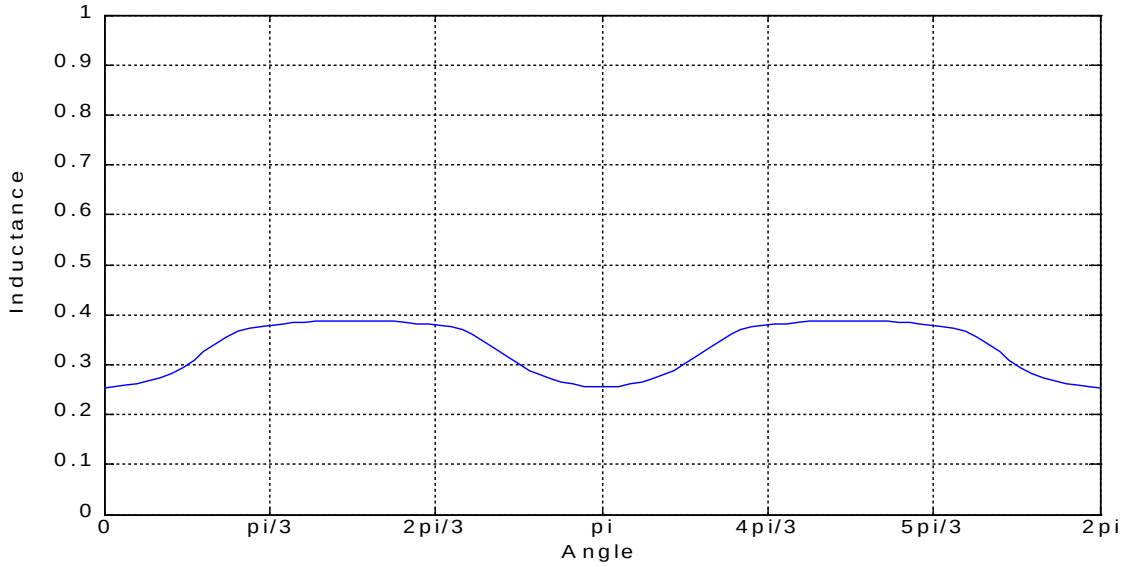

Figure 59

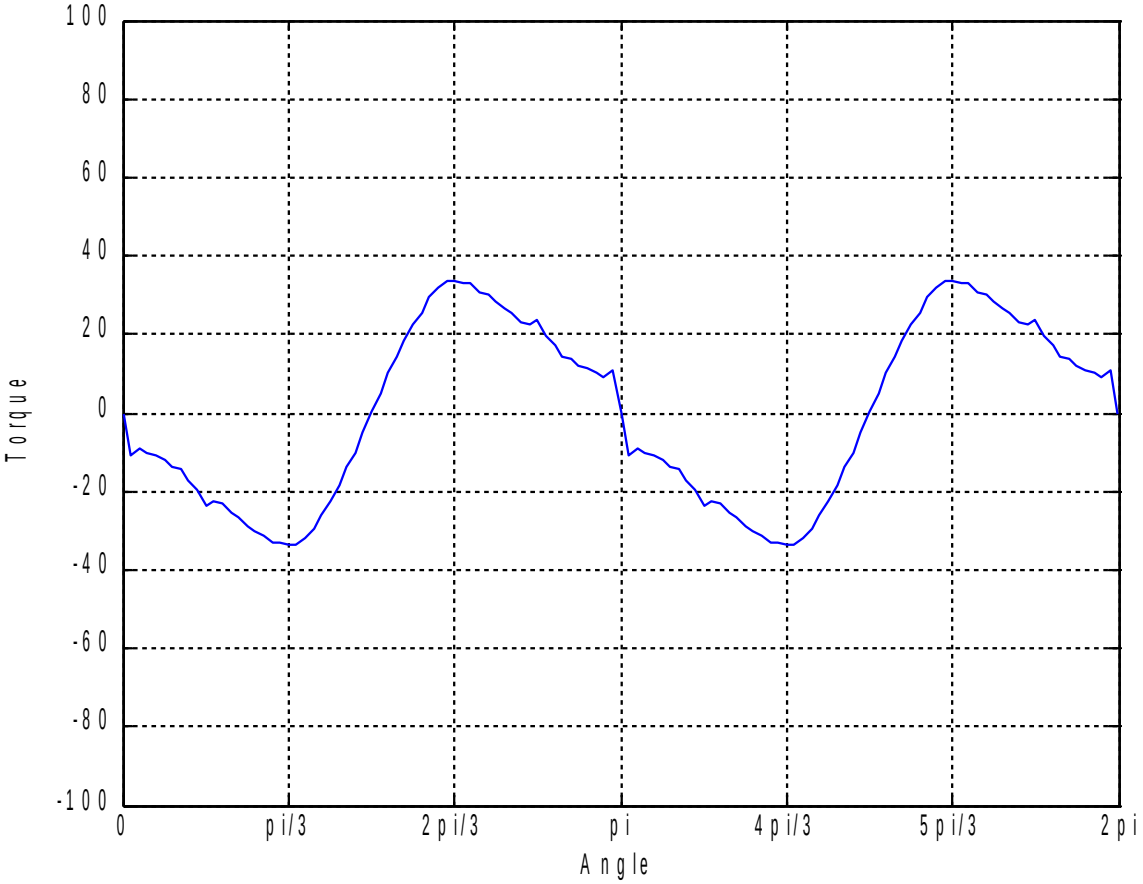

Figure 60

MMF = 4000 At, φ=30°

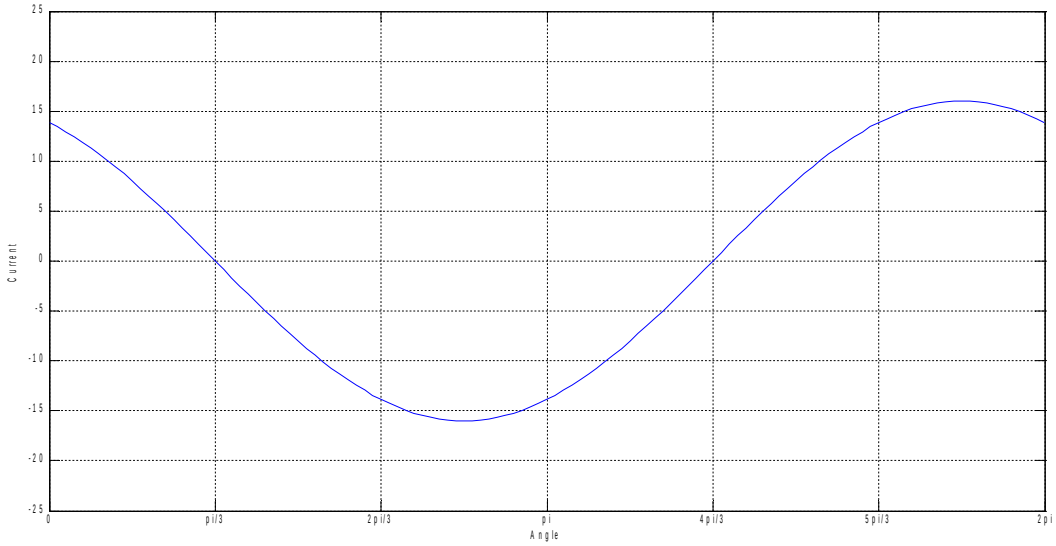

Figure 61

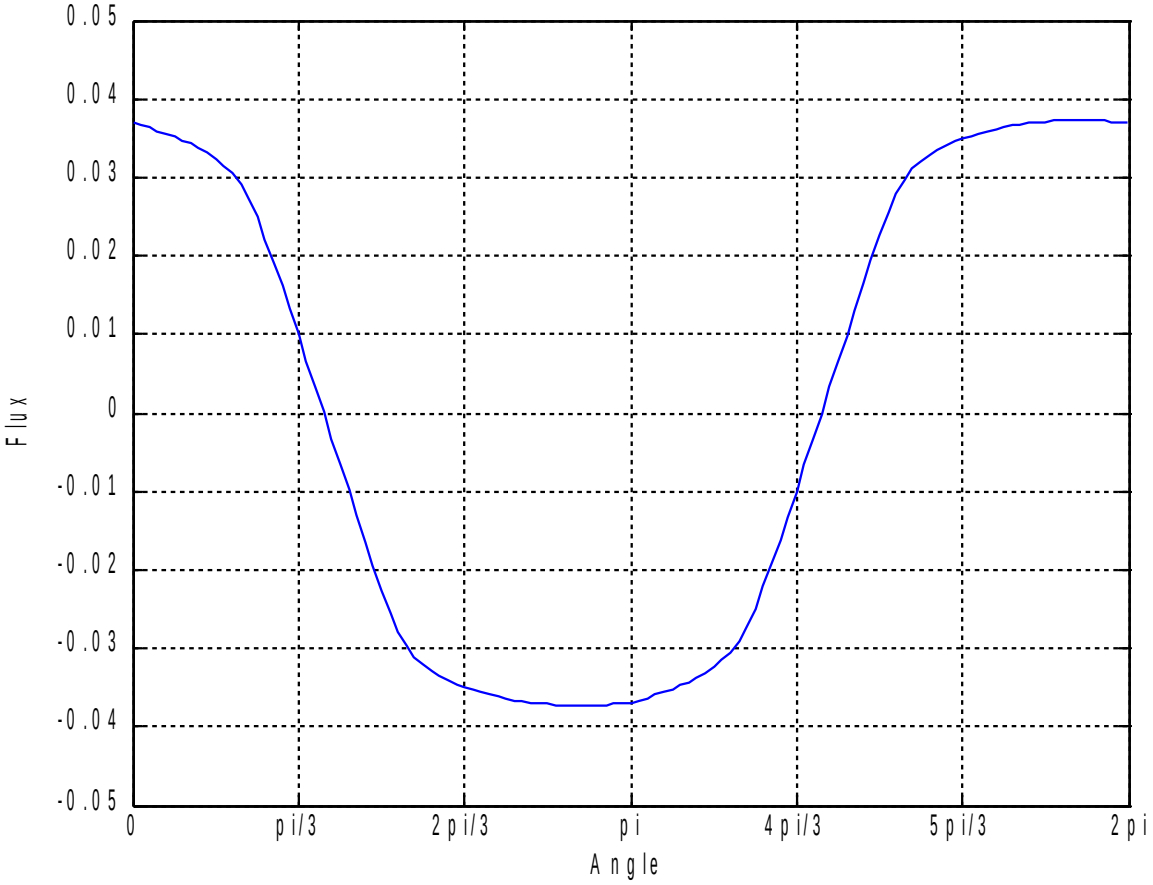

Figure 62

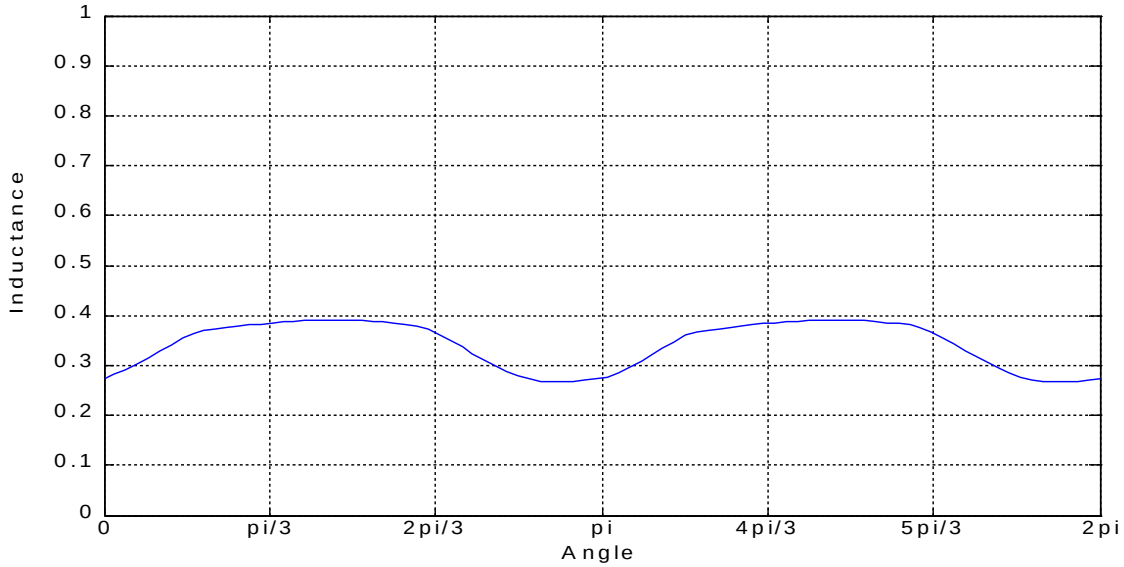

Figure 63

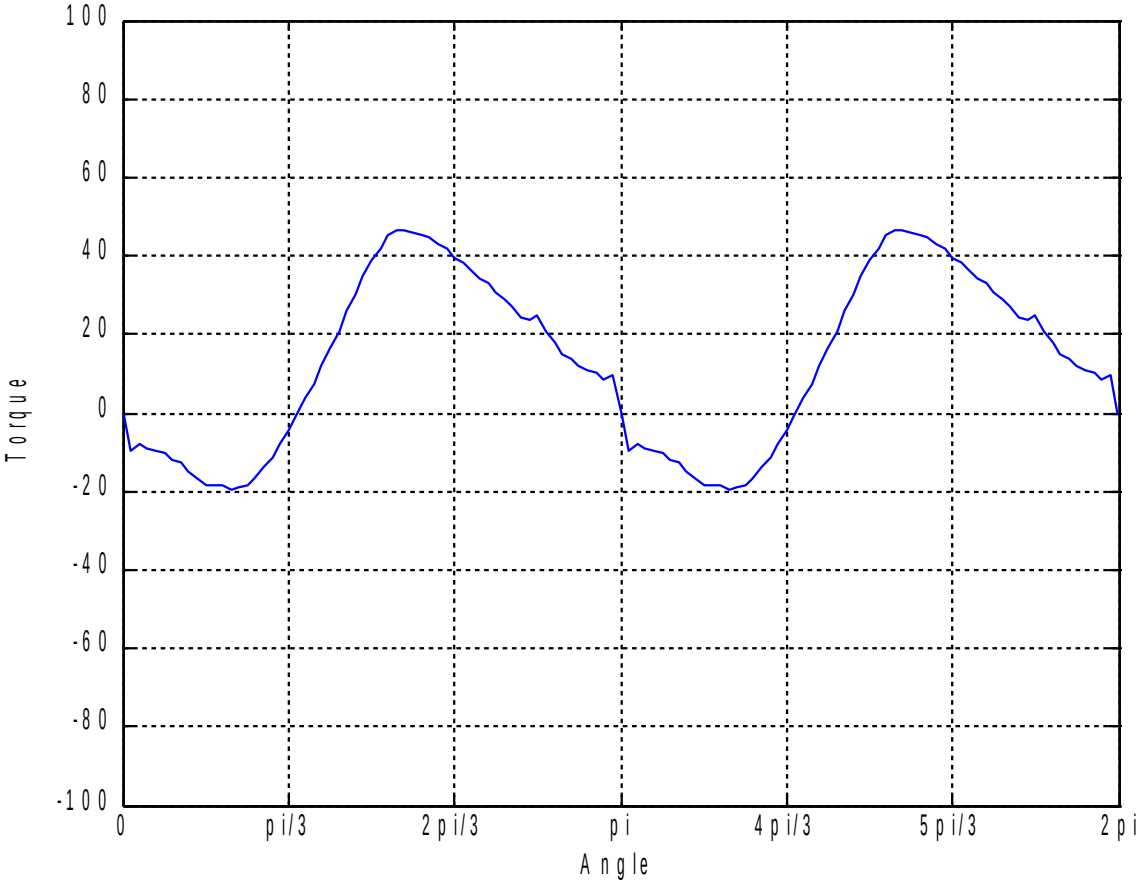

Figure 64

MMF = 4000 At, φ=60°

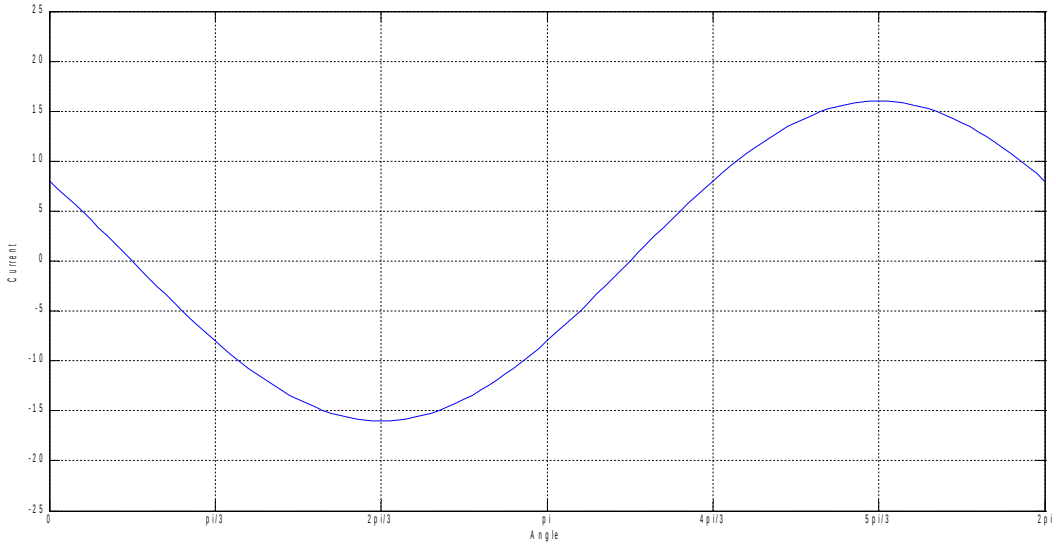

Figure 65

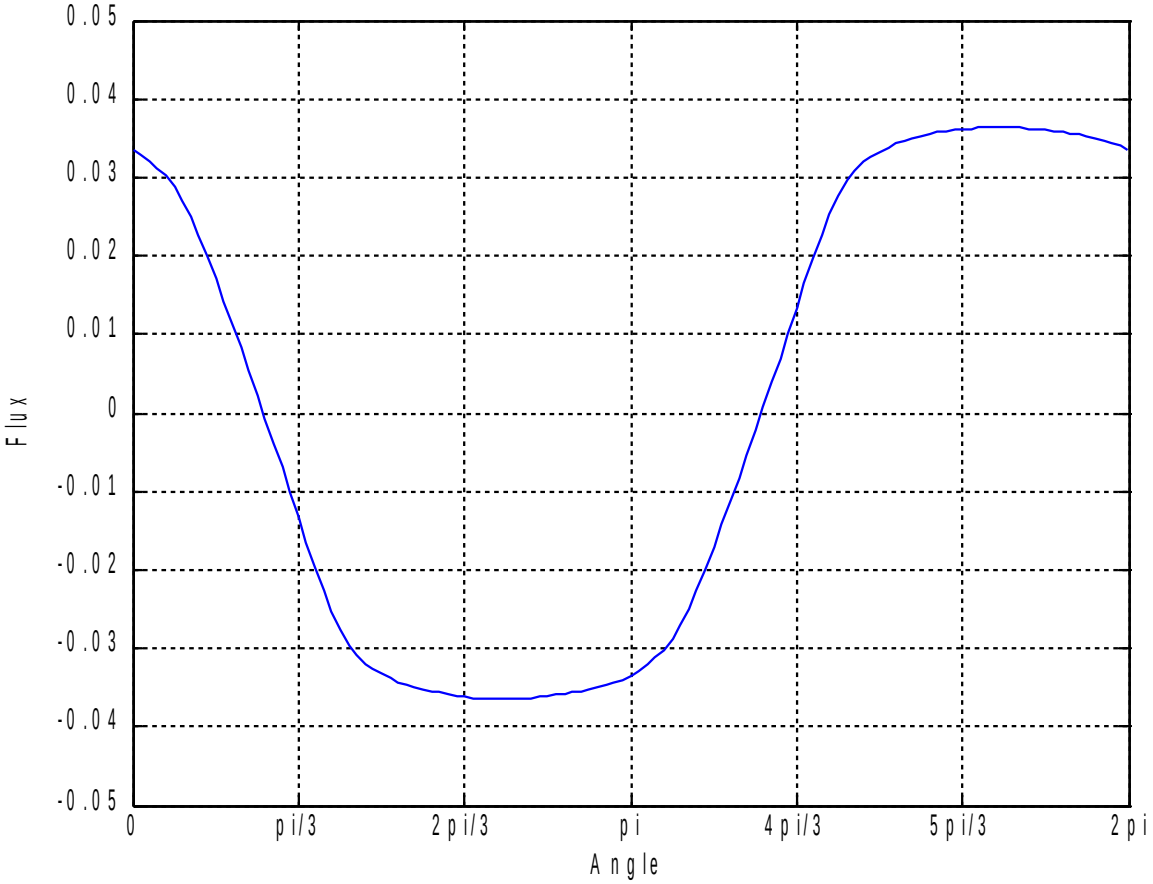

Figure 66

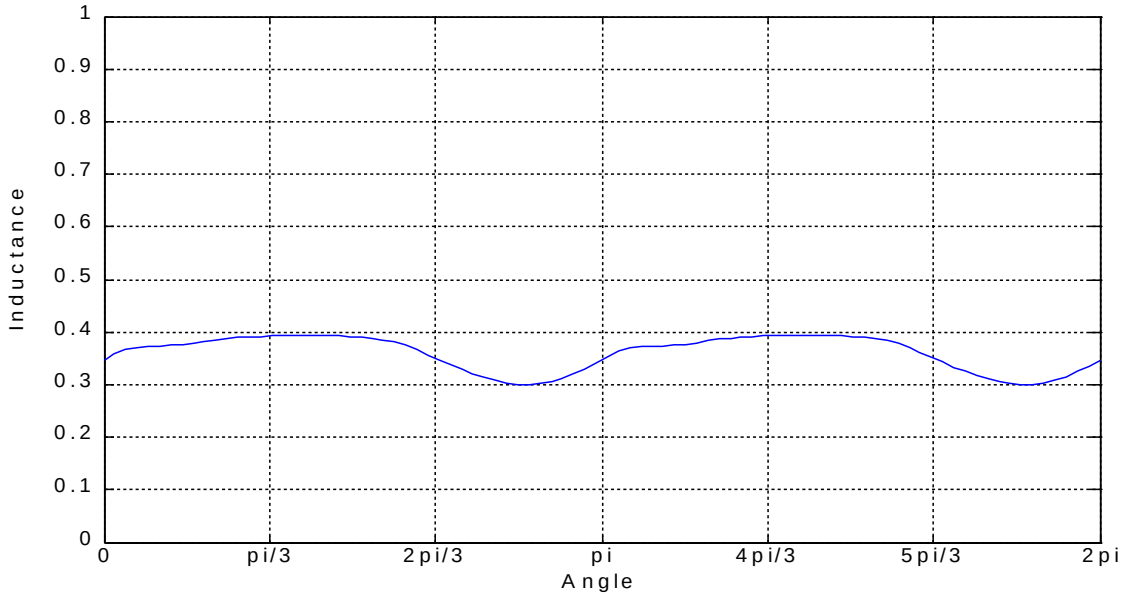

Figure 67

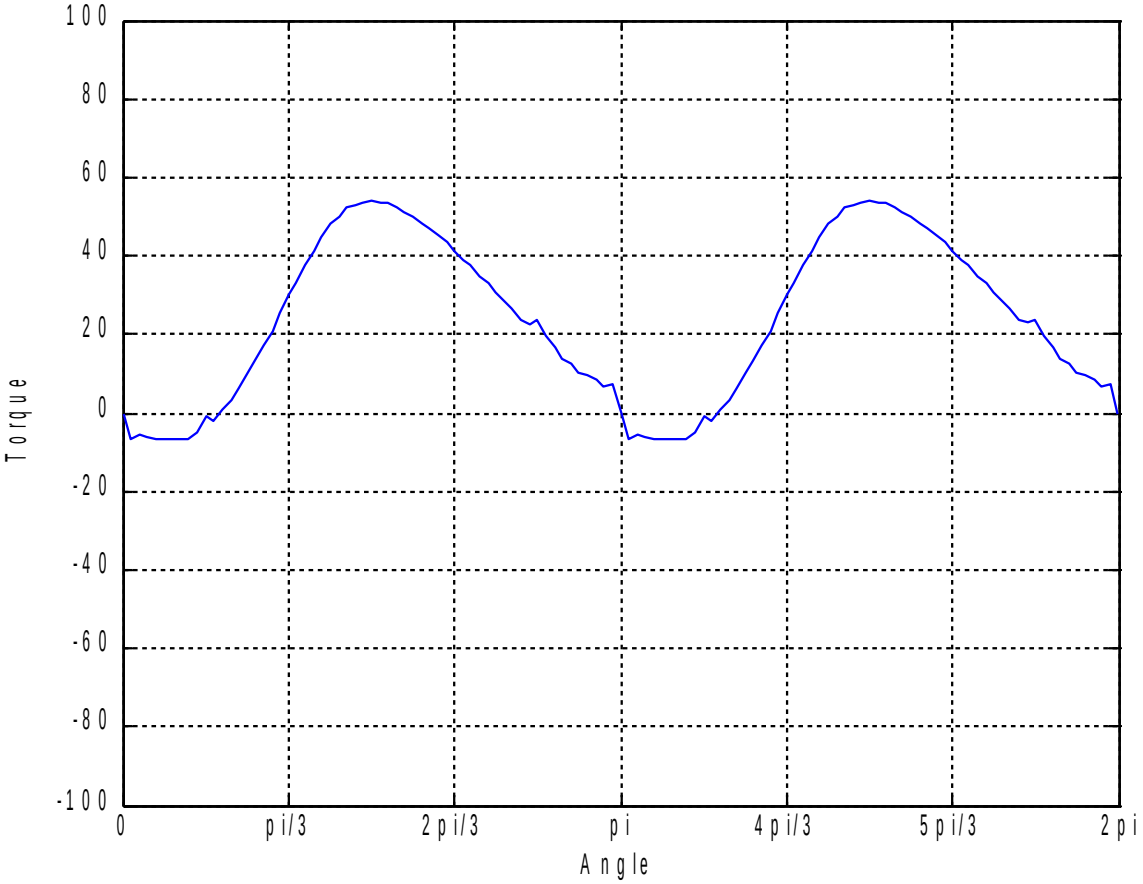

Figure 68

MMF = 4000 At, φ=90°

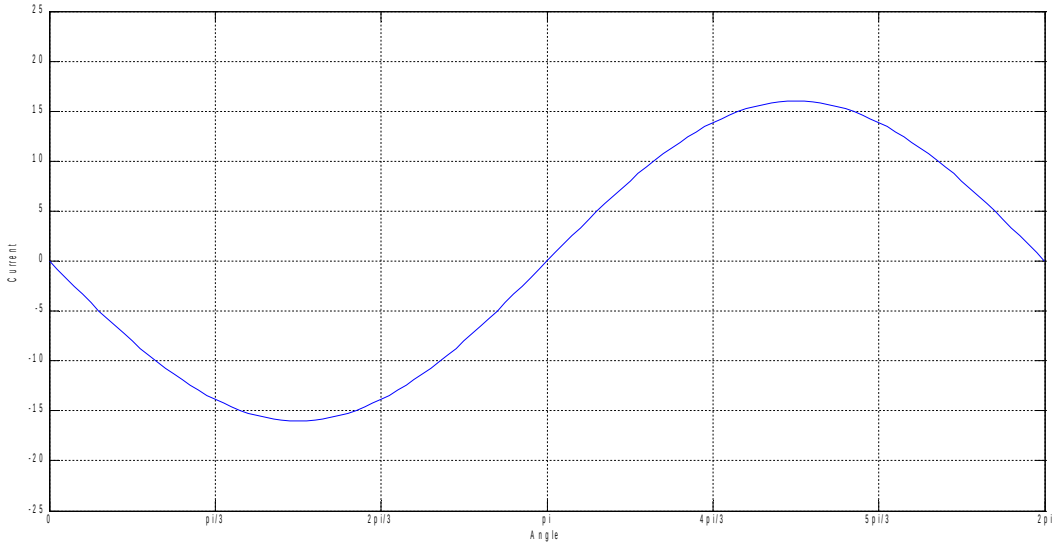

Figure 69

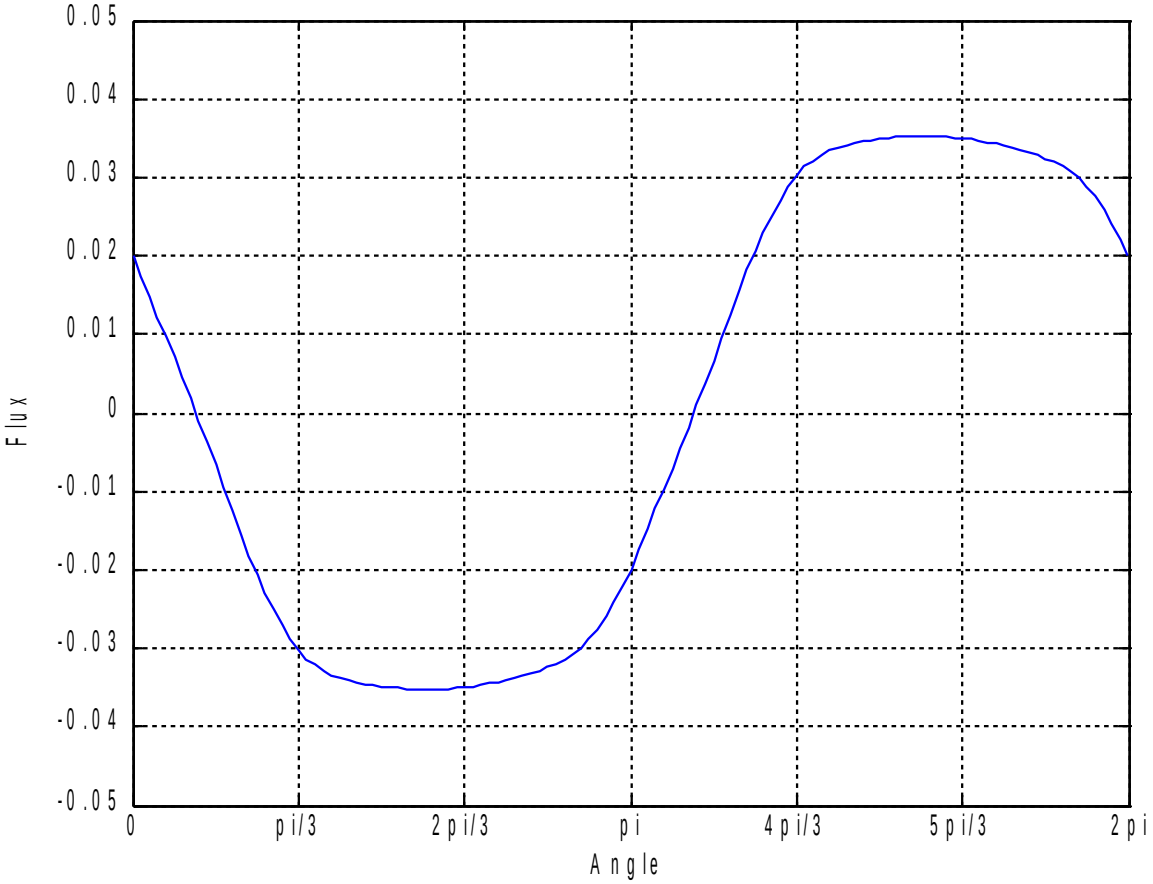

Figure 70

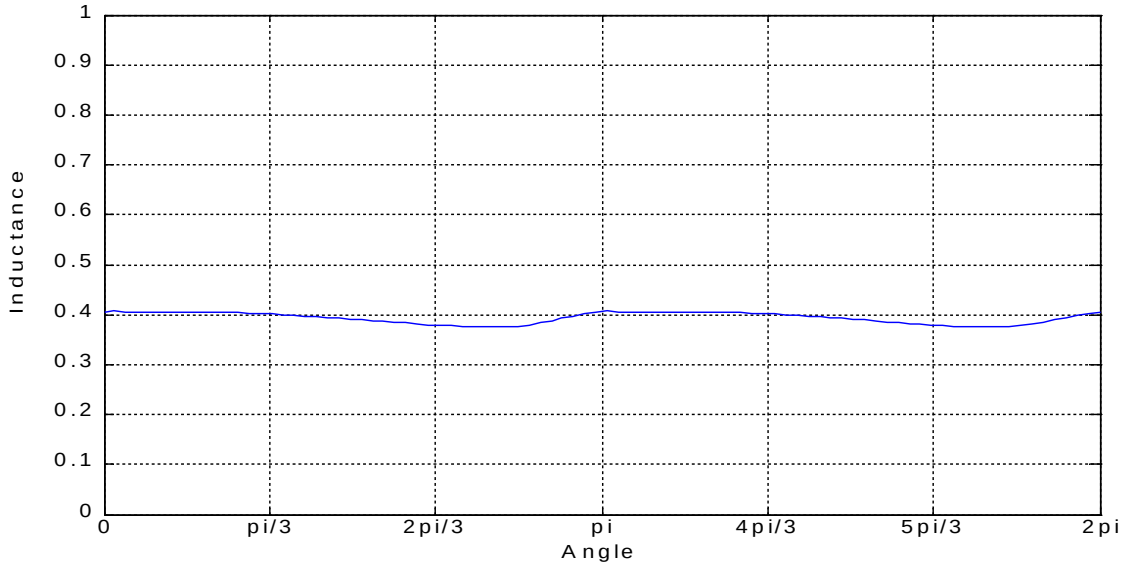

Figure 71

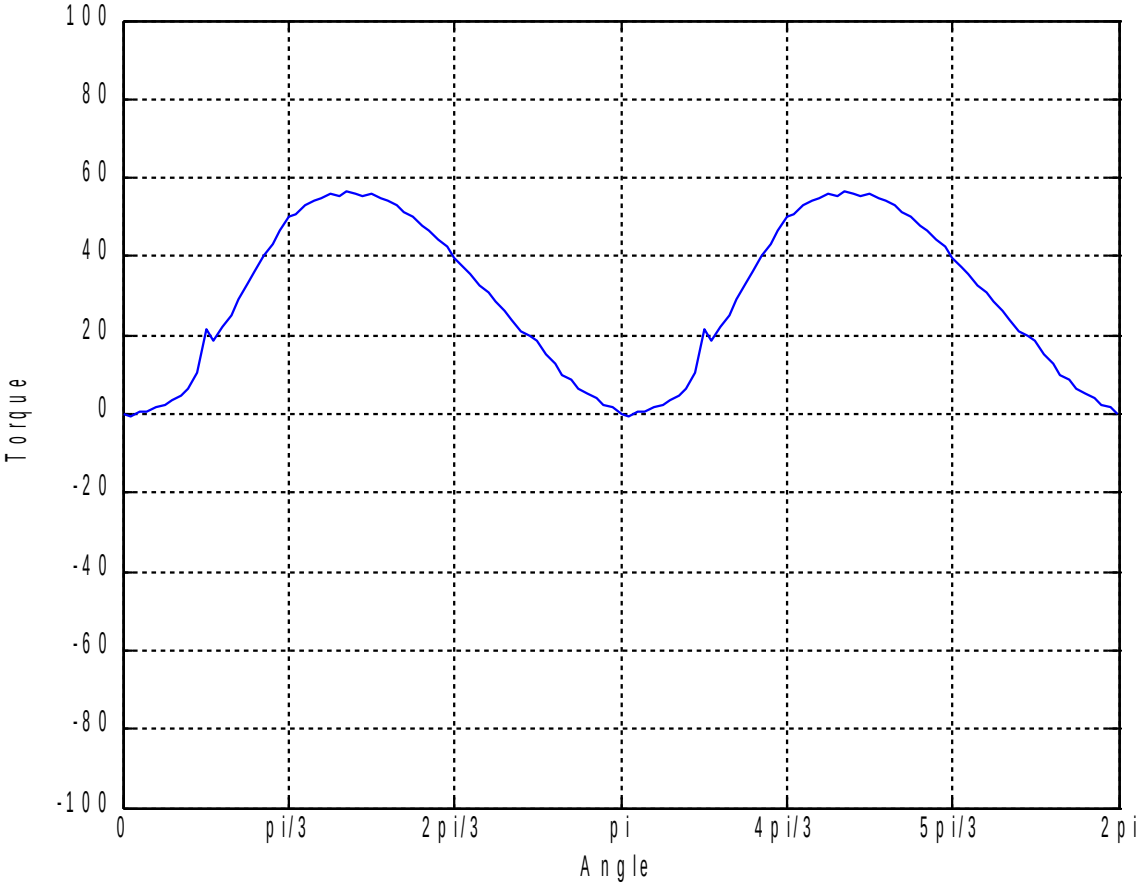
100
80
60
40
20
0
-20
-40
-60
-80
-100
Torque
0
pi/3
2pi/3
pi
4pi/3
5pi/3
2pi
Angle

Figure 72

3. MACHINE WITH 4 POLES

3.1 Model of the machine

Once that the 2-poles machine magnetic analysis is completed, it's possible to make the same thing for a 4-poles machine with the same equivalent structure. The geometrical model is represented in the figure below

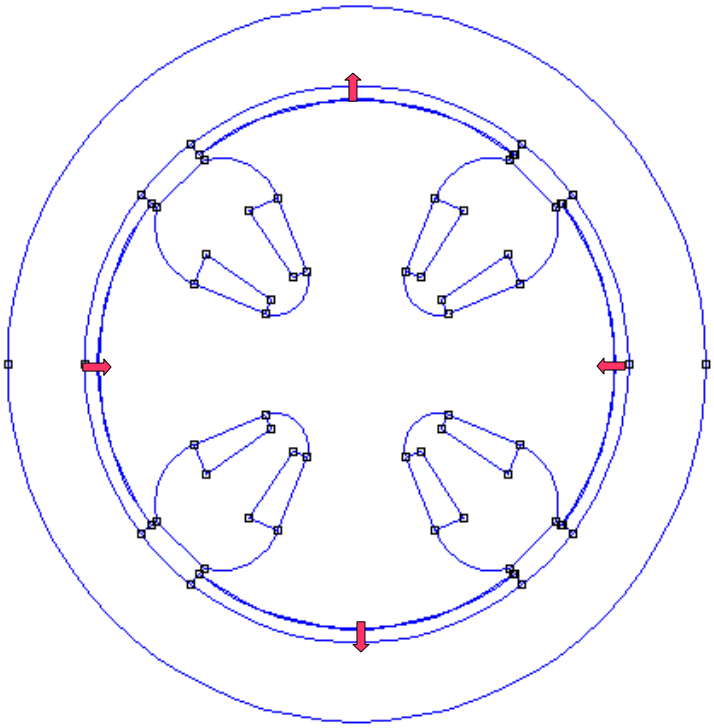

Figure 73

Once again, the first steps of the work is the magnetic calculus, which gives some indications about the behaviour of the machine, which is going to be verified later with the simulating process.
The analysis takes in account several parameters of the machine, in particular its geometry and the characteristics of the magnets.

3.2 Analytic calculus

The first value to calculate is the average magnetic flux density on in the air gap of the machine. To get it, it is necessary to increase the value of the thickness of the gap (only in the mathematical analysis) to consider the effects of the geometry of the caves on the magnetic distribution, by a coefficient called Carter's, which depends by the thickness and by the wideness of them. In this project, Carter's coefficient is estimate to be k_{Car}=1,2. This is kind of a high value, but it seems to fit with the shape of the machine, which have a low number of poles – and so a higher wideness of the caves compared with the whole lateral surface of the internal stator.
This way is possible to get the average magnetic flux density value:

$$B = B_R \frac{1}{1 + \frac{\mu_r g'}{d}}$$

eq. 1

The values involved are:

- B_R = 0,4211 T
- μ_r = 1,43486
- g = 0,0005 m
- g' = k_{Car} g
- d = 0,005 m

In the and, the average B value is equal to 0,359 T.
The value of the flux passing through the magnetic circuit is a function of it following the equation:

$$\Phi_0 = B D \frac{l_{stk}}{p},$$

eq. 2

which gives a value of the flux, when the machine is in the aligned position, of 0,0107 Wb.

In this case the winding is coupled with four arms, so the analysis will have to take in account the equivalent inductance of the system. As for the 2-poles model, there is an inner stator with concentrated windings and an outer rotor with Permanent Magnets mounted on the internal surface. The orientation of the magnetic field given by the PMs is the one shown in Figure 15.
The rotation of the rotor makes the flux induced in the internal part of the magnetic circuit change, producing at the terminals of the windings an electromotive force, that is the output of the system.
The geometrical definitions and the hypothesis about the magnetic behaviour of the machine are just like the ones made for the 2-poles machine.
Once again, it is assumed that the magnetic characteristics and the geometrical shapes of the magnets are the same for all the P Ms, so the flux produced by them is identical

$$\Phi_{m1} = \Phi_{m2} = \Phi_{m3} = \Phi_{m4} = \Phi_m$$

eq. 25

Because of the magnetic flux conservation, it can be assumed that the flux passing through each arm of the inner stator and in the air gap are the same as well:

$$\Phi_{m1} = \Phi_{g1} = \Phi_1 = \Phi_2 = \Phi_3 = \Phi_4$$

eq. 26

From now on, the analytic calculus of the flux 1 will be considered; the magnets-due flux evolution in time $\Phi_{0(t)}$ is given by

$$\Phi_{0(t)} = \vartheta_{(t)} \Phi_M \ ,$$

eq. 10

If $S_{(t)}$ is the surface on which we have the superposition of the permanent magnets with the inner stator, this surface depends on time by the law

$$S_{(t)} = \vartheta_{(t)} rl \ ,$$

eq. 11

having defined $\vartheta_{(t)}$ as the angle of superposition. If the rotational speed is imposed at a value ω_r, constant, we have a dependence of ϑ by time, as shown by its evolution (Figure 16)

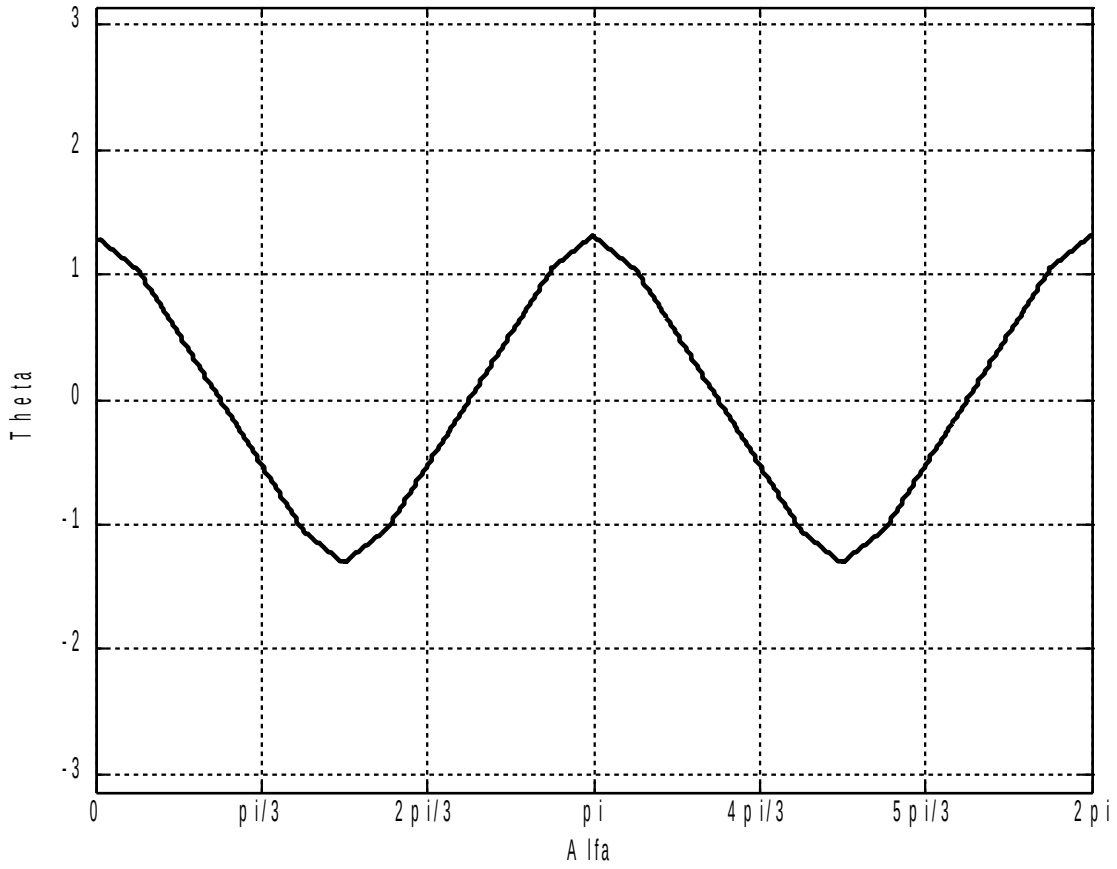

Figure 74

The wideness of the magnets has been chosen equal to

$$\beta = \frac{5\pi}{12} \ .$$

This variation of the superposition angle between the two iron-made surfaces makes the magnetic

reluctance of the air gap change as well. This will generate the variation of the coupled flux inducing the emf at the terminals of the windings.
The purpose now is to calculate the flux flowing through the arm 1 of the stator, the one coupled with winding 1. This flux, in the hypothesis of linearity – valid for low values of current, and in particular for the no-load analysis – is given by the sum of the fluxes originated by the magnets and the current.
It is possible to write the equation (Ampere's law):

$$6\,N\,i_{(t)} = \int H\,dl = R_{TOT(t)}\,\Phi_{(t)}$$

eq. 27

from which it is possible to extract the values of the magnetic flux due to the current, which, summed with the magnets-due, gives the total one:

$$\Phi_{(t)} = \frac{3\,N\,i_{(t)}}{2\,R_{(t)}} + \Phi_{0(t)}\,,$$

eq. 28

The total reluctance opposed by the machine to the flux is given by the product of the reluctance on each arm of the inner stator times the number of them.
This is the plot of one of these reluctances:

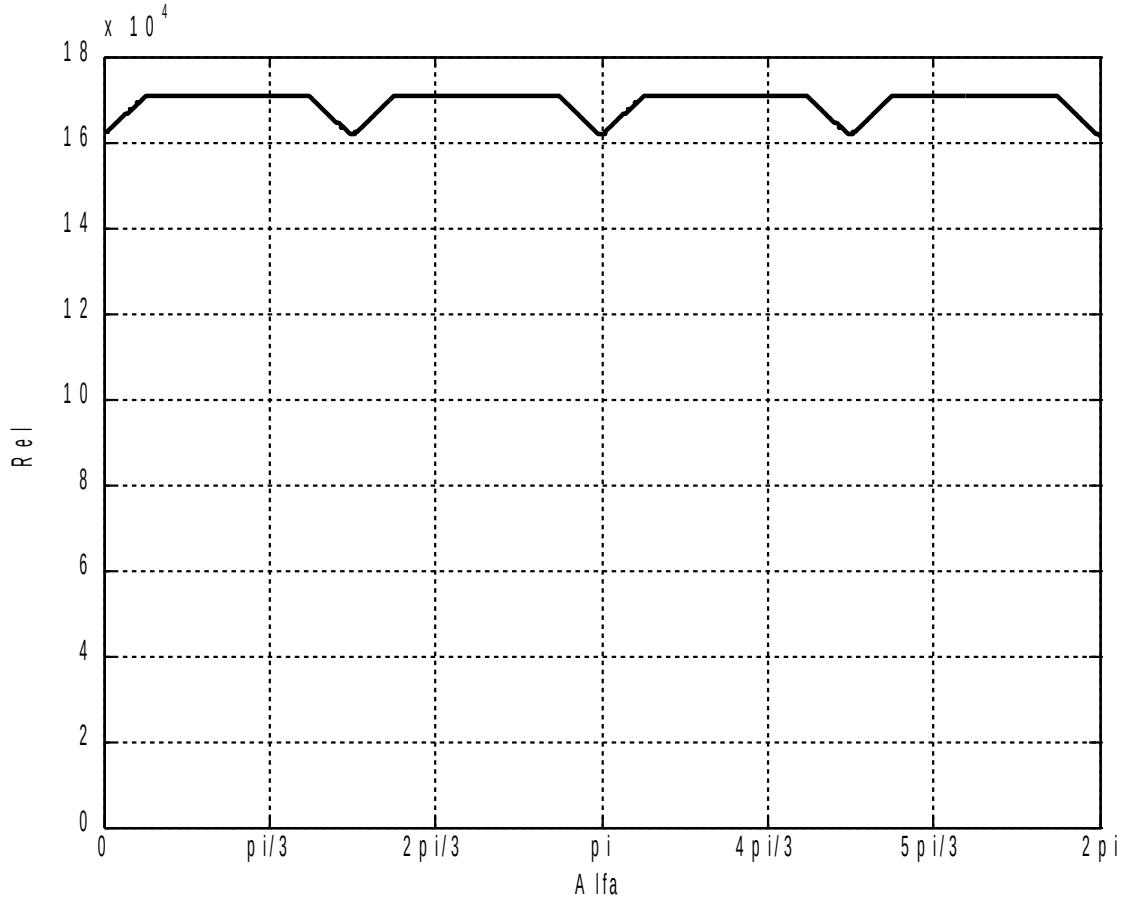

Figure 75

As it can be seen, the reluctance in this case is the half of the one with 2 poles: this is because of the half wideness of the useful path for the flux.

It is possible to plot the evolution valid for the flux passing through arm 1:

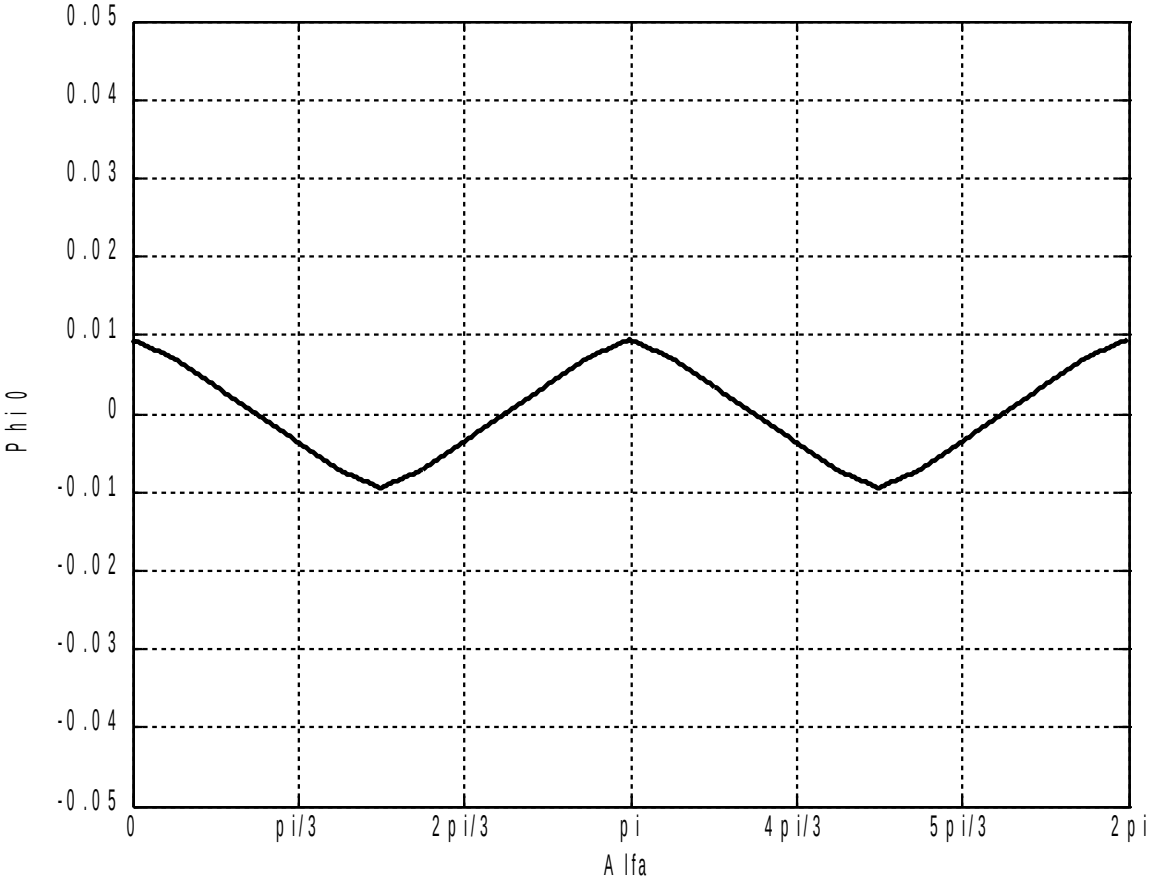

Figure 76

Now it's easy to get the formulation of the coupled flux:

$$\lambda_{(t)} = N\Phi_{(t)} = \frac{3N^2 i_{(t)} + 2N\vartheta_{(t)}\Phi_M}{2R_{(t)}}$$

eqs. 28

These formulations can be re-written in another way

$$\lambda_{(t)} = L_{(t)} i_{(t)} + \lambda_{0(t)}$$

eqs. 29

Proceeding as did for the 2-poles machine, the first electric values to be calculated are the no-load electromotive forces at the terminals of the windings. They are given by the derivative by respect to time of the coupled fluxes, but having previously imposed the no-load condition.

This way the value of $e_{0(t)}$ can be calculated

$$e_{0(t)}=\frac{d\lambda_{01}}{dt}=-\frac{d}{dt}\left(\frac{N\vartheta_{(t)}\Phi_M}{R_{(t)}}\right);$$

eq. 30

The result of the derivative gives

$$e_{0(t)}=-\frac{N\Phi_M}{2R_{(t)}^2}\left(\frac{d\vartheta_{(t)}}{dt}R_{(t)}-\frac{dR_{(t)}}{dt}\vartheta_{(t)}\right).$$

eq. 31

it is possible to see that the resulting formula (for number of spires) is exactly the same found for the previously analysed machine. This is also true for the no-load condition flux, as it can be seen

The Figure 20 shows the evolution in time of the electromotive force per spire:

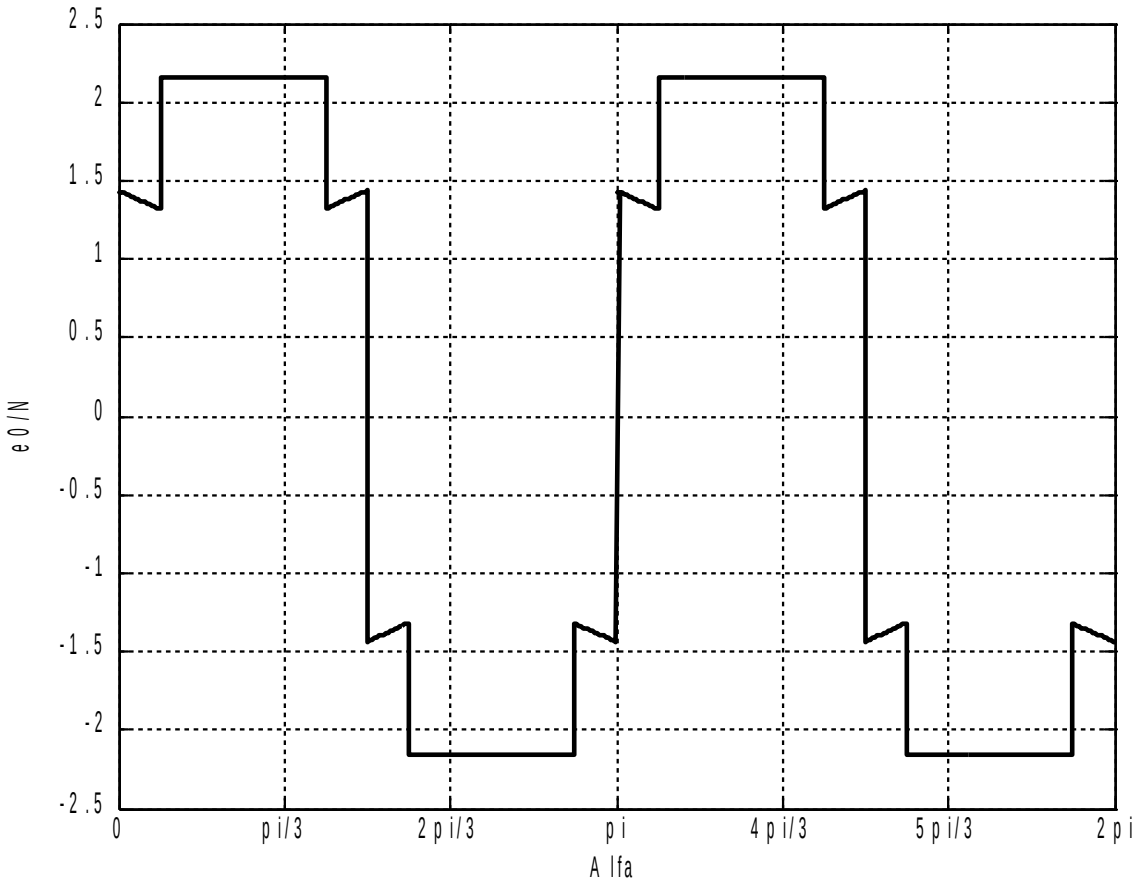

Figure 77

Also in this case, the emf found is the half of the previous one.

In order to calculate the expression of the magnetic torque it is necessary to find the one of the magnetic coenergy; in this case, it is given by the sum of the four values of coenergy given by the four windings.

$$W'_m = W'_{m1} + W'_{m2} + W'_{m3} + W'_{m4} \quad .$$

eq. 32

That is to say

$$W'_m = \int_{i_{01}}^{i_1} \lambda_1 di + \int_{i_{02}}^{i_2} \lambda_2 di + \int_{i_{03}}^{i_3} \lambda_3 di + \int_{i_{04}}^{i_4} \lambda_4 di \ ,$$

eq. 33

where the i_{0j} are the currents needed to de-magnetize the system by one of the windings when in the others doesn't flow any current. As the expression of the flux is the one got before,
it is possible to obtain the expressions of i_0

$$i_0 = \frac{-\Phi_M R}{N} \ .$$

eq. 34

As said before, coenergy cannot be computed analytically, because of the non-linear behaviour of the system.
Hence, the most powerful tool to use is the FEMM analysis.

3.3 FEMM Simulation

As did for the 2-poles machine, the behaviour of the 4-poles one has been simulated with a finite elements software.
This is the model used:

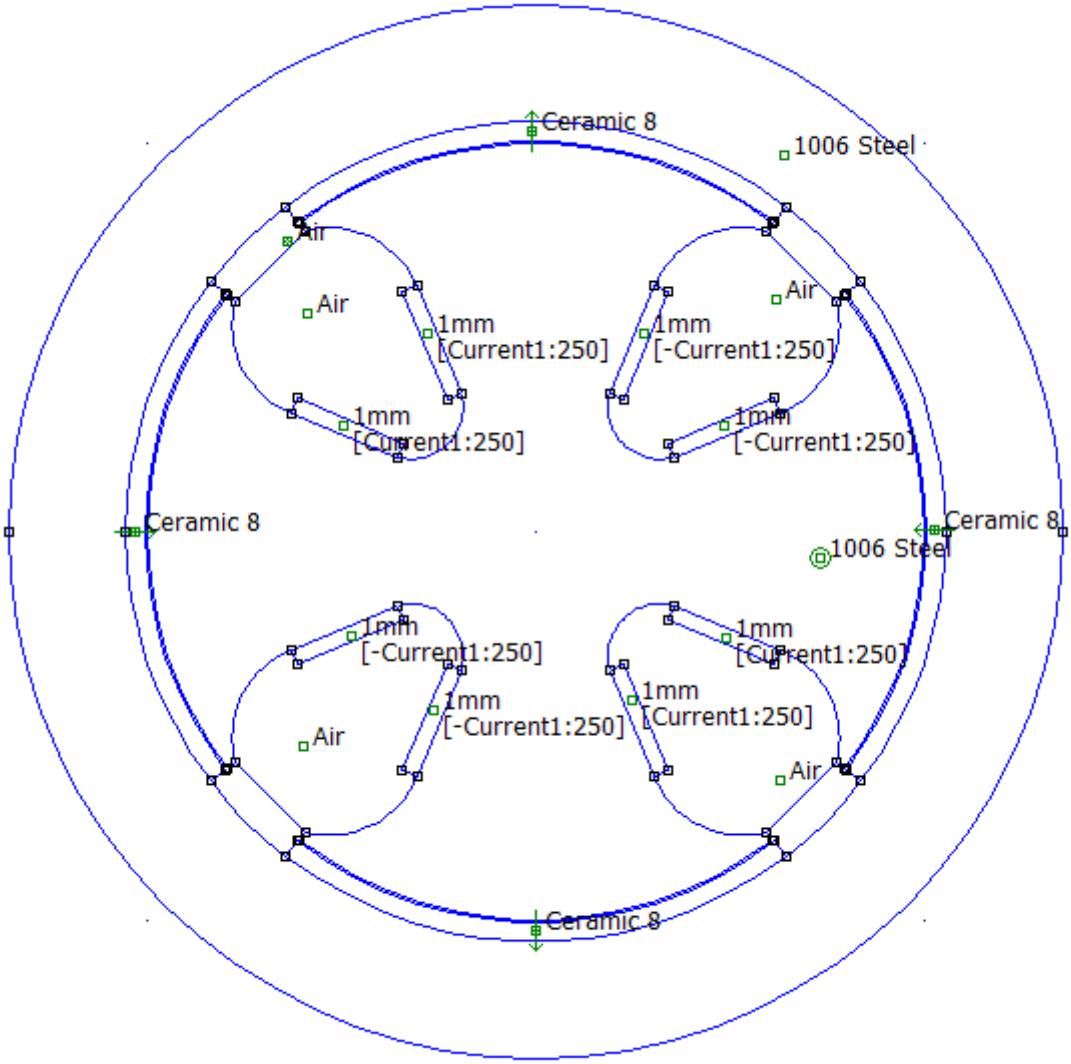

Figure 78

In this case there are four windings.
Each one will be coupled with a correspondent flux, but the four fluxes, for the assumptions made, are all equal, so it's enough to report the evolutions of one of them for each feeding condition.

The firsts evolutions plotted are the ones obtained with no current flowing in the windings. As a consequence, the reported torque is the cogging torque.

There are also detailed pictures of the evolutions.

The representation of the flux and of the cogging torque are below:

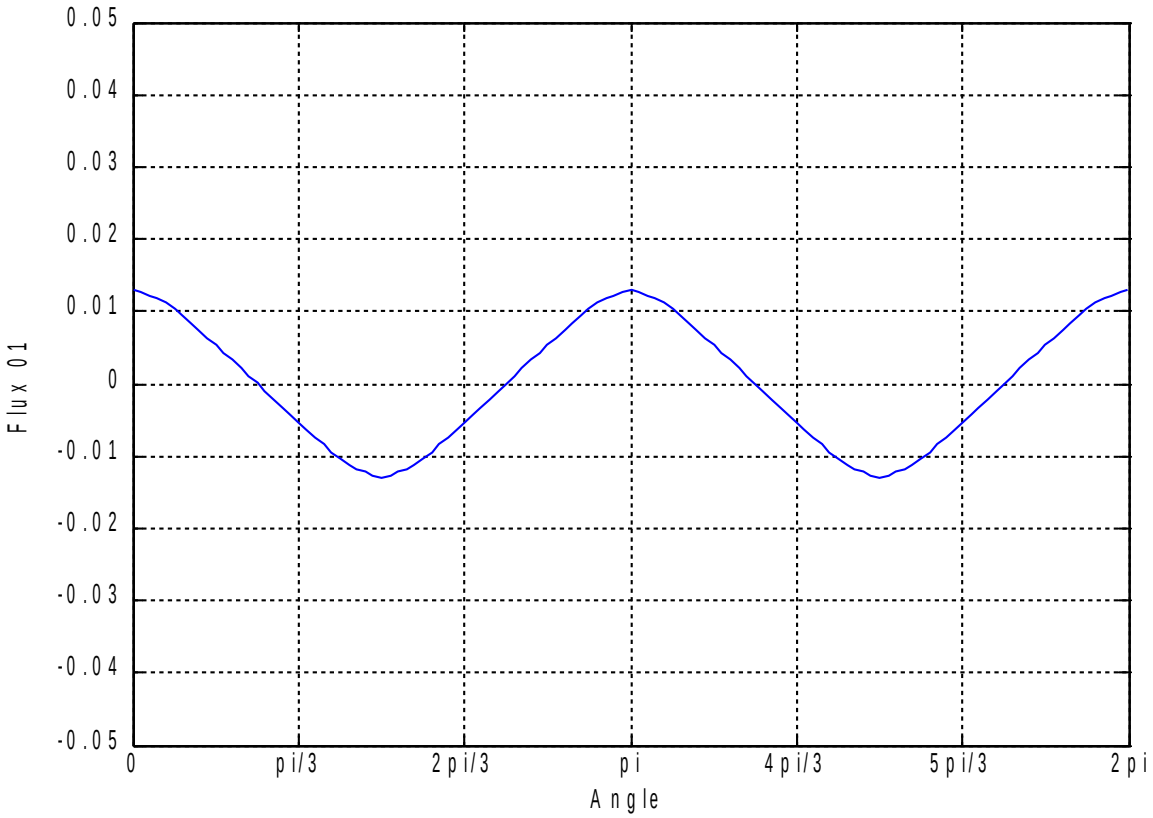

Figure 79

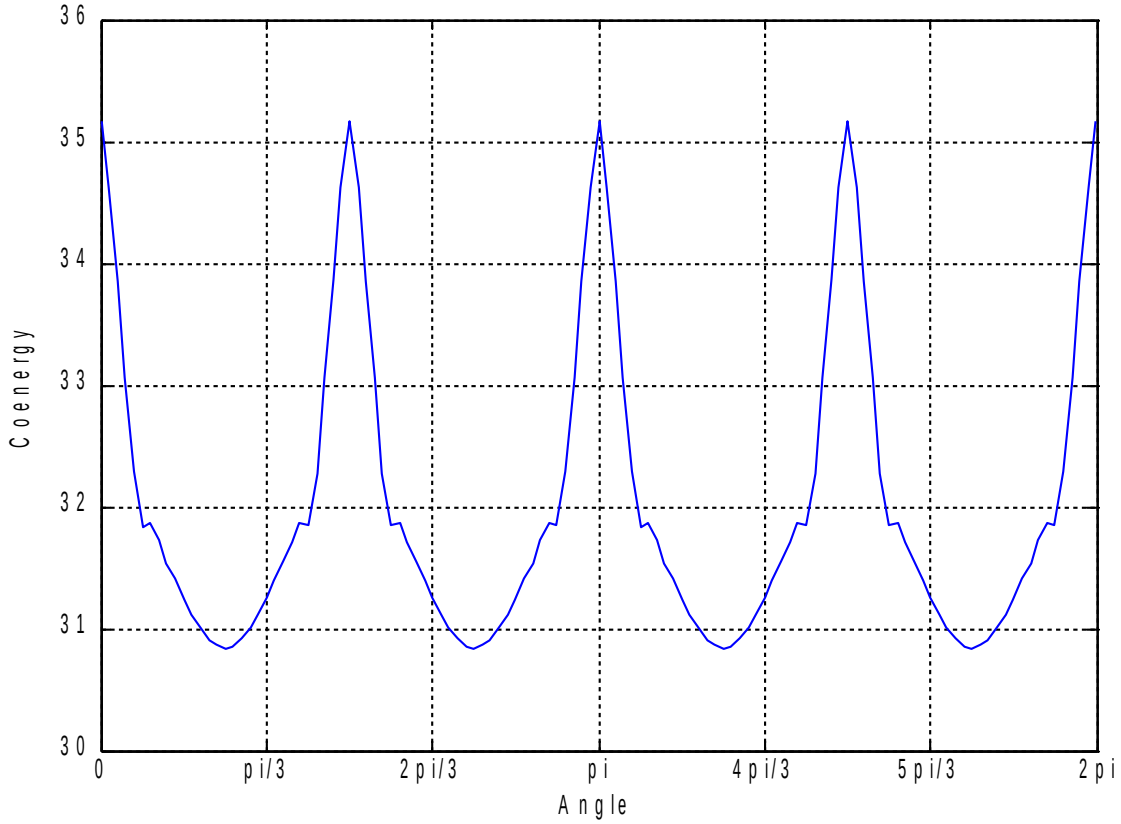

Figure 80

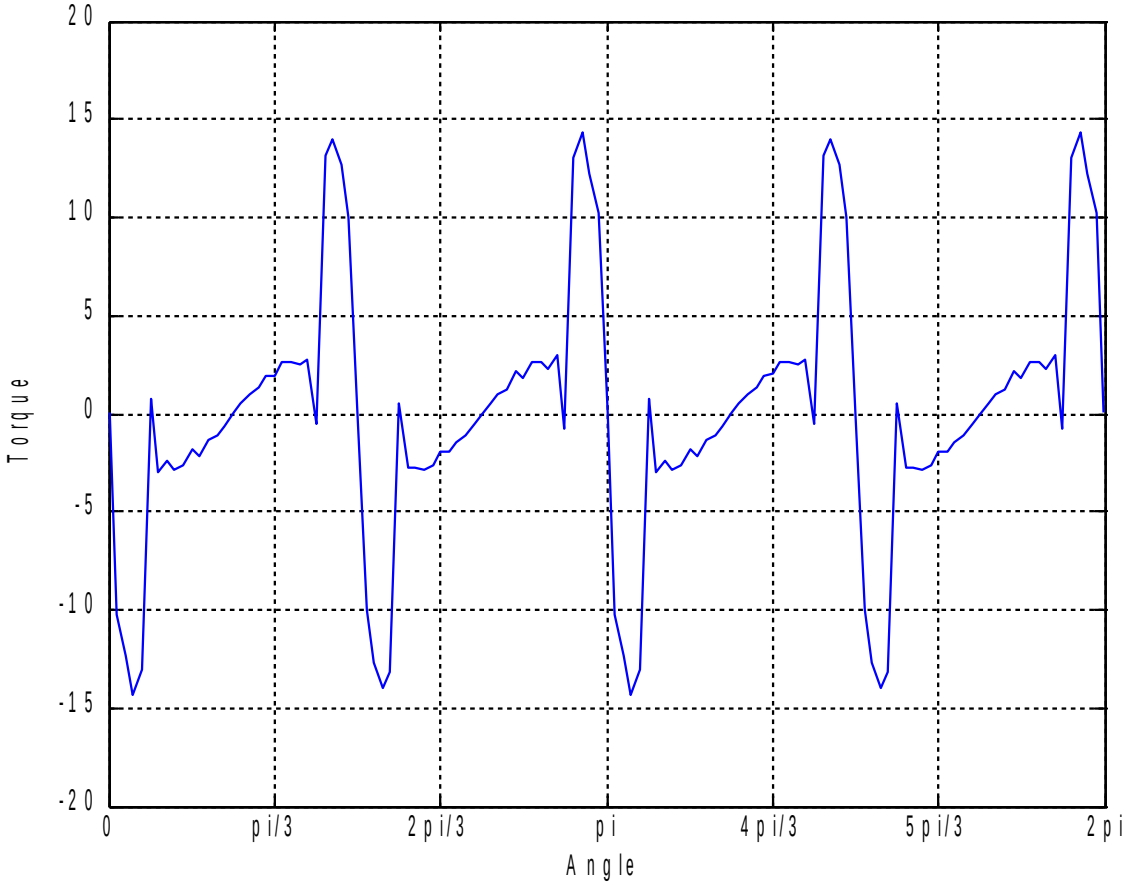

Figure 81

It is now possible to get the evolutions of the electromechanical parameters of the machine when it's fed by a sinusoidal current.
Hence, from now on, evolutions will be plotted for different values of feeding current, $i_{(t)}$, which follows the cosinusoidal behaviour:

$$i_{(t)} = I_M \cos(2\omega t + \varphi)$$

eq. 32

Values changing for each simulation are both the peak value and the angular phase.
Cosinusoidal law has been chosen instead of sinusoidal one so as to have $i_{(t)}$ and $\Phi_{0(t)}$ in phase when $\varphi=0$.

MMF=250 At, φ=0

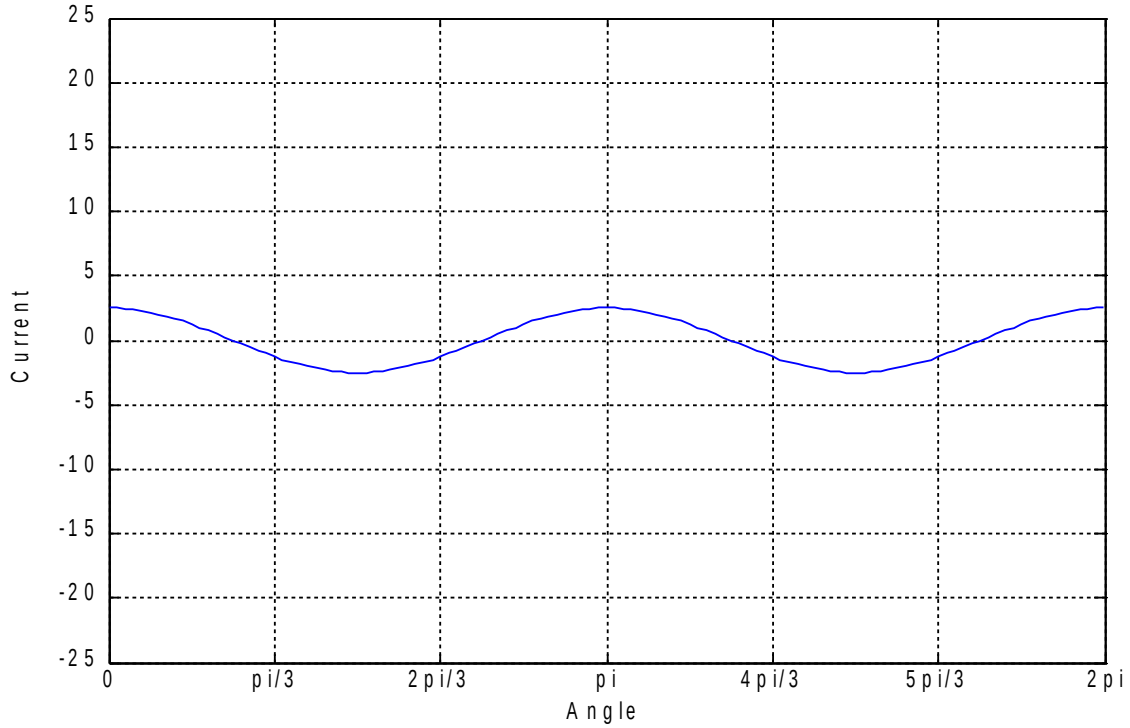

Figure 82

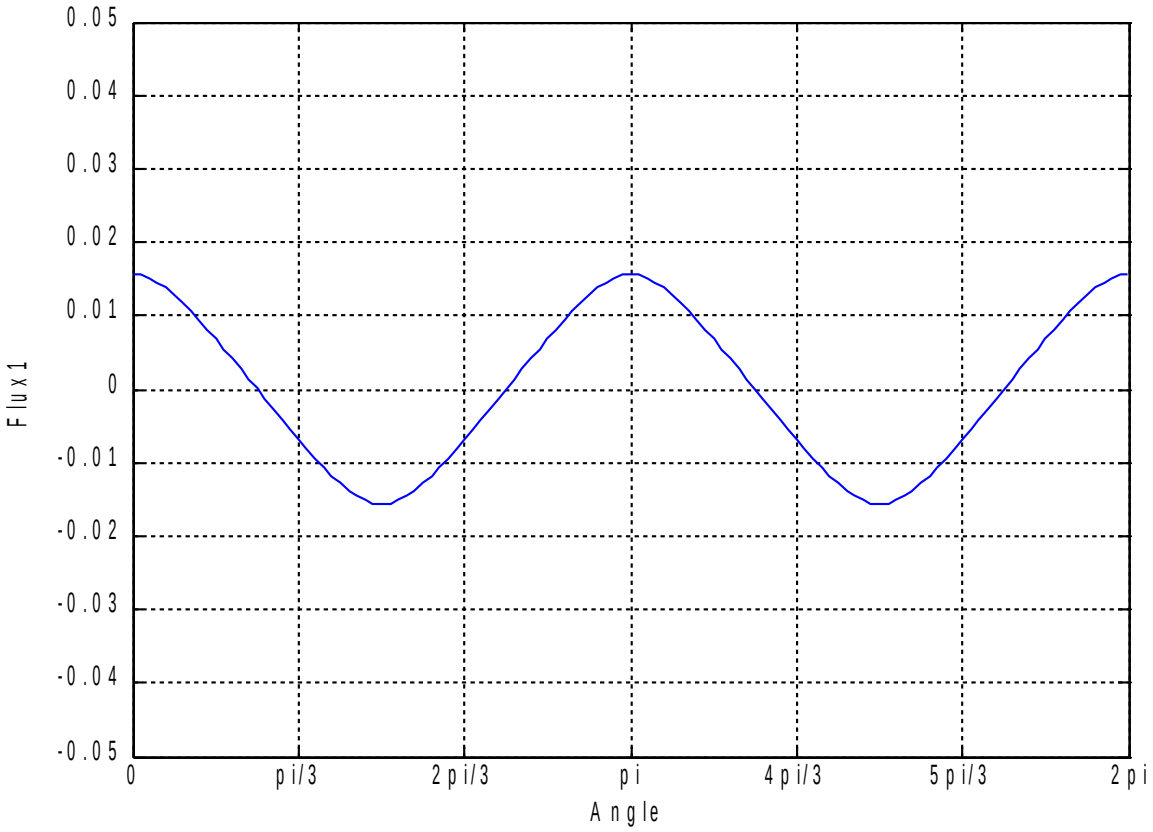

Figure 83

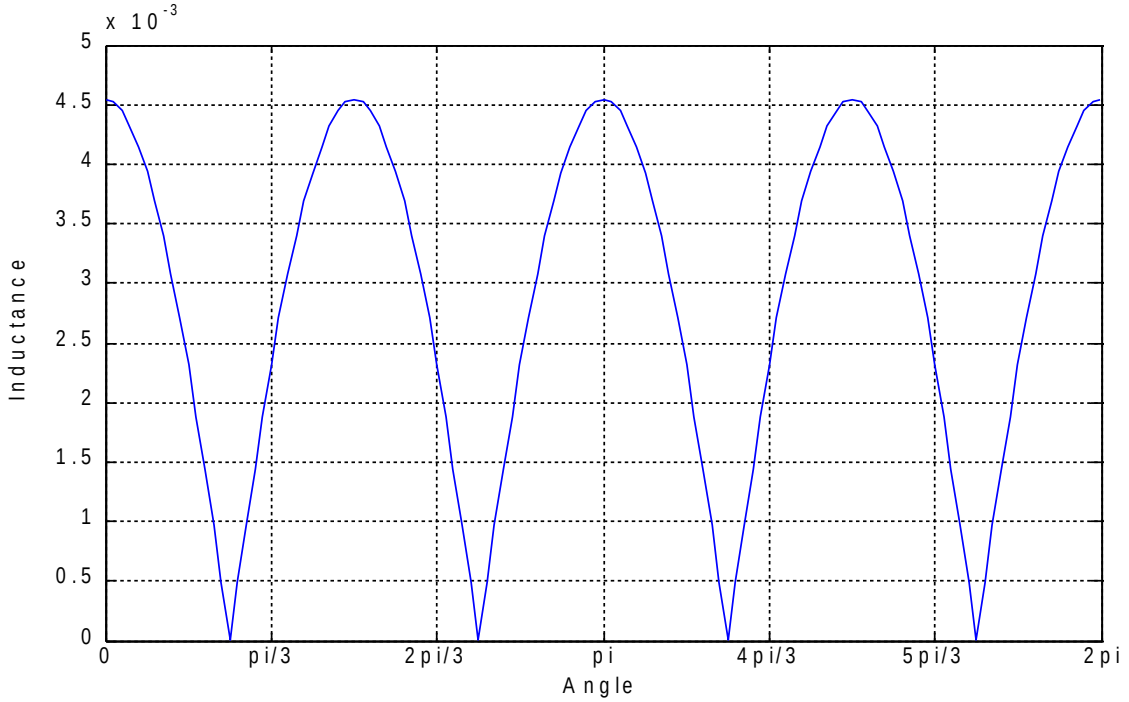

Figure 84

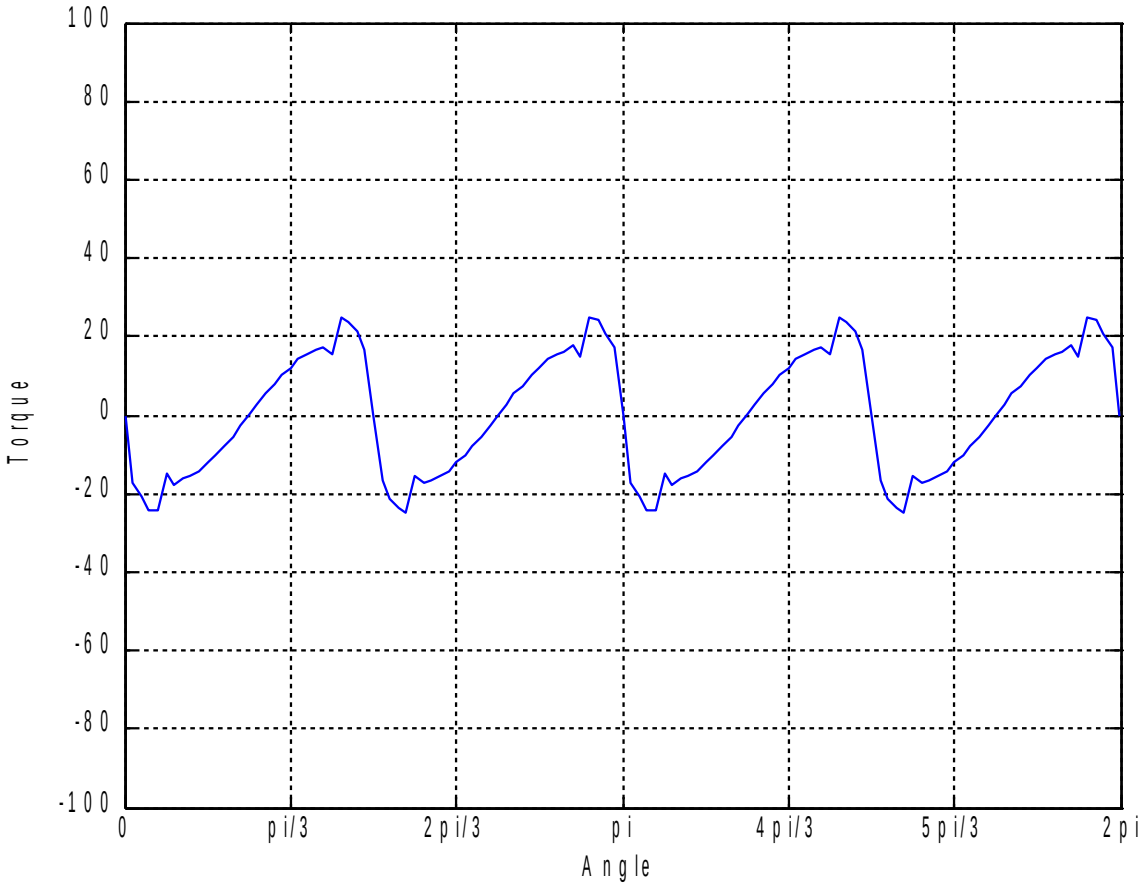

Figure 85

MMF = 250 At, φ=30°

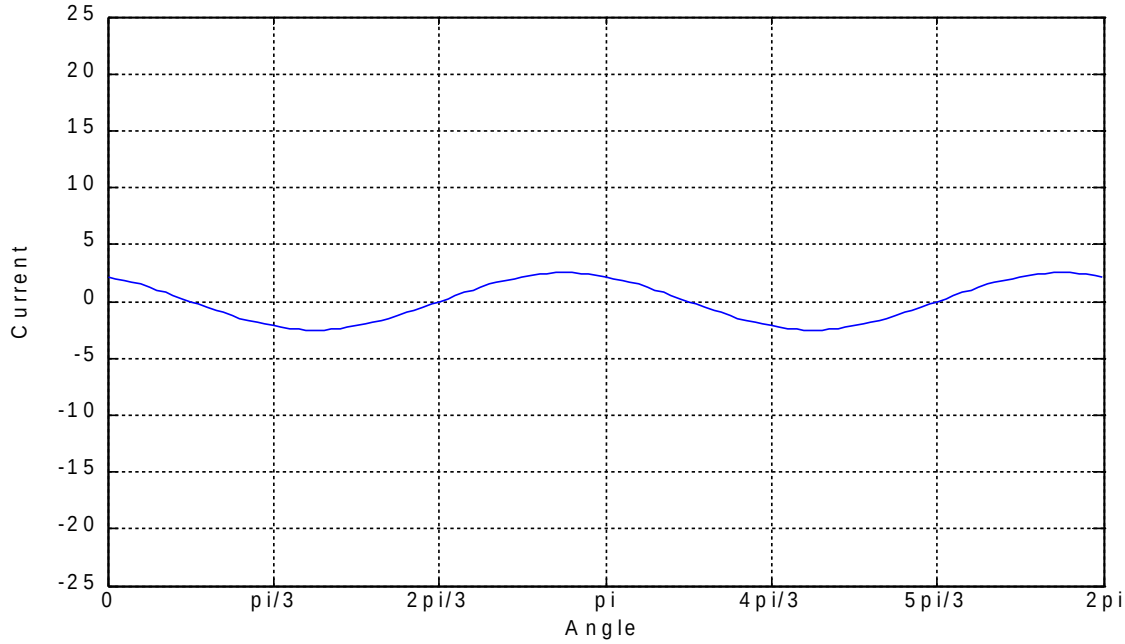

Figure 86

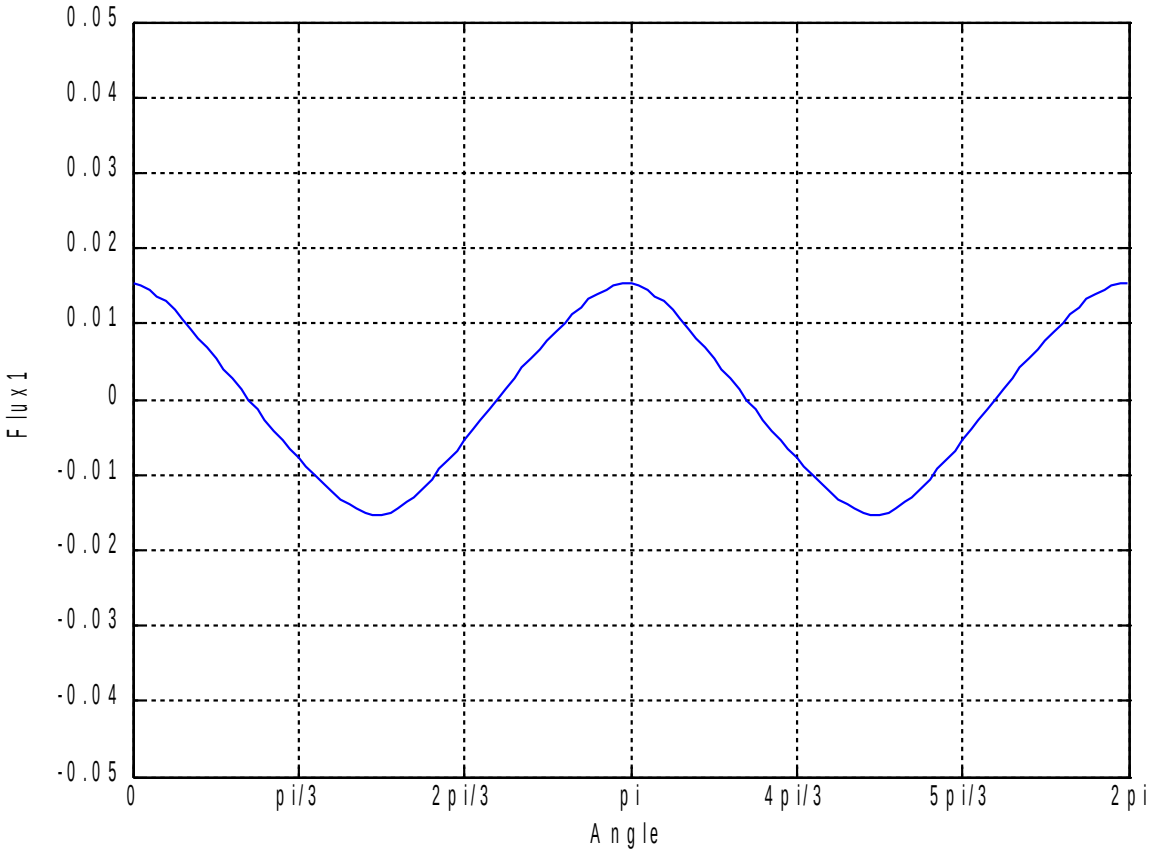

Figure 87

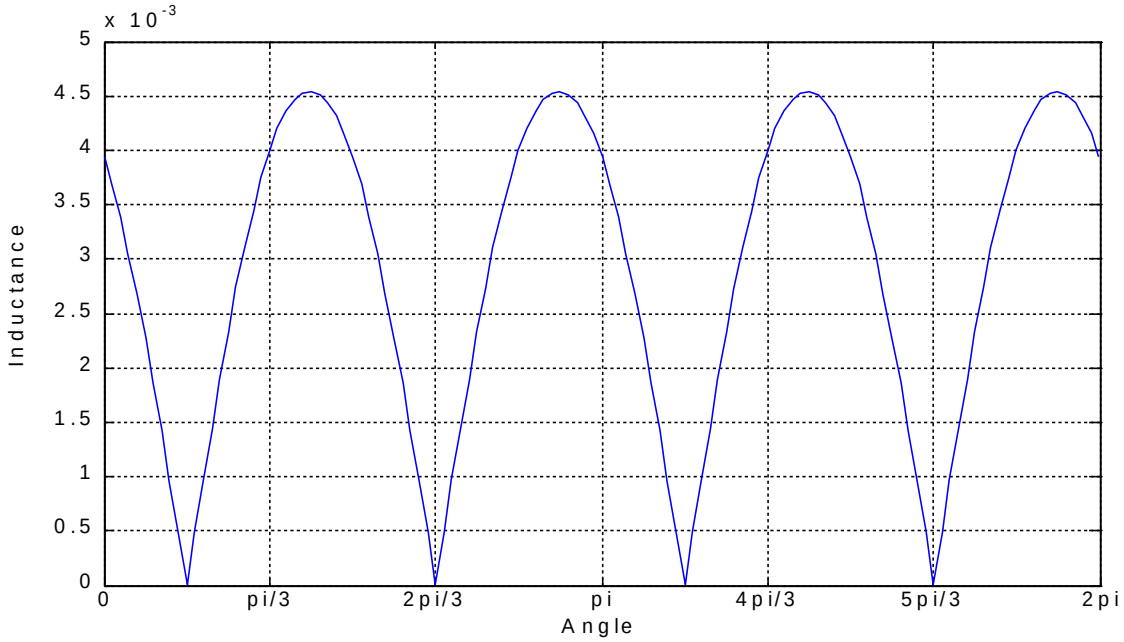

Figure 88

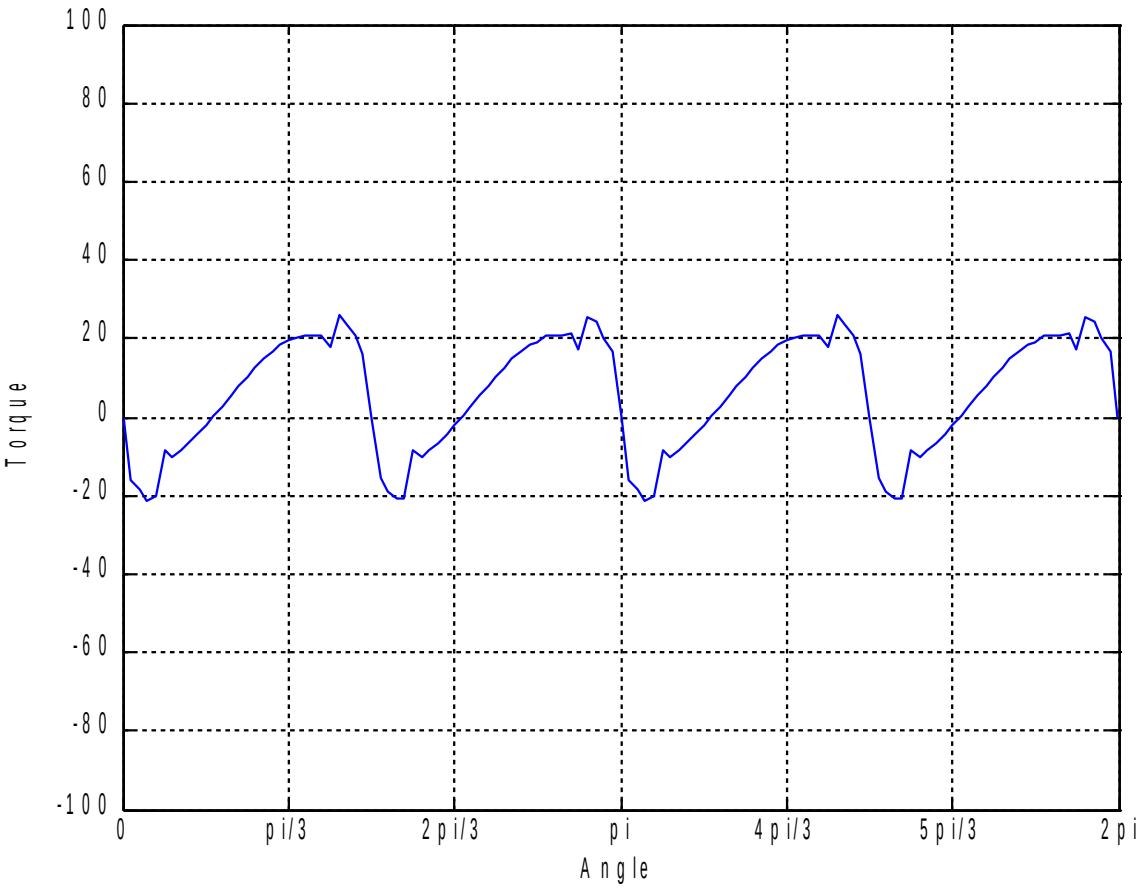

Figure 89

MMF = 250 At, φ=60°

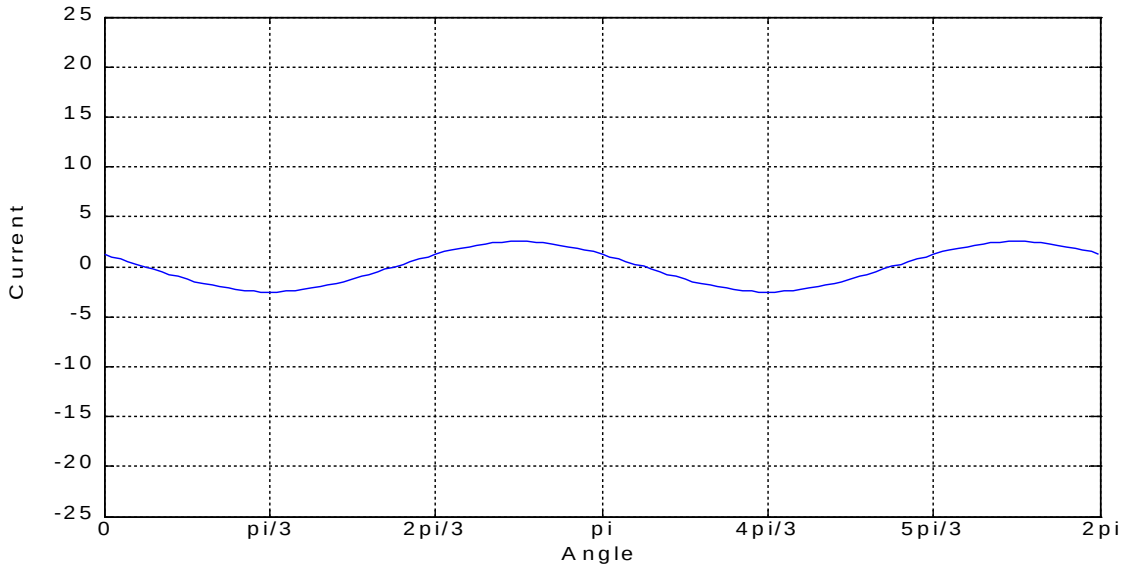

Figure 90

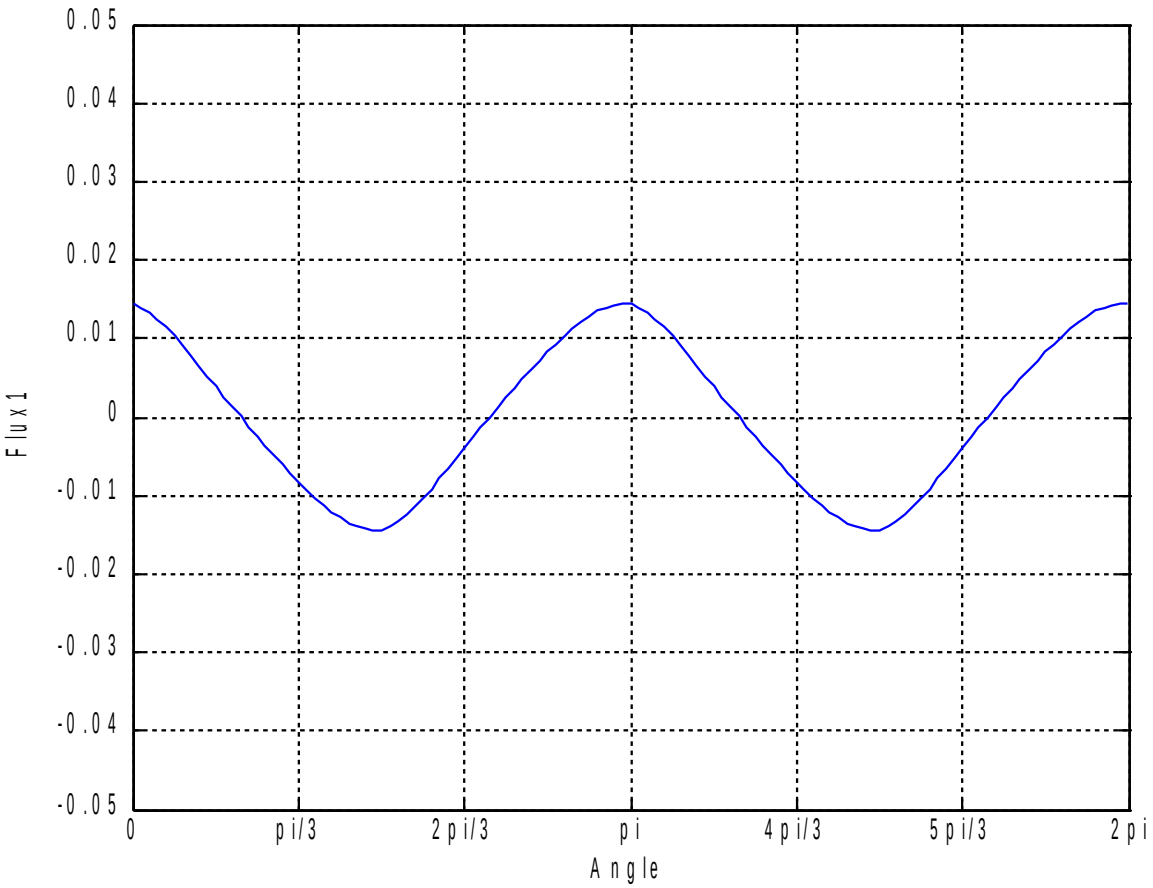

Figure 91

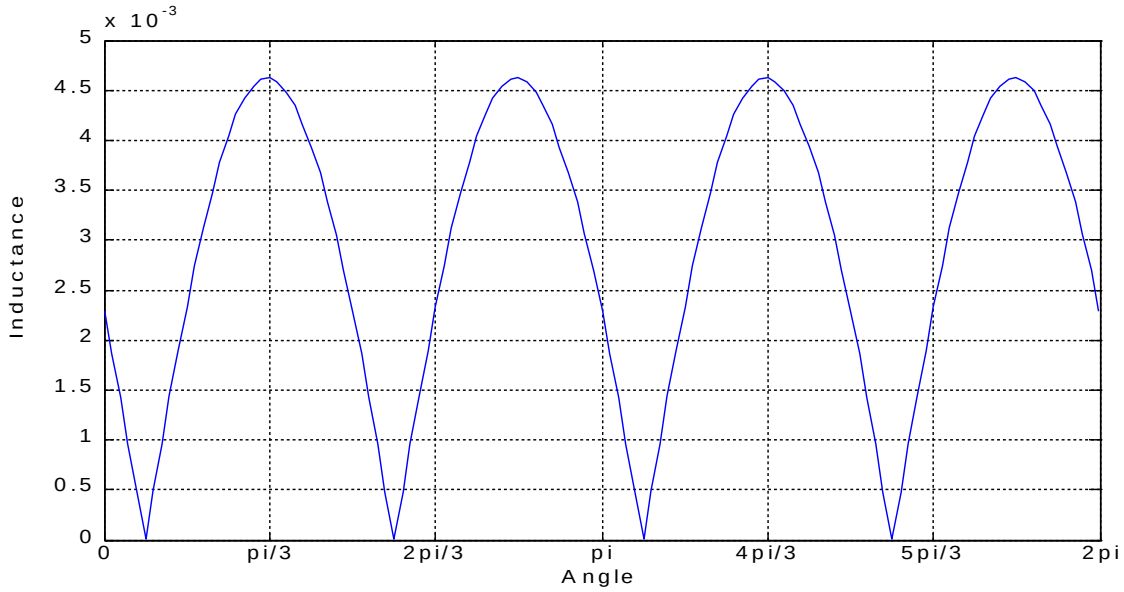

Figure 92

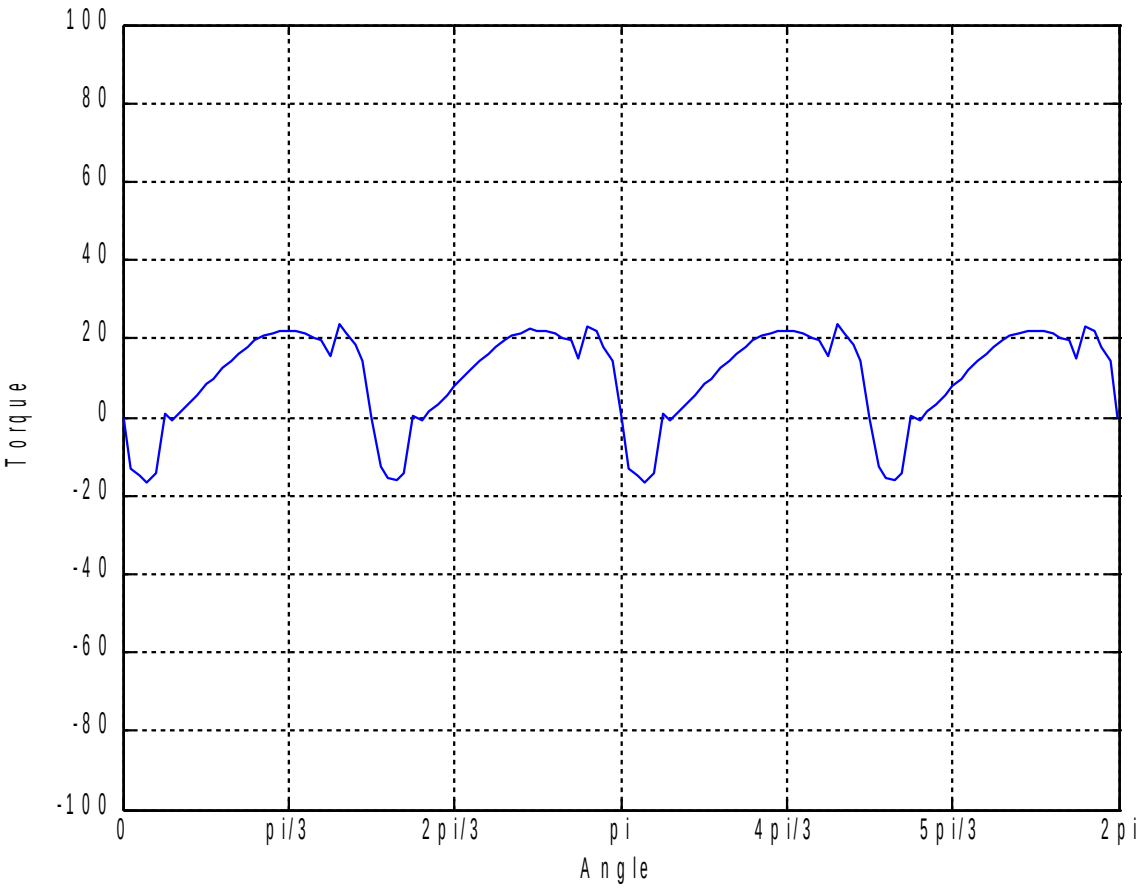

Figure 93

MMF = 250 At, φ=90°

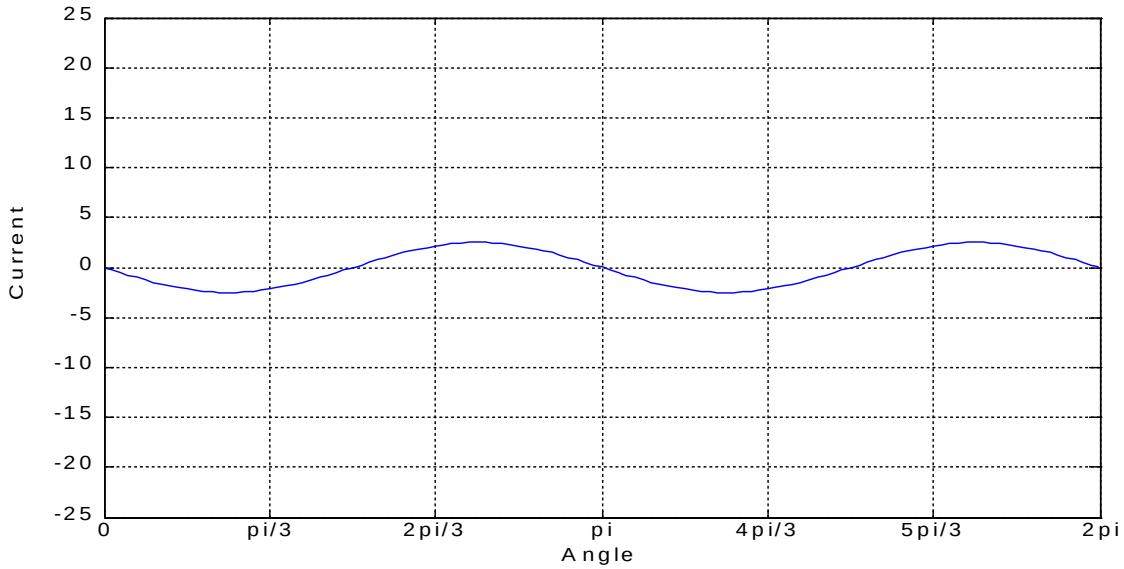

Figure 94

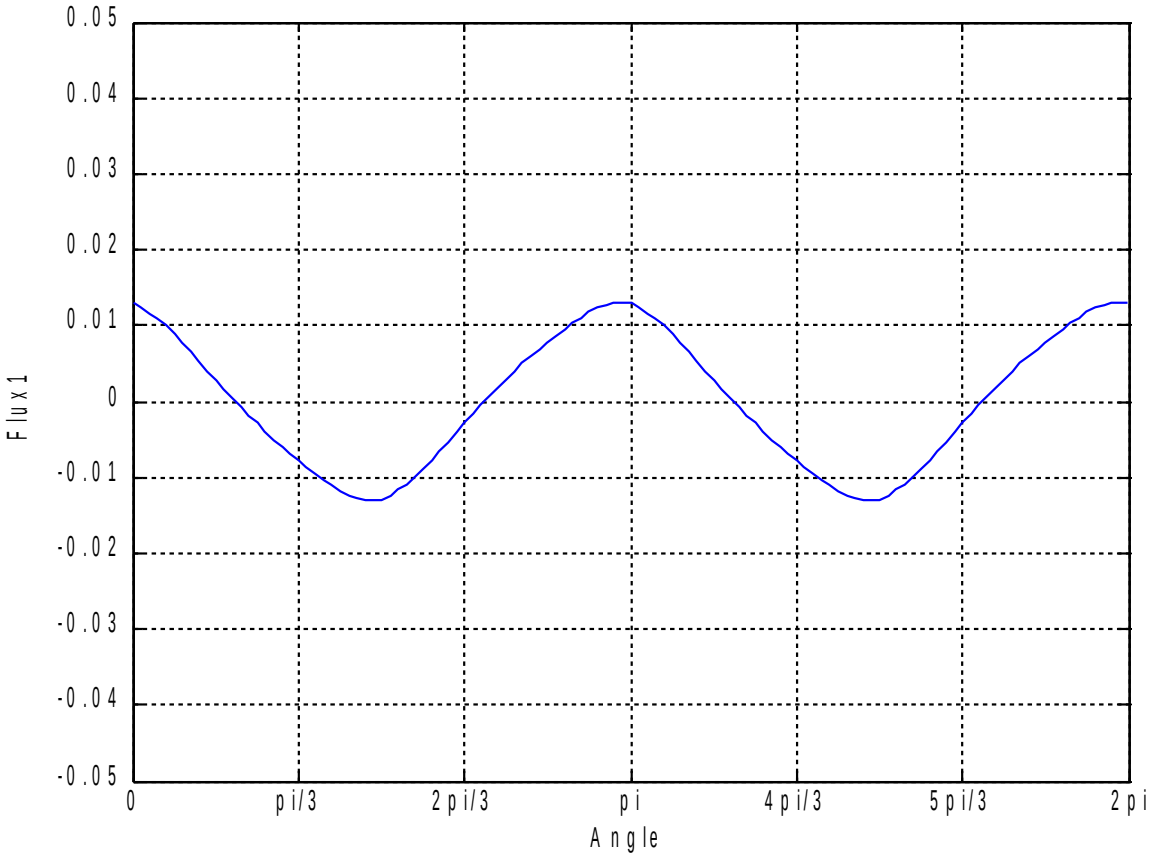

Figure 95

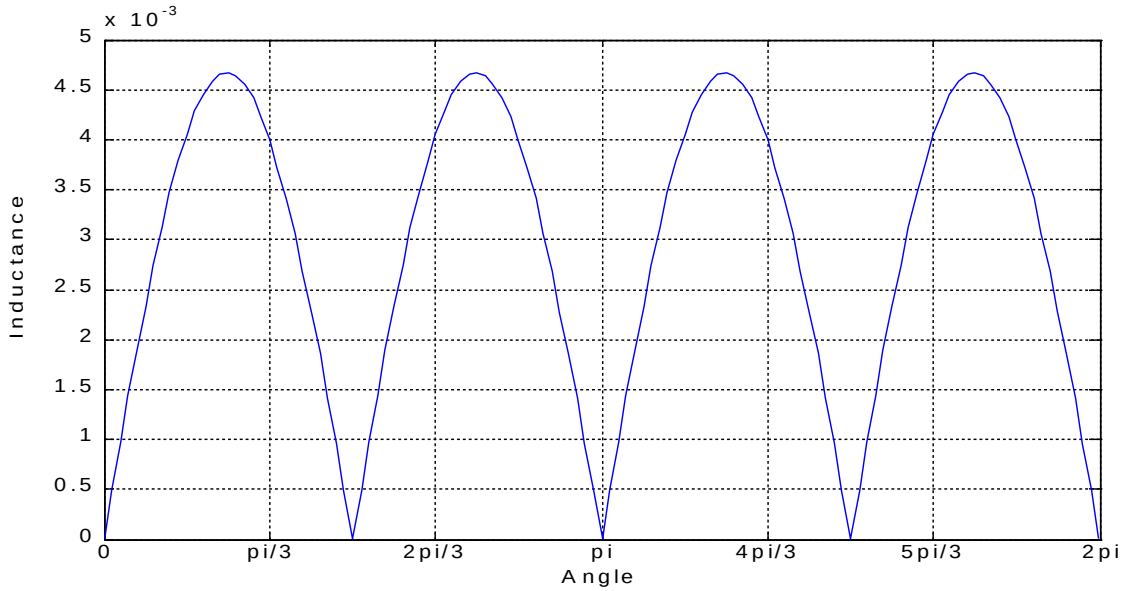

Figure 96

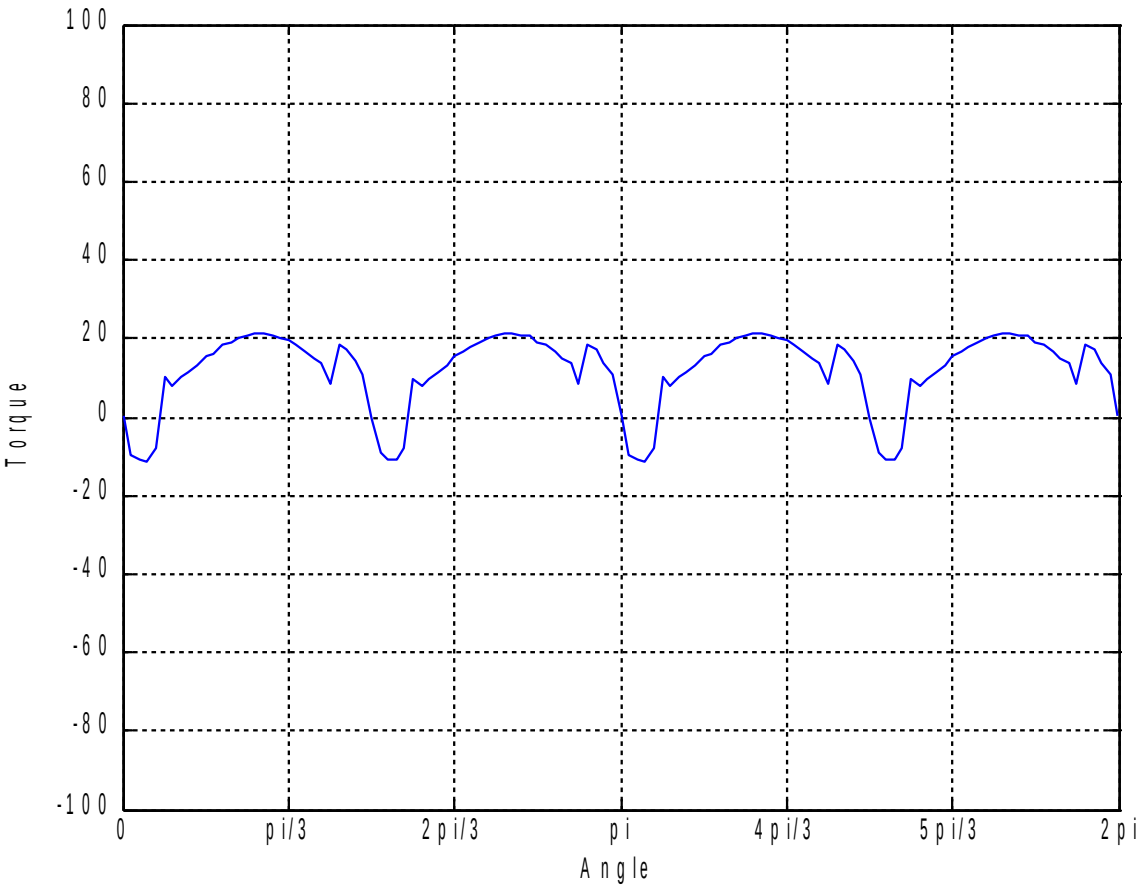

Figure 97

MMF = 500 At, φ=0°

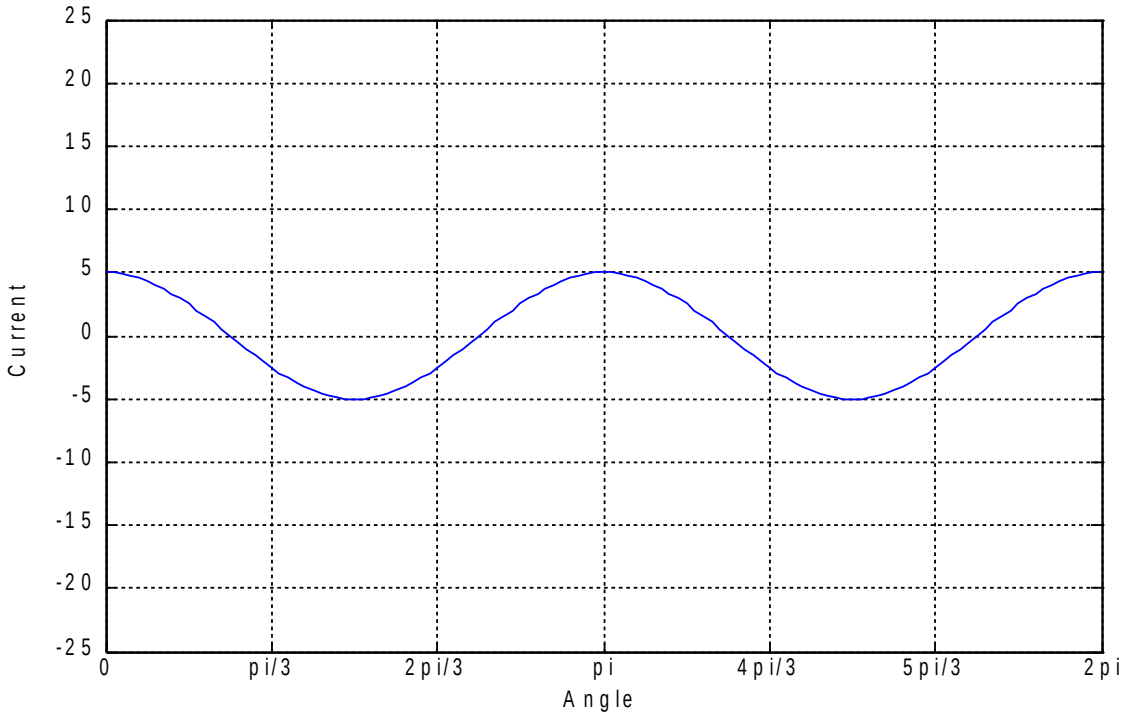

Figure 98

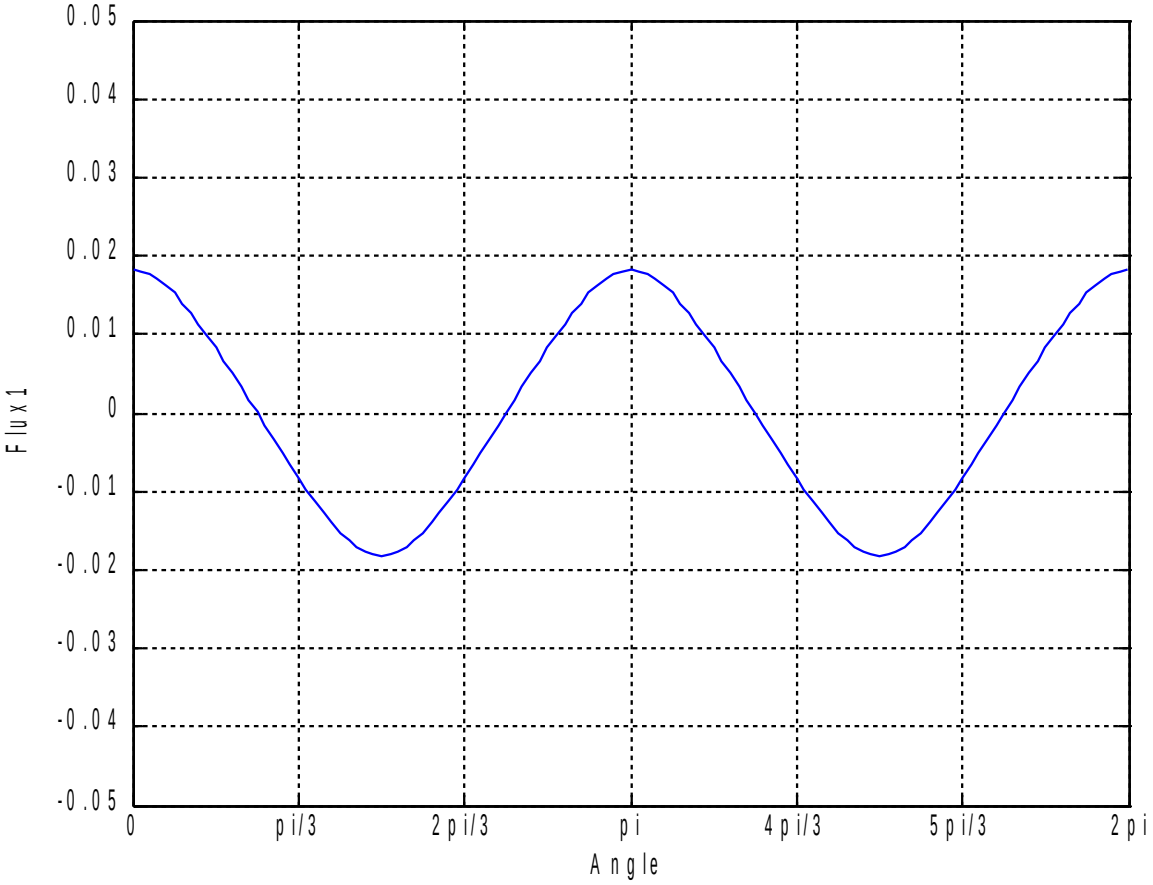

Figure 99

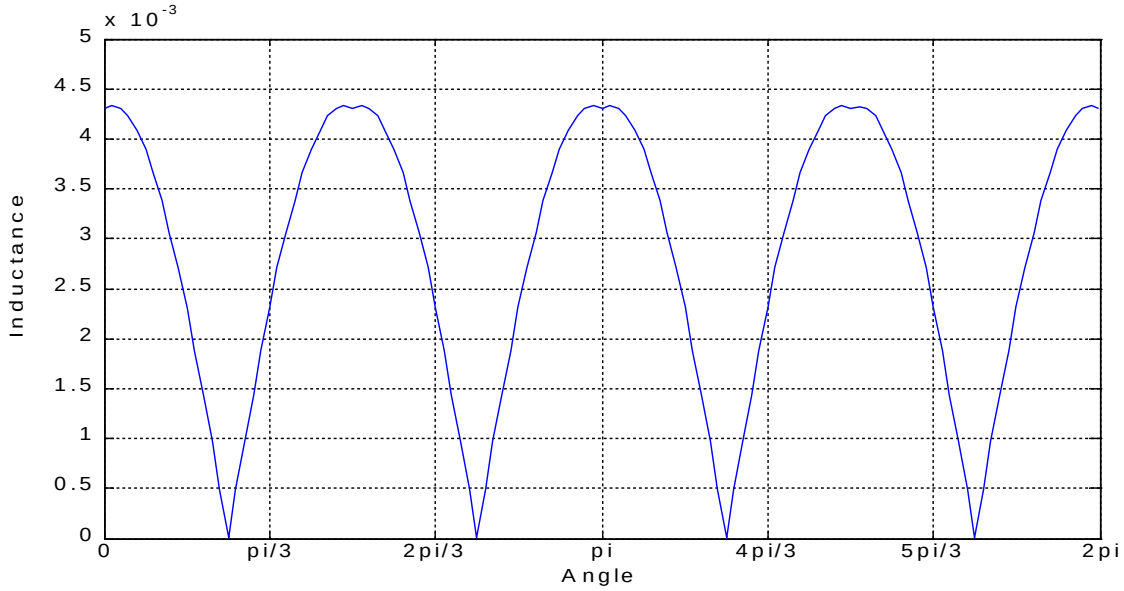

Figure 100

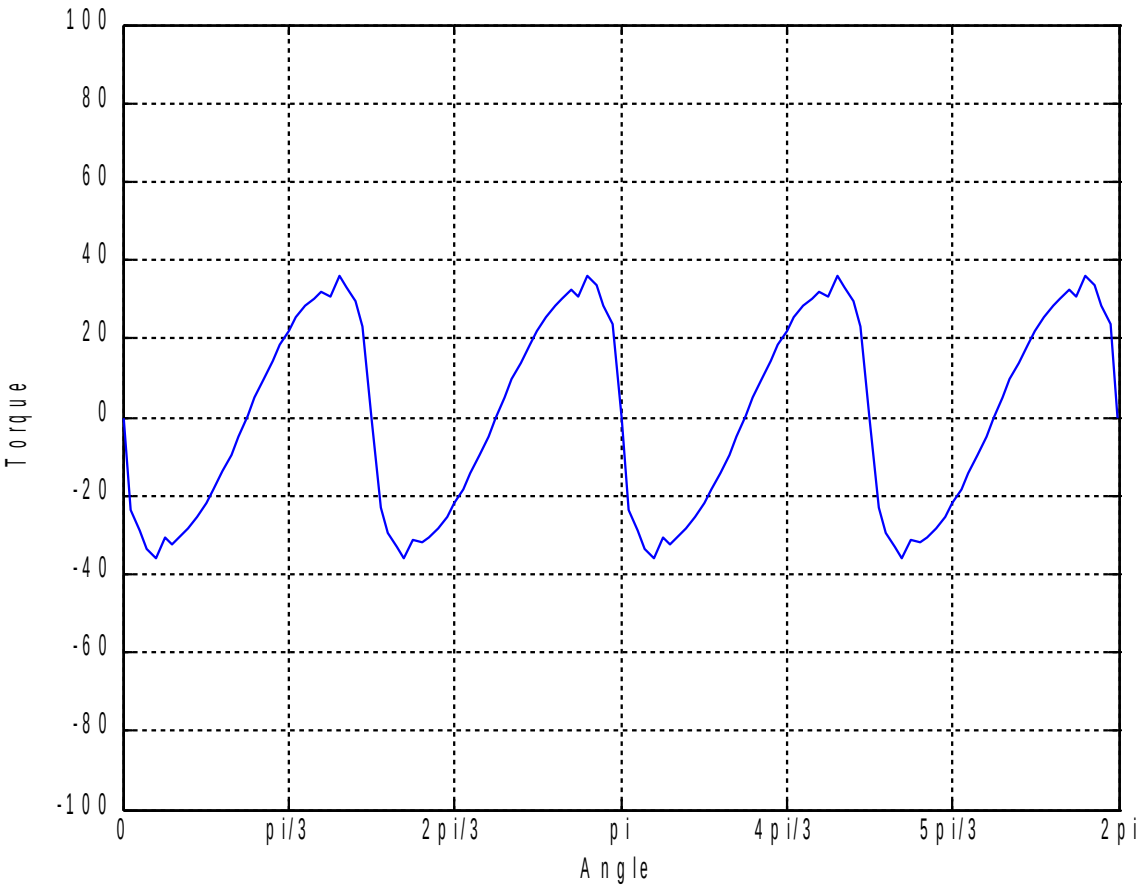

Figure 101

MMF = 500 At, φ=30°

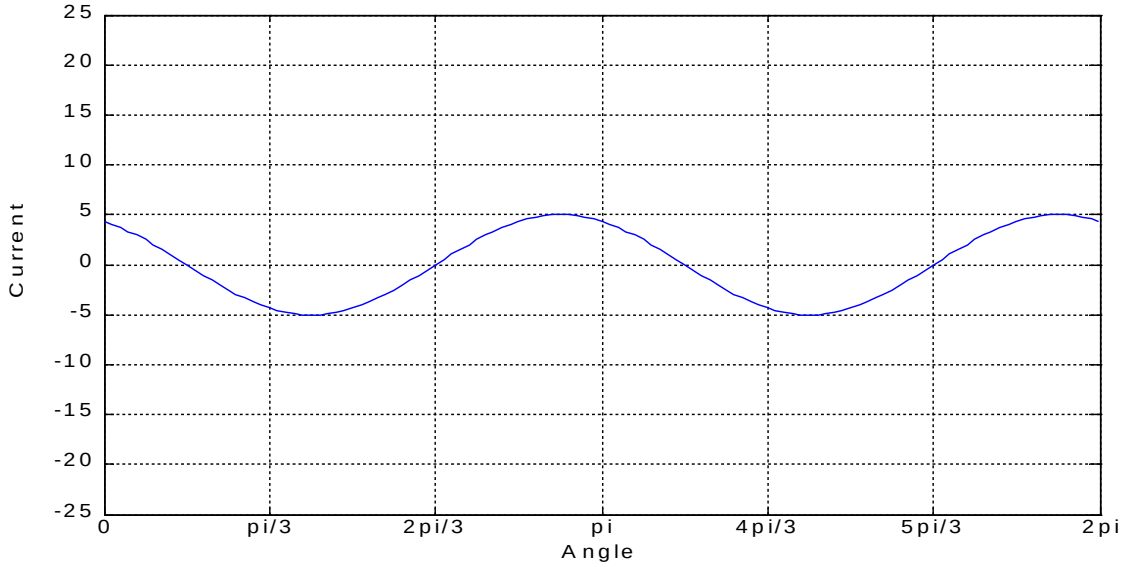

Figure 102

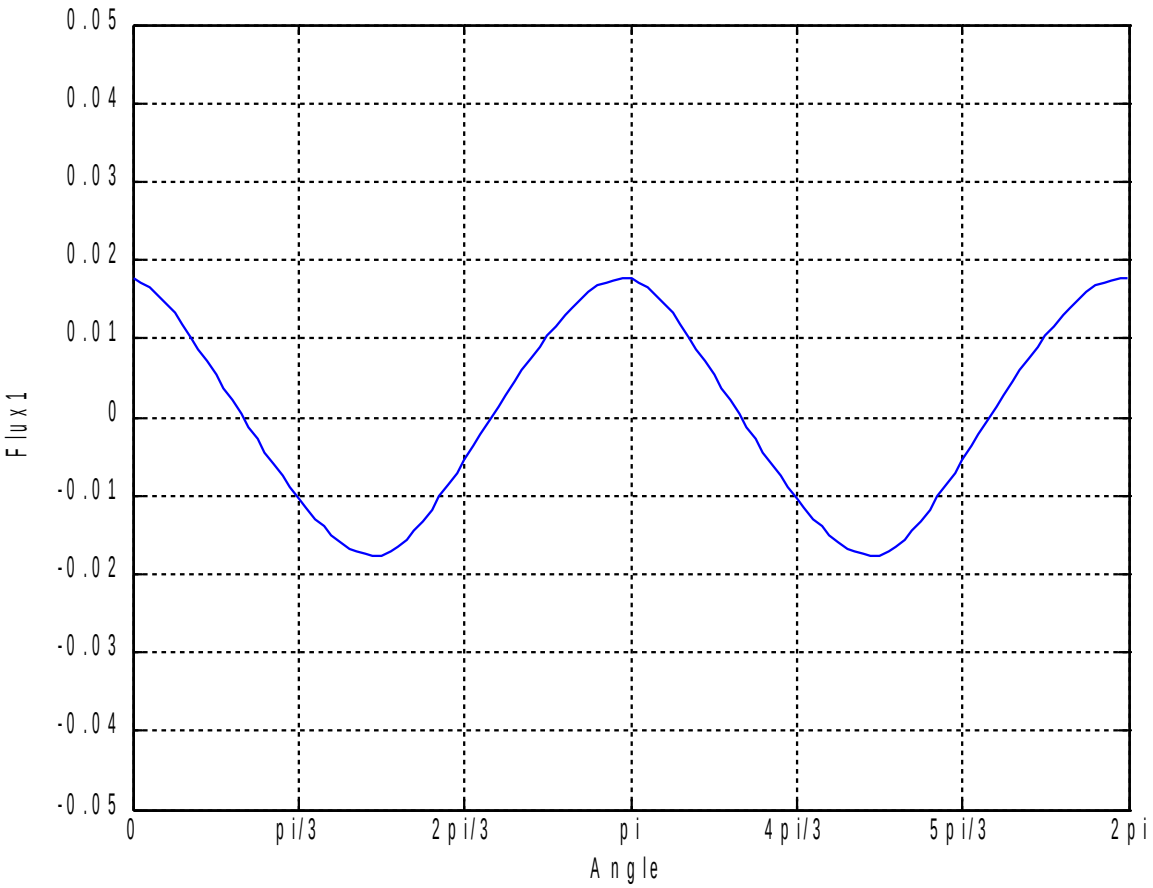

Figure 103

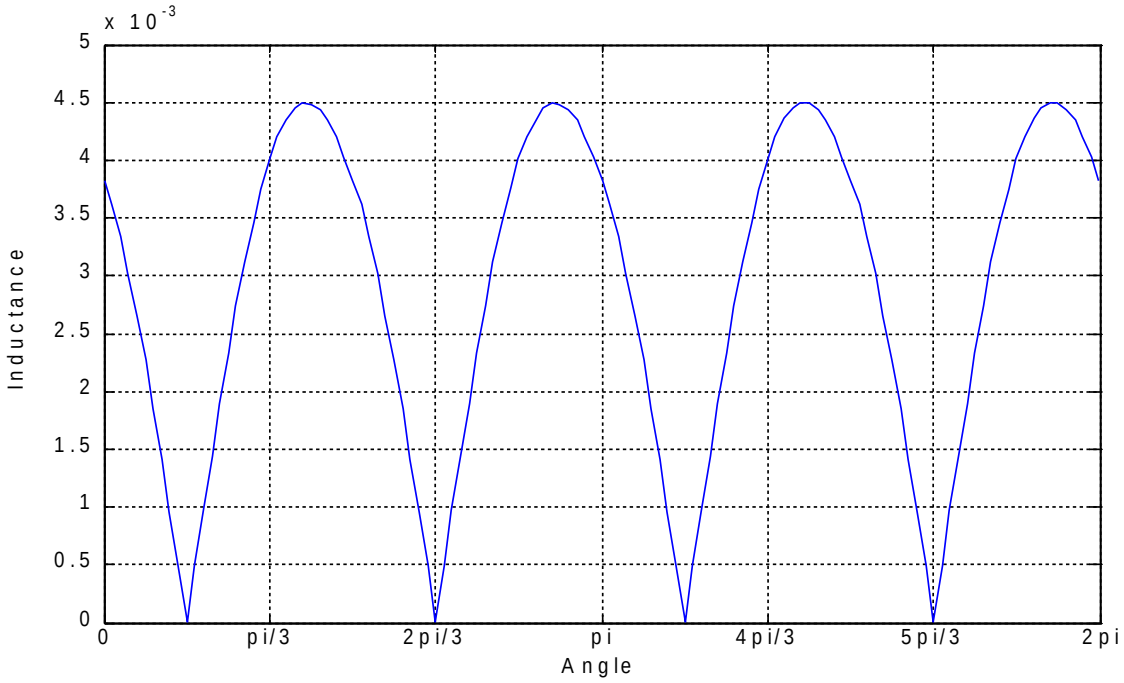

Figure 104

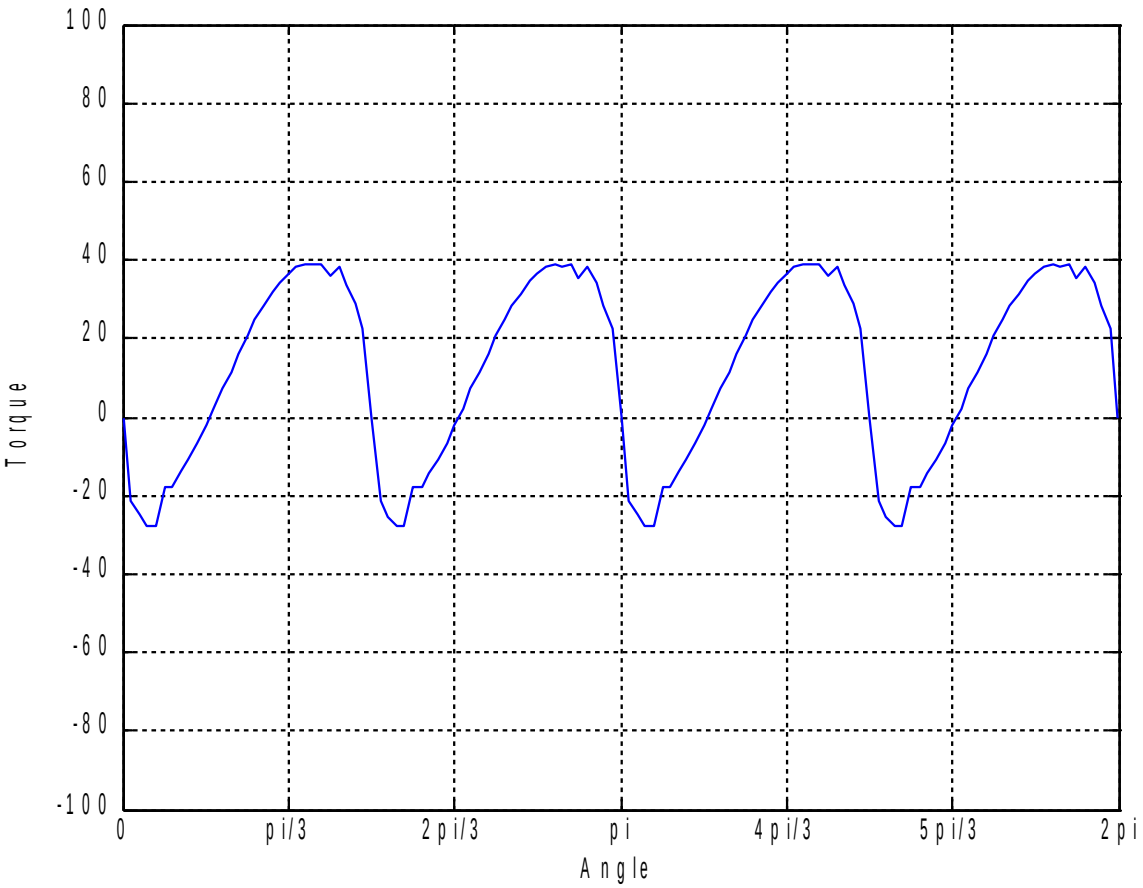

Figure 105

MMF = 500 At, φ=60°

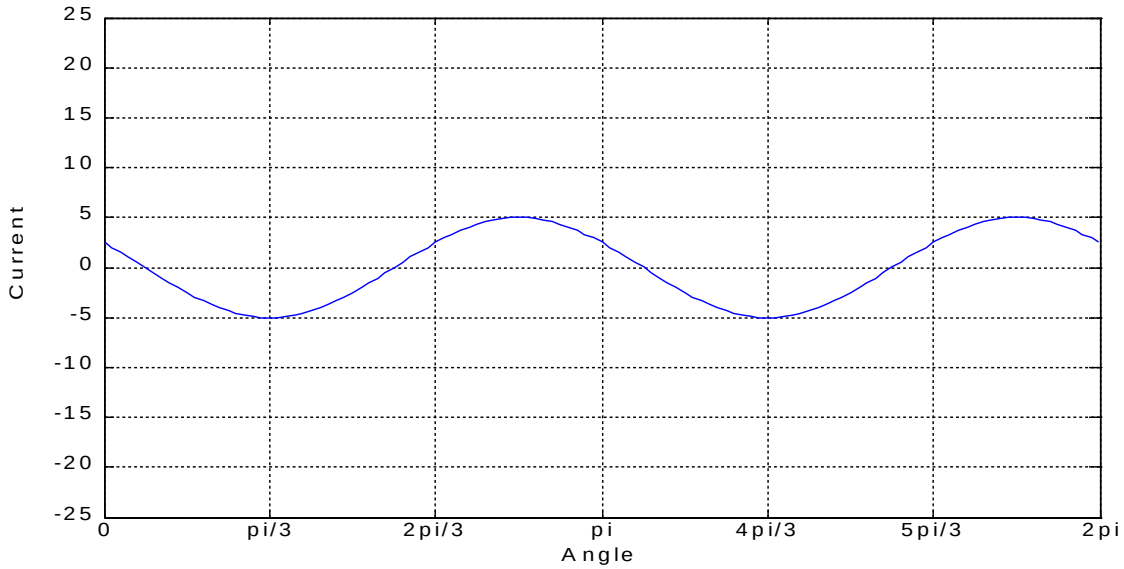

Figure 106

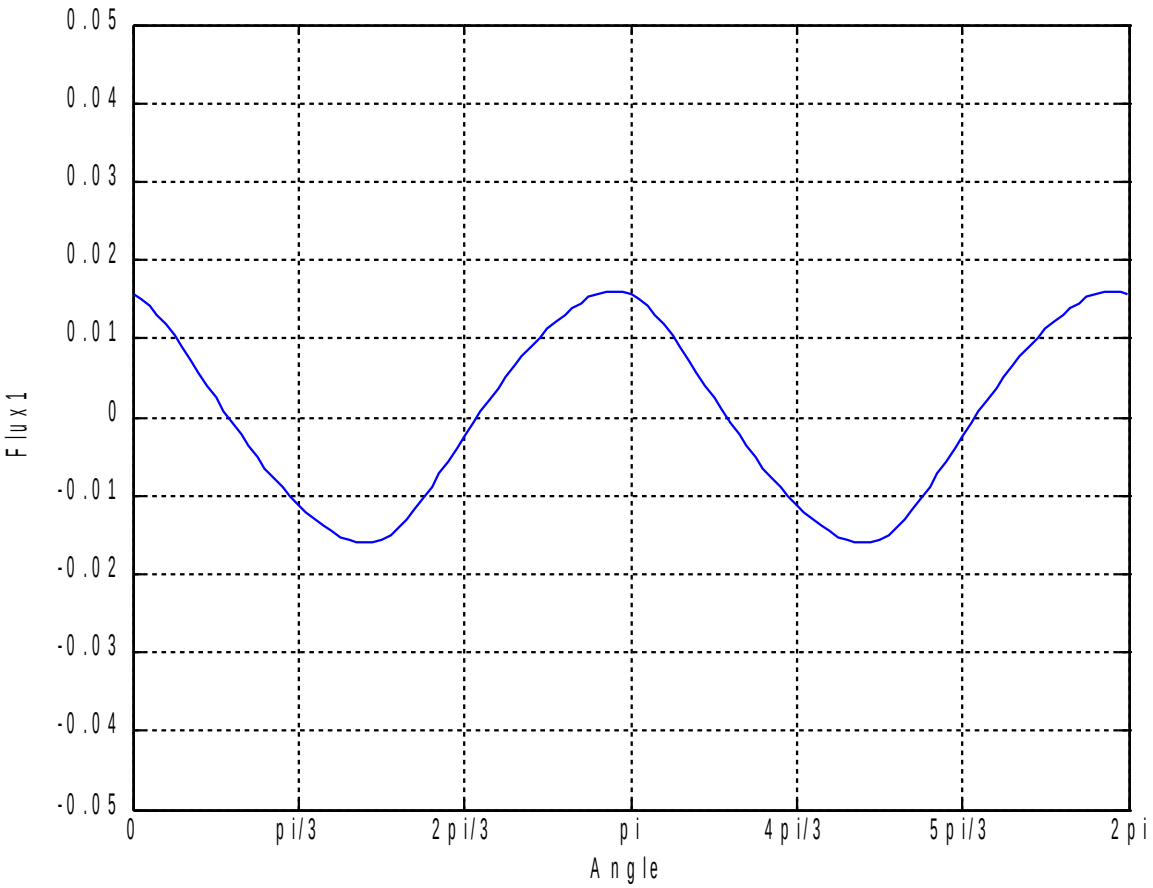

Figure 107

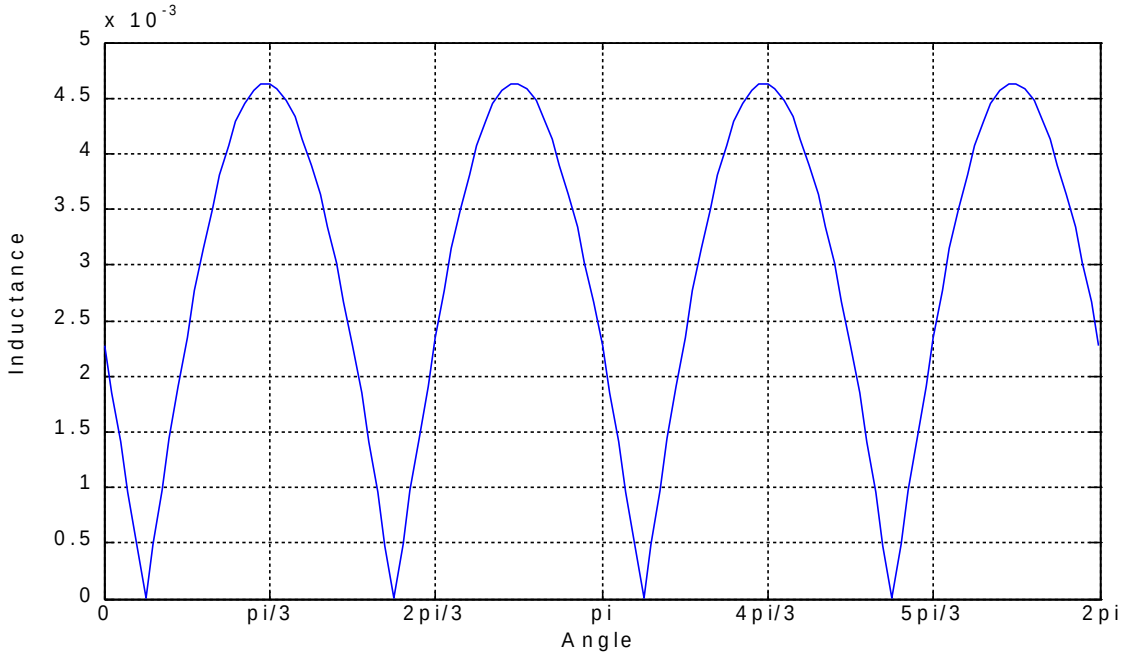

Figure 108

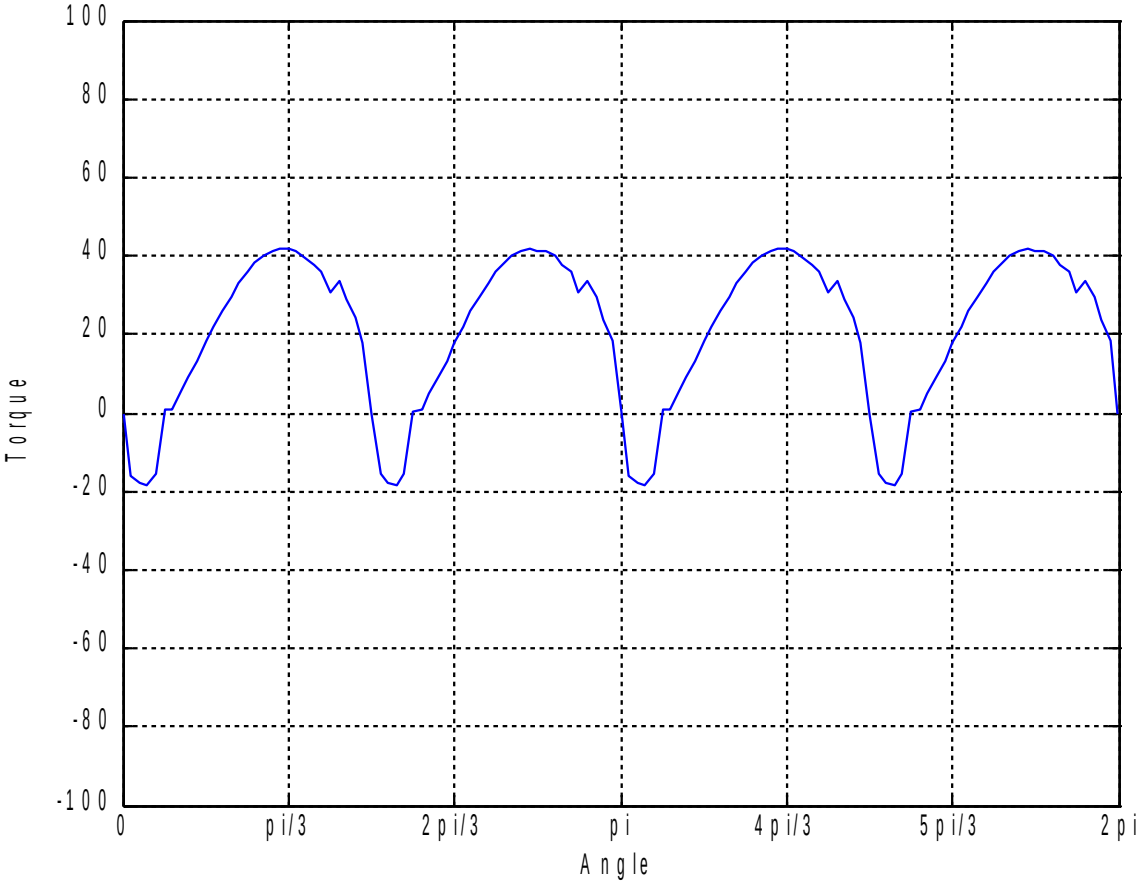

Figure 109

MMF = 500 At, φ=90°

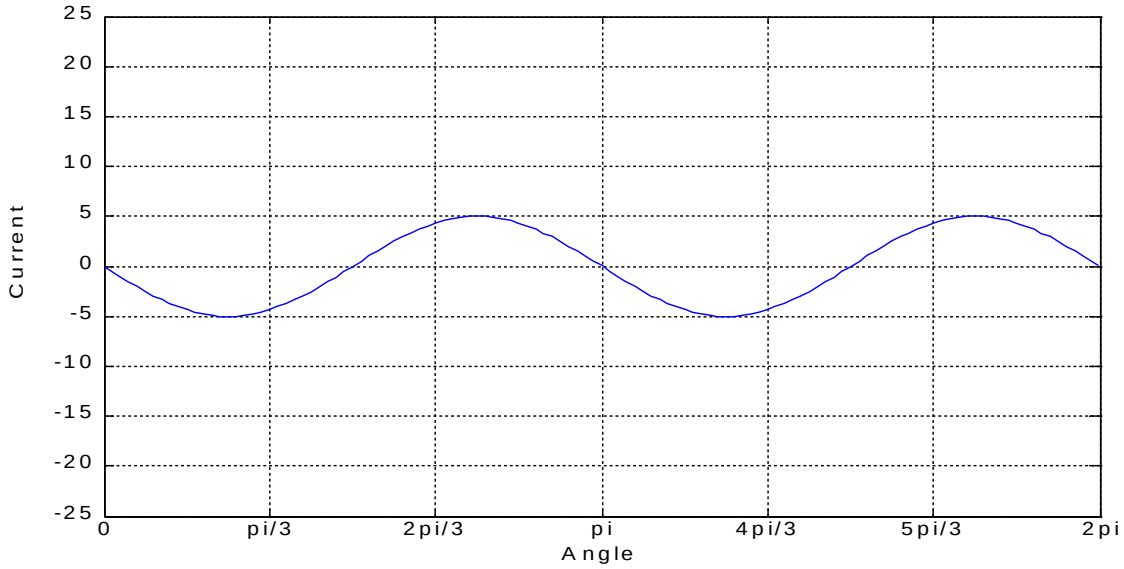

Figure 110

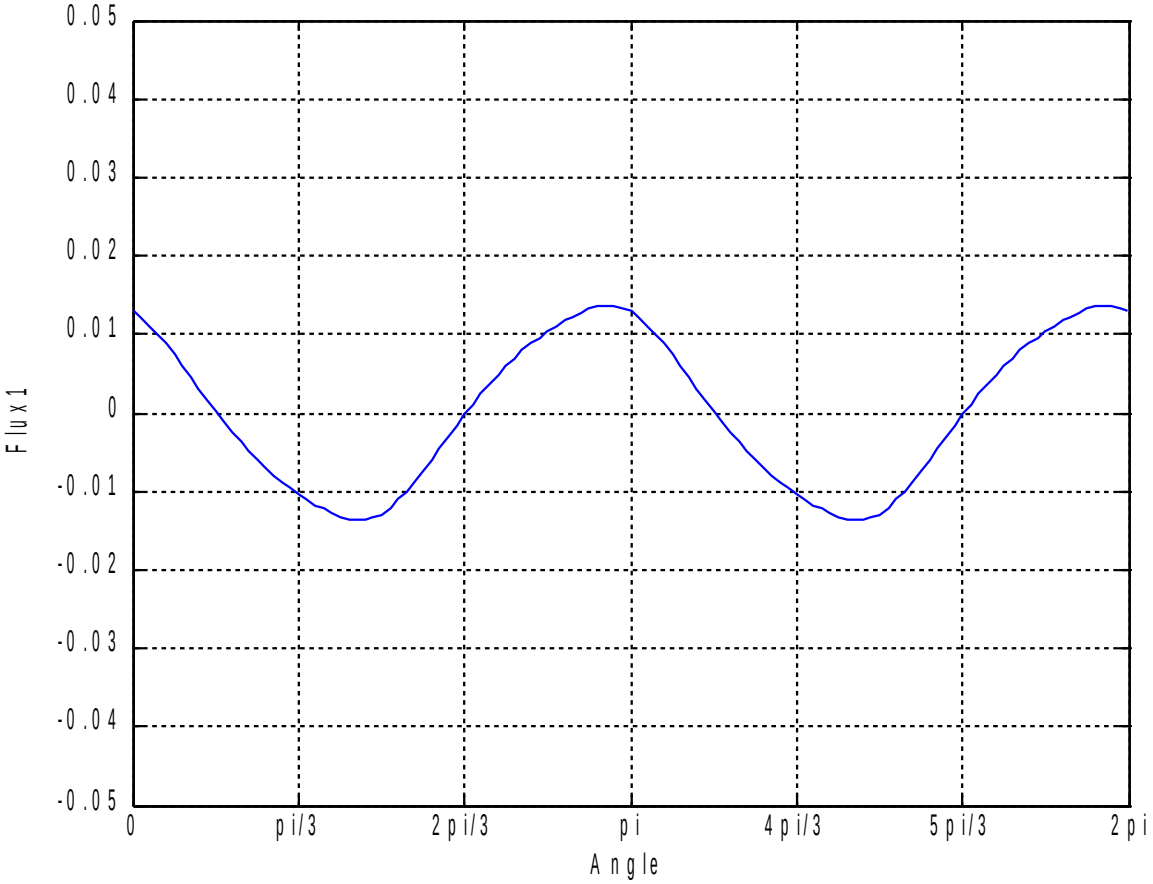

Figure 111

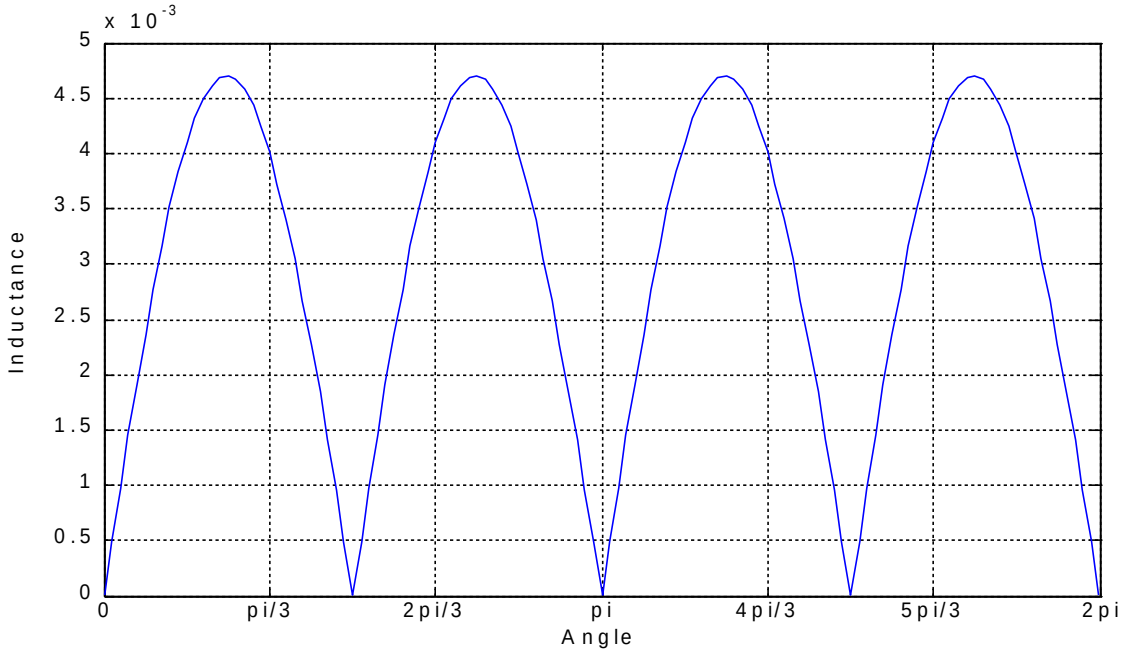

Figure 112

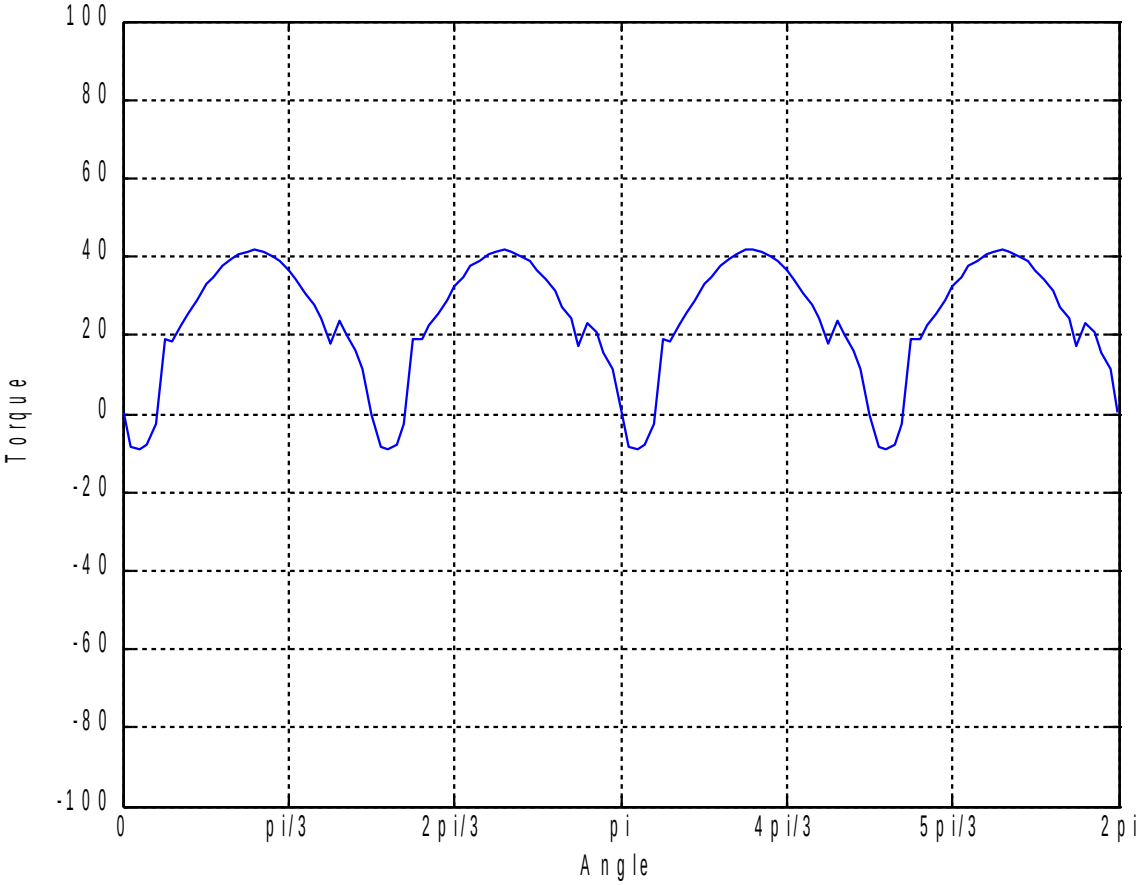

Figure 113

MMF = 750 At, φ=0°

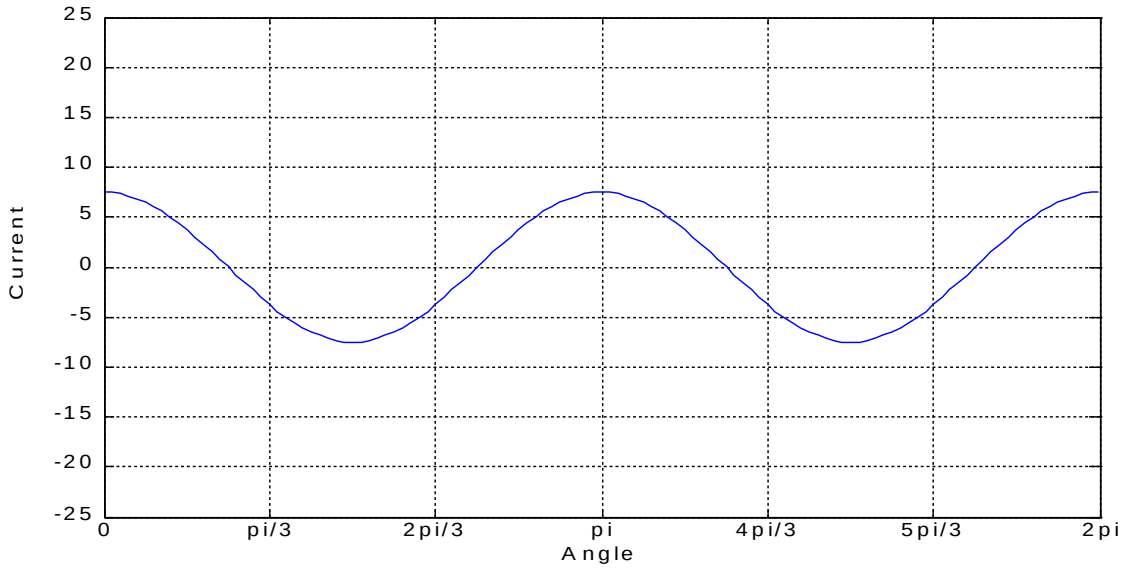

Figure 114

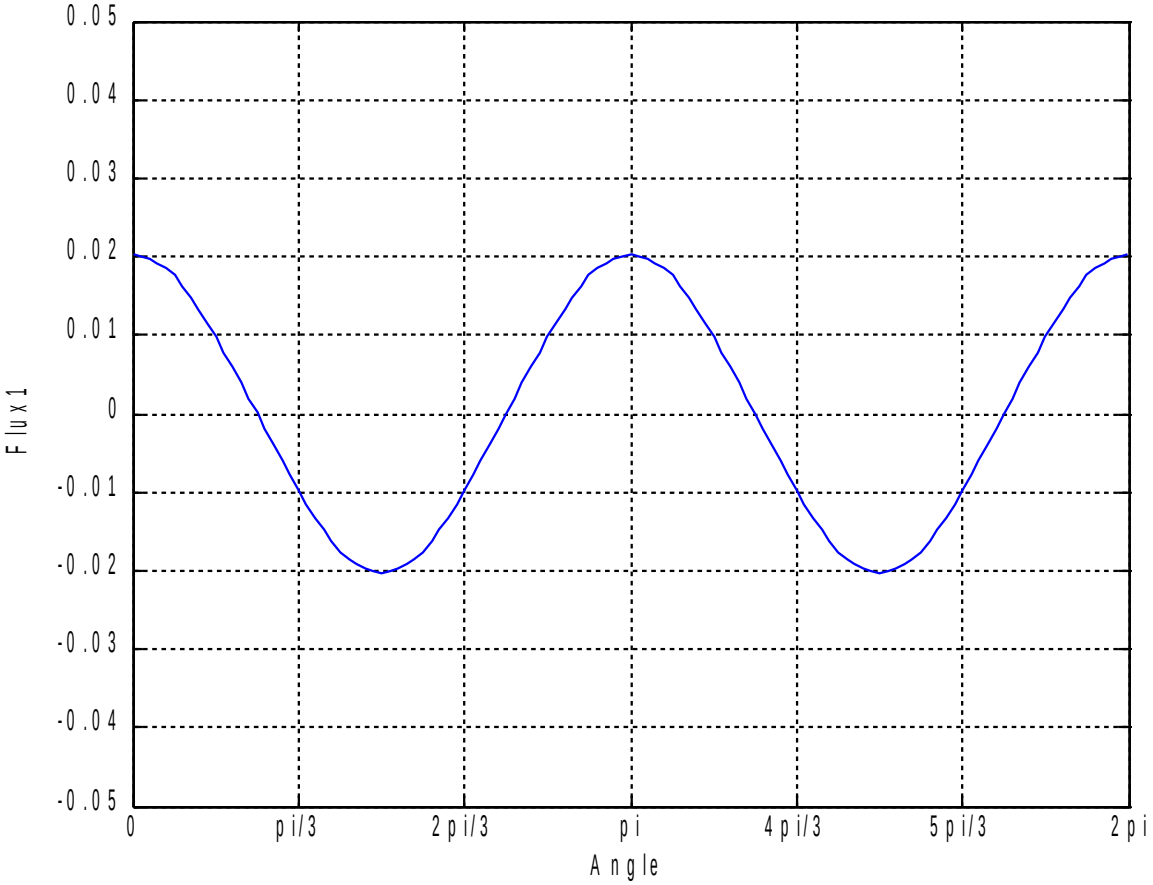

Figure 115

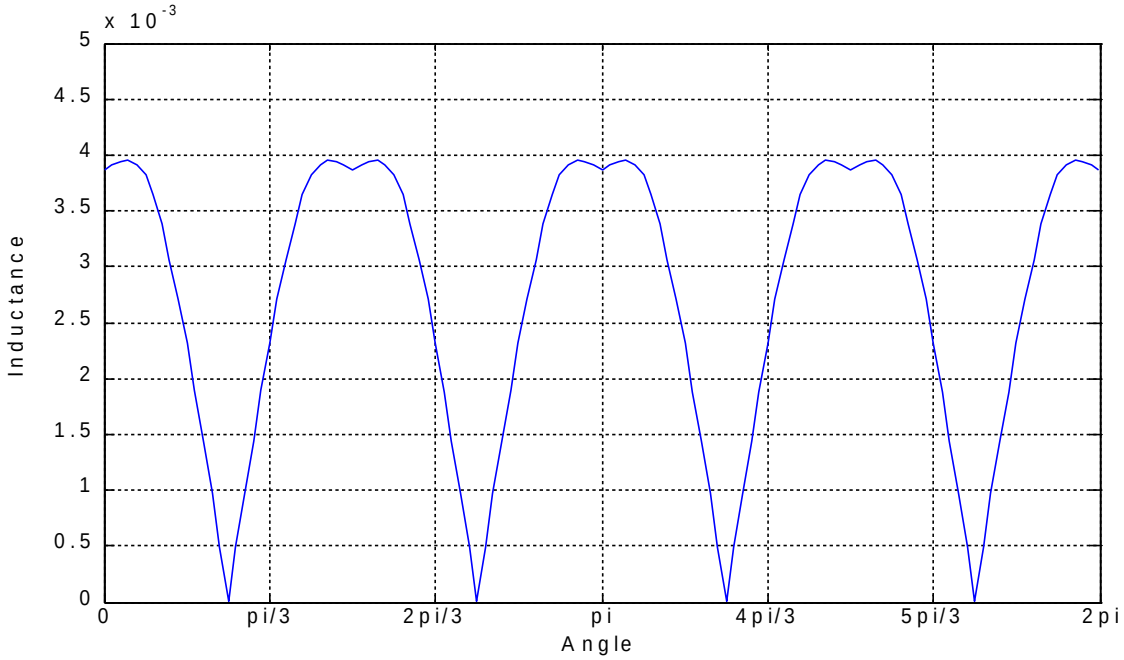

Figure 116

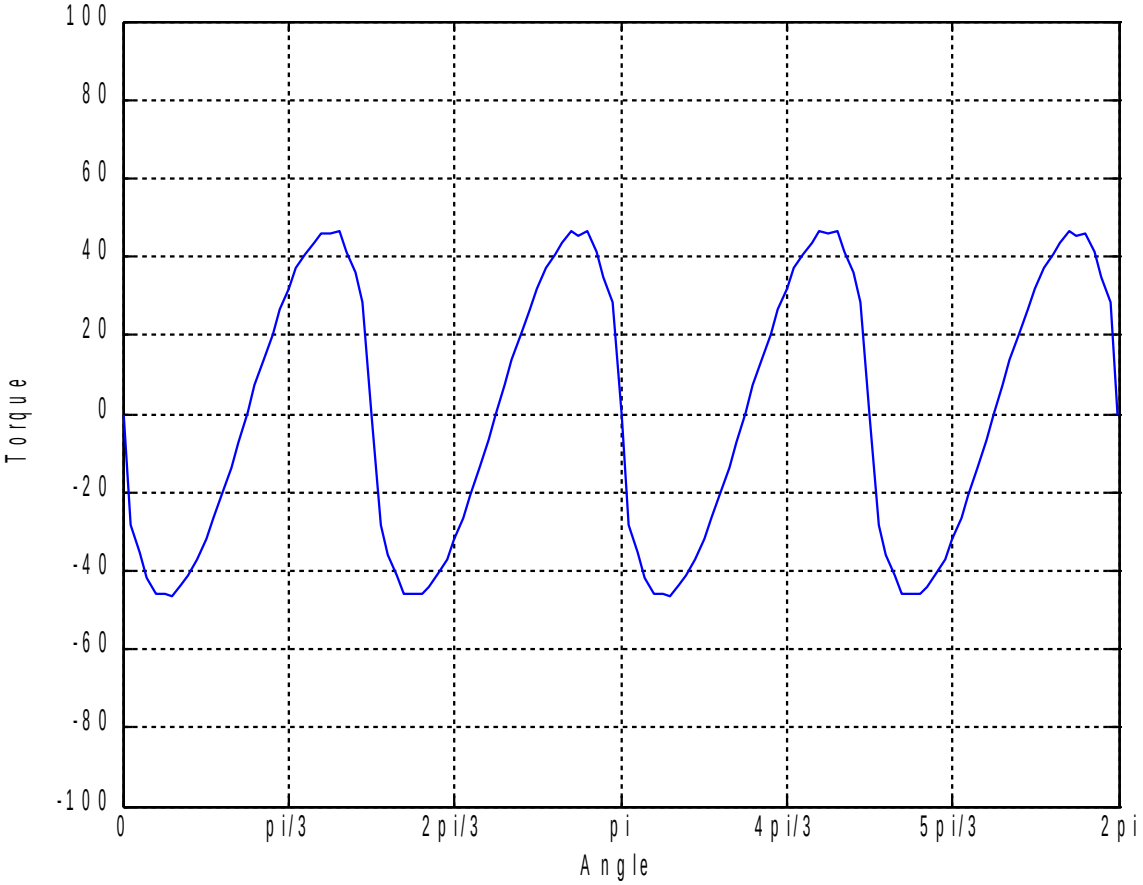

Figure 117

MMF = 750 At, φ=30°

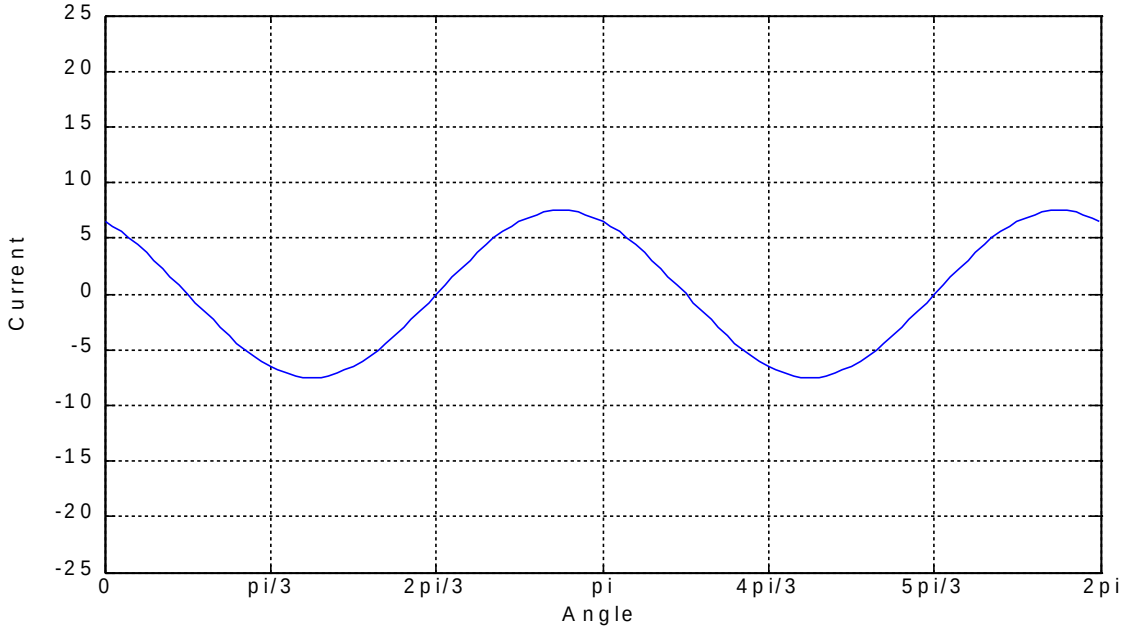

Figure 118

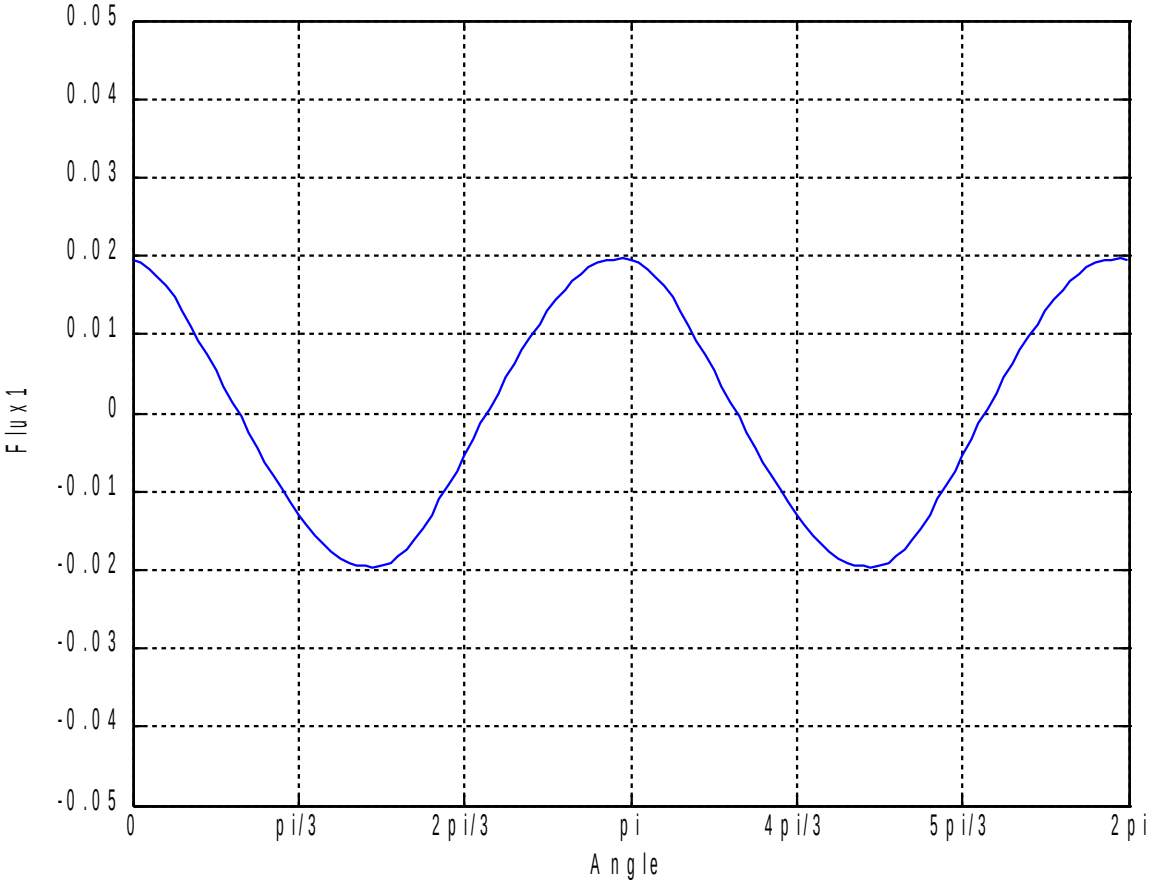

Figure 119

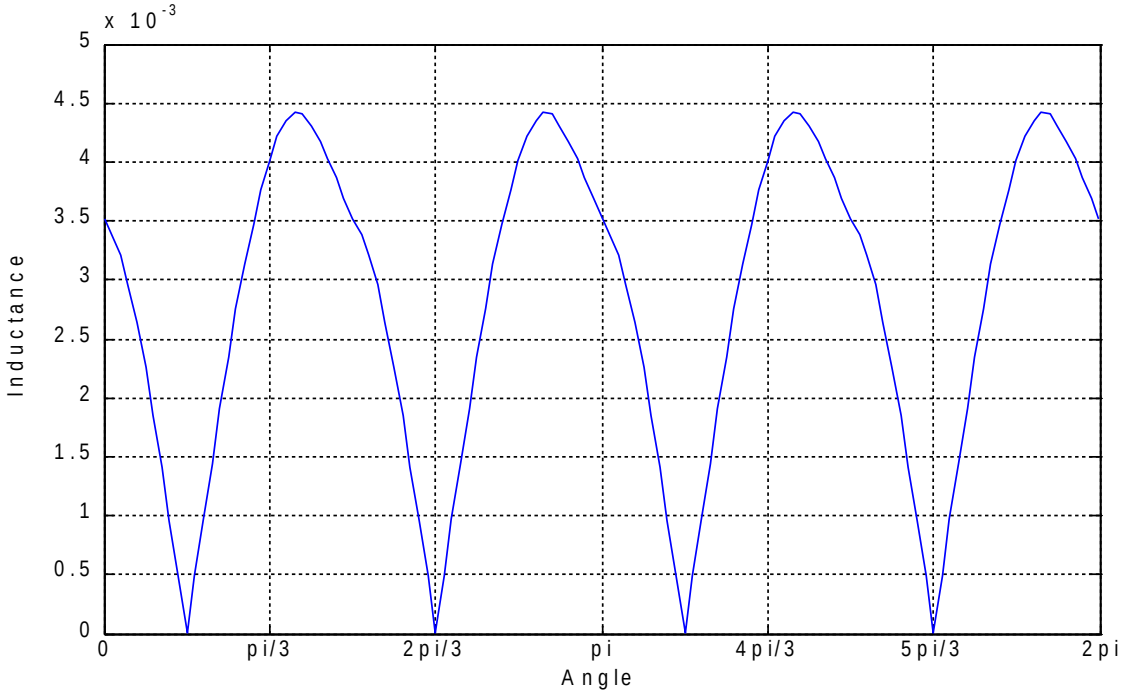

Figure 120

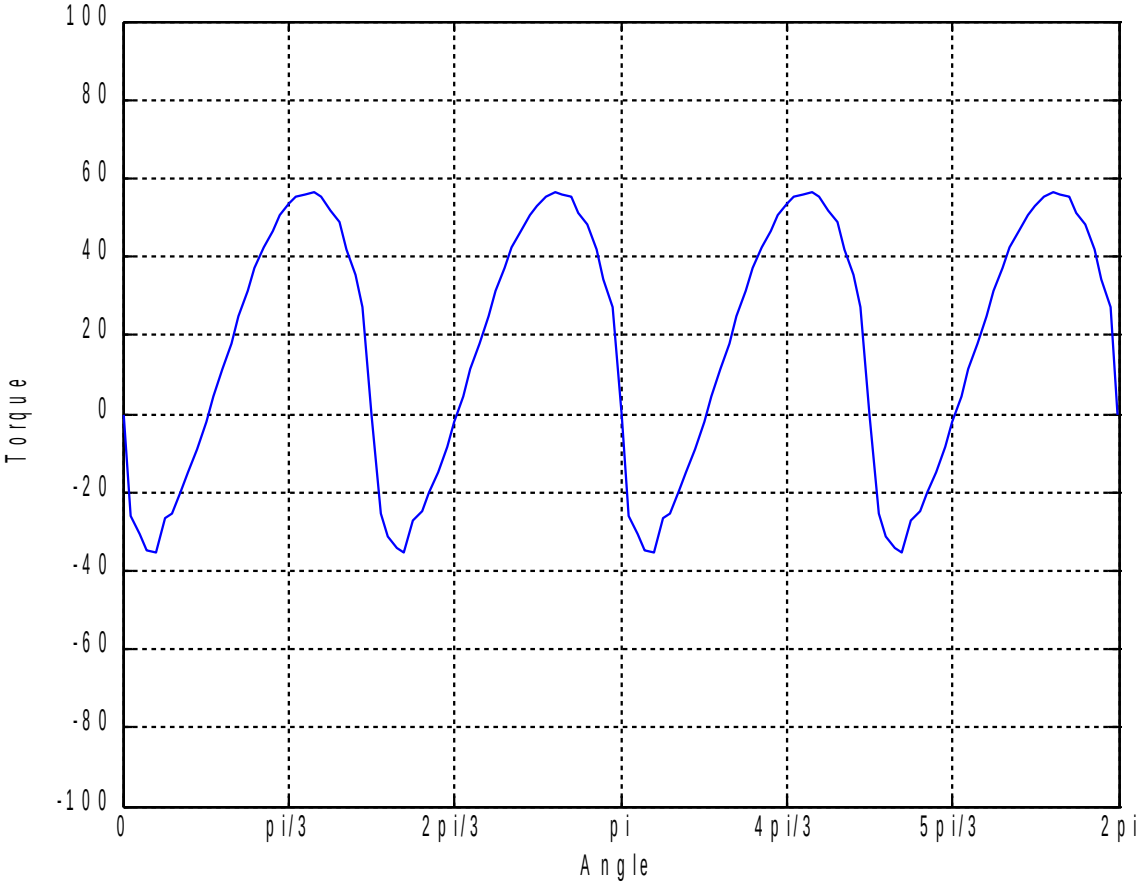

Figure 121

MMF = 750 At, φ=60°

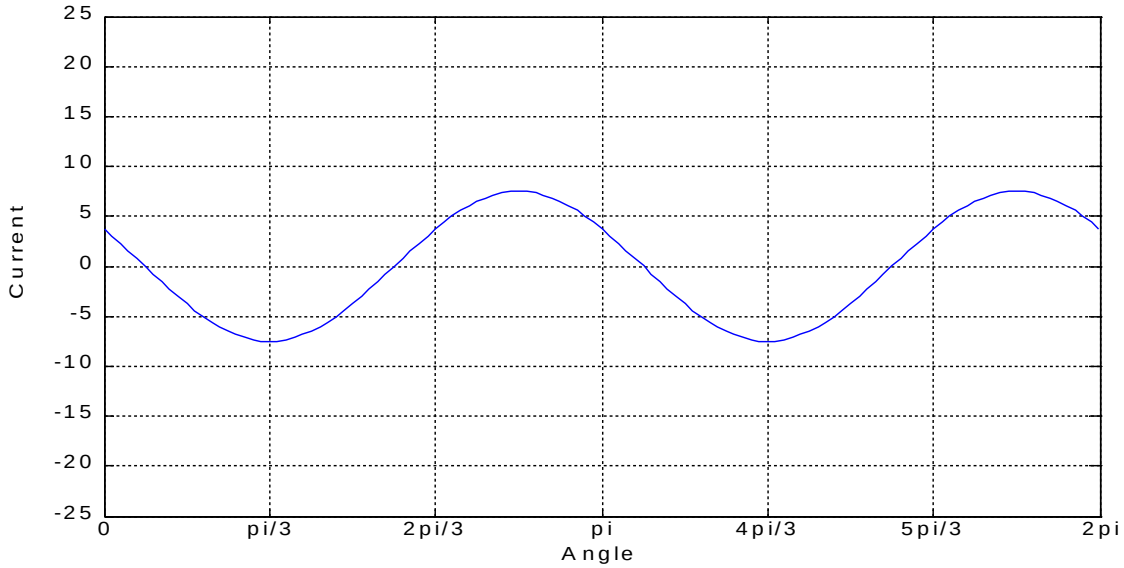

Figure 122

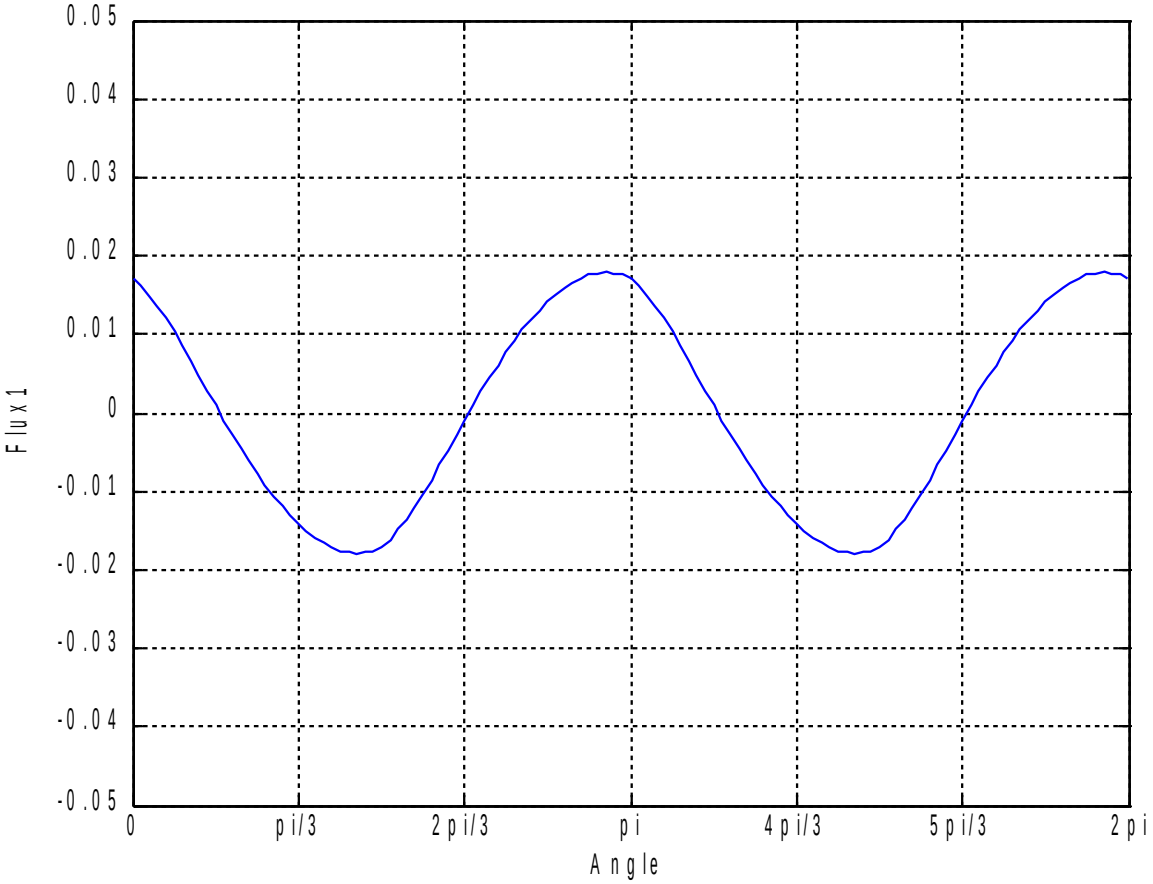

Figure 123

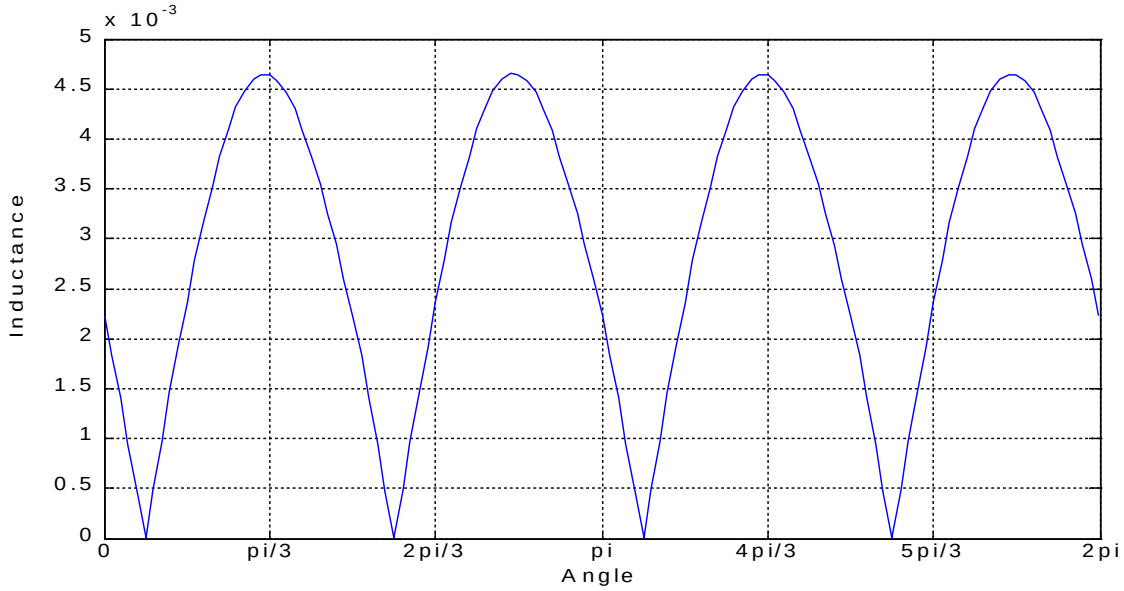

Figure 124

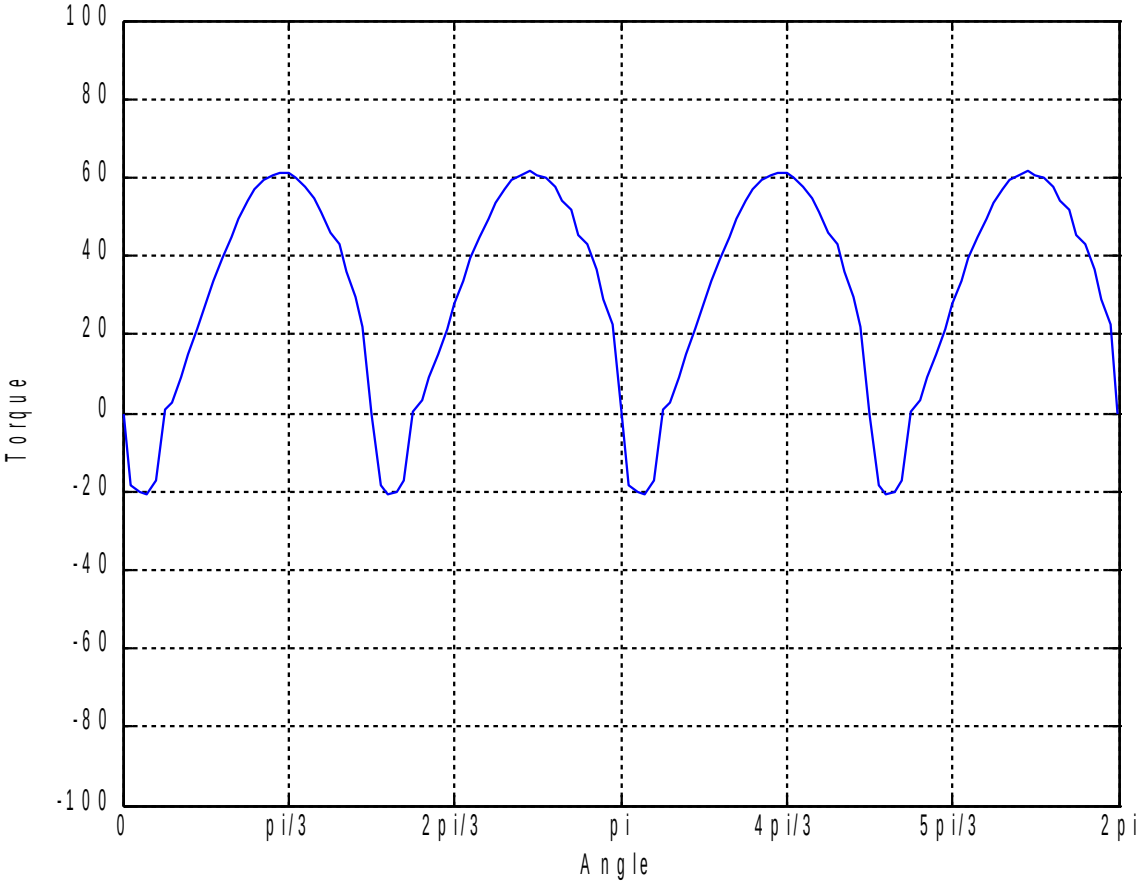

Figure 125

MMF = 750 At, φ=90°

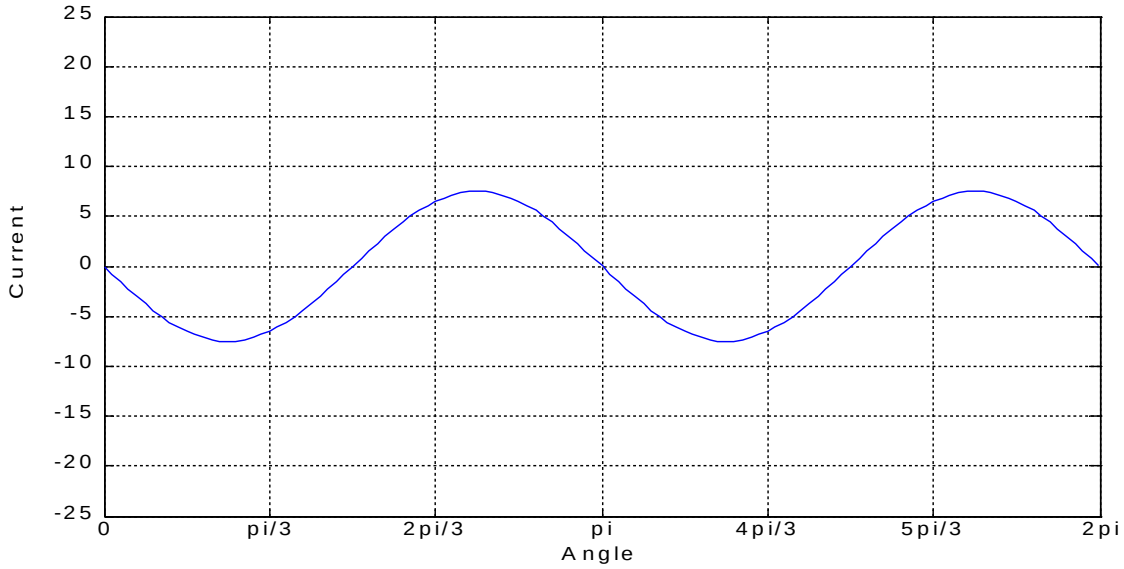

Figure 126

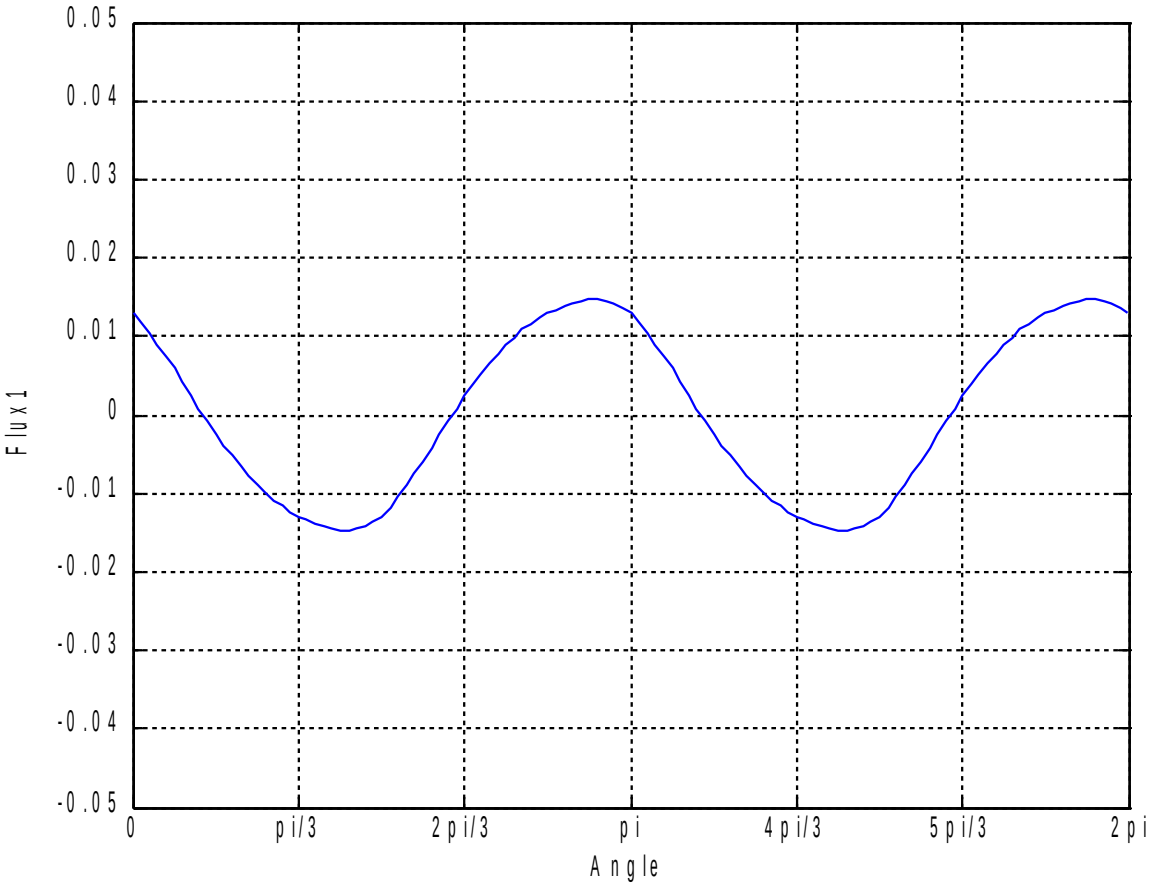

Figure 127

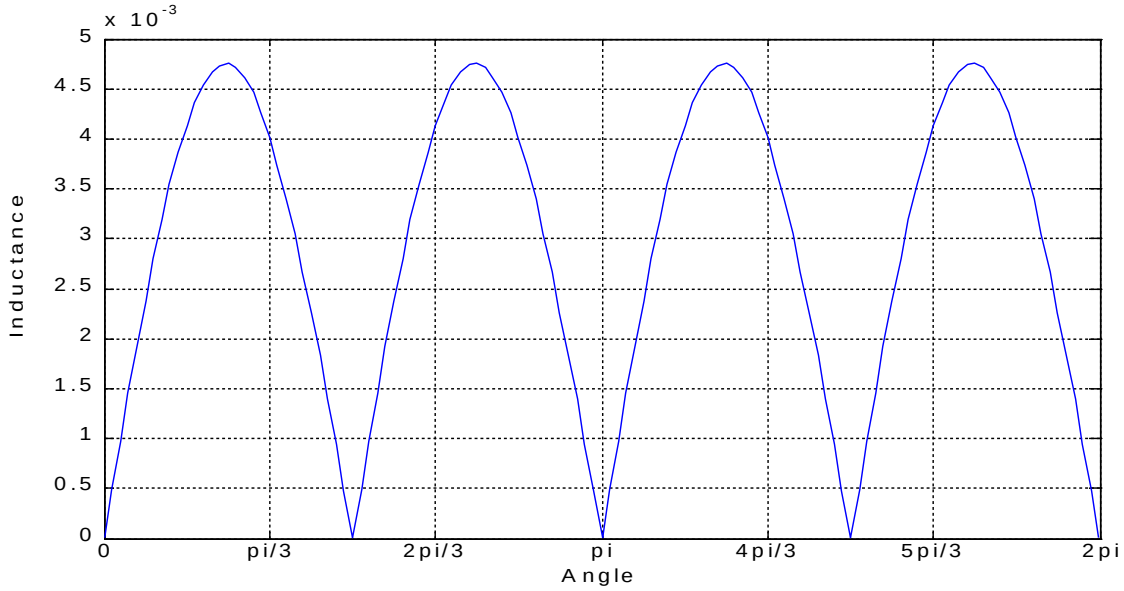

Figure 128

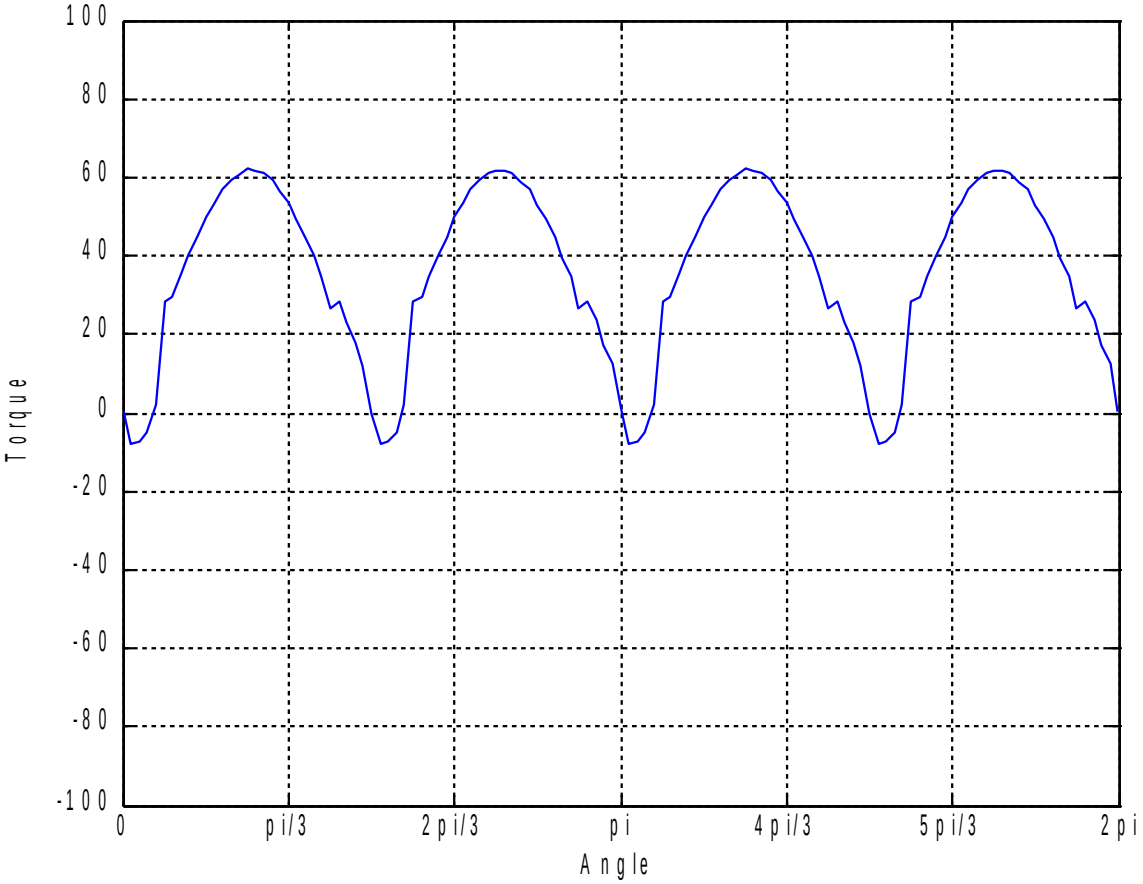

Figure 129

MMF = 1000 At, φ=0°

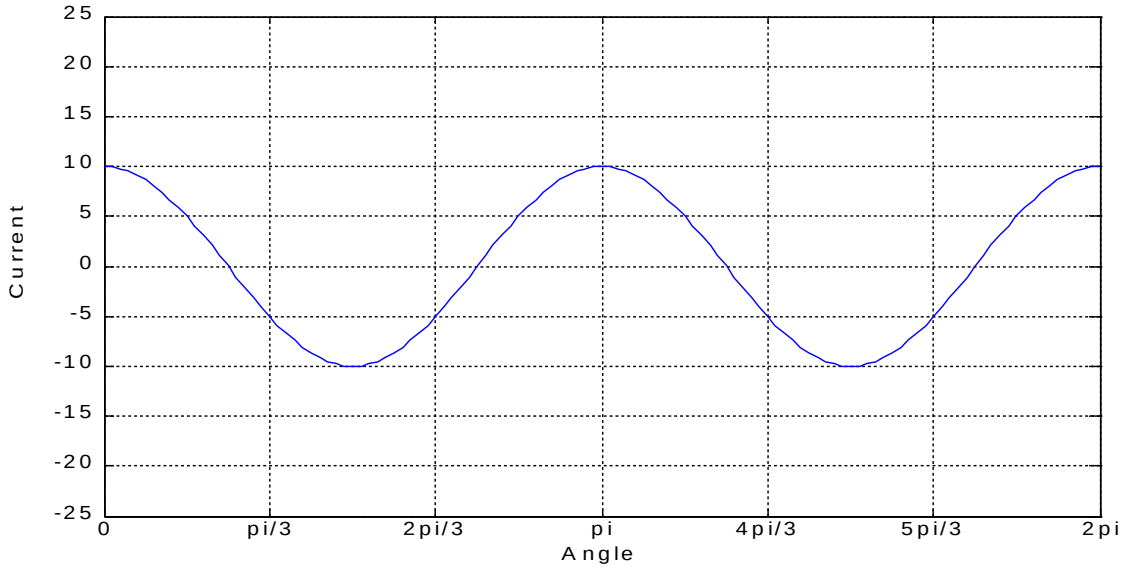

Figure 130

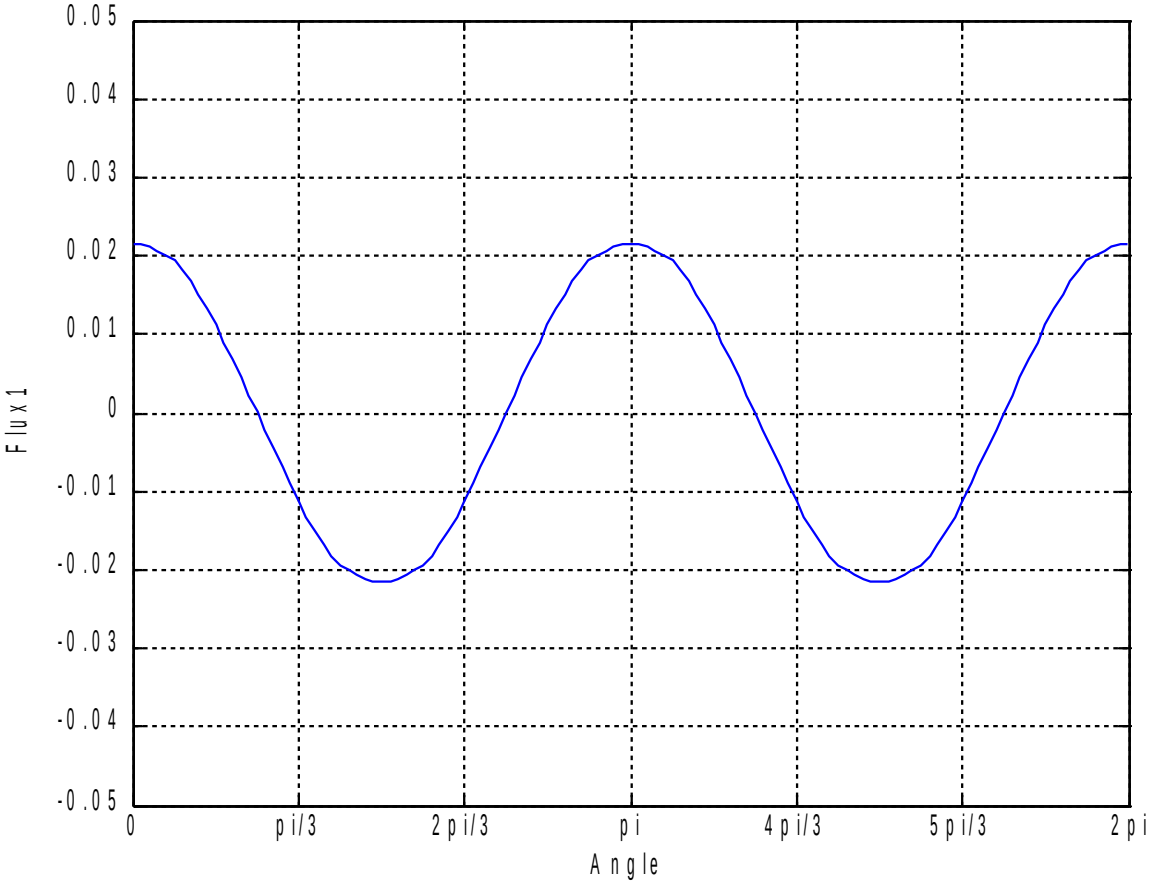

Figure 131

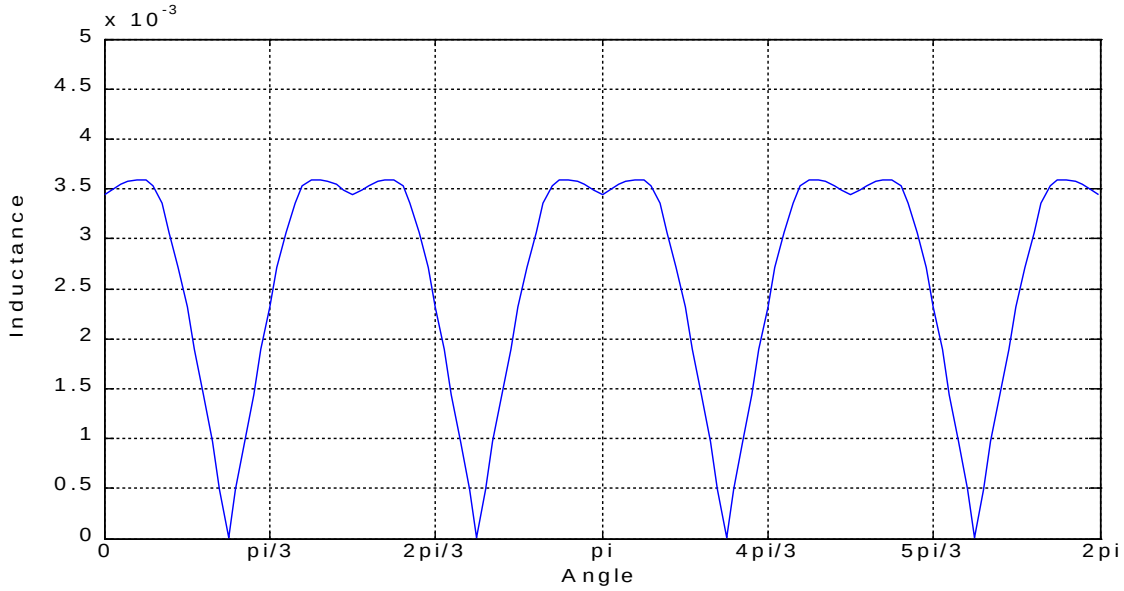

Figure 132

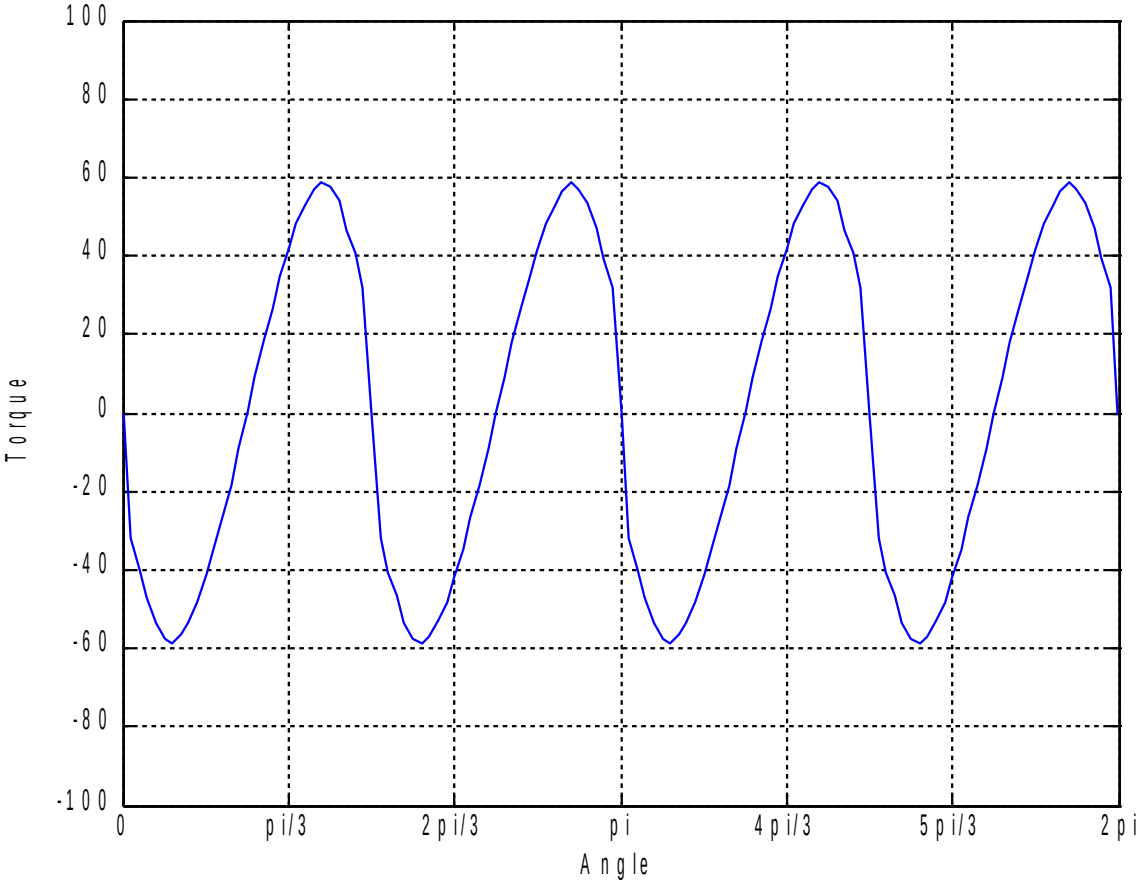

Figure 133

MMF = 1000 At, φ=30°

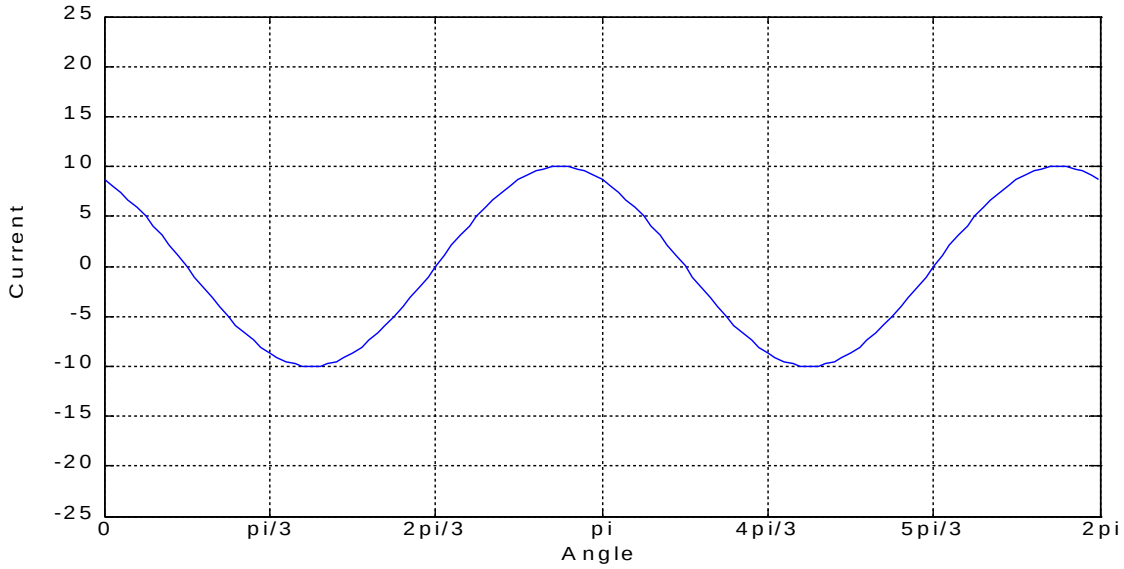

Figure 134

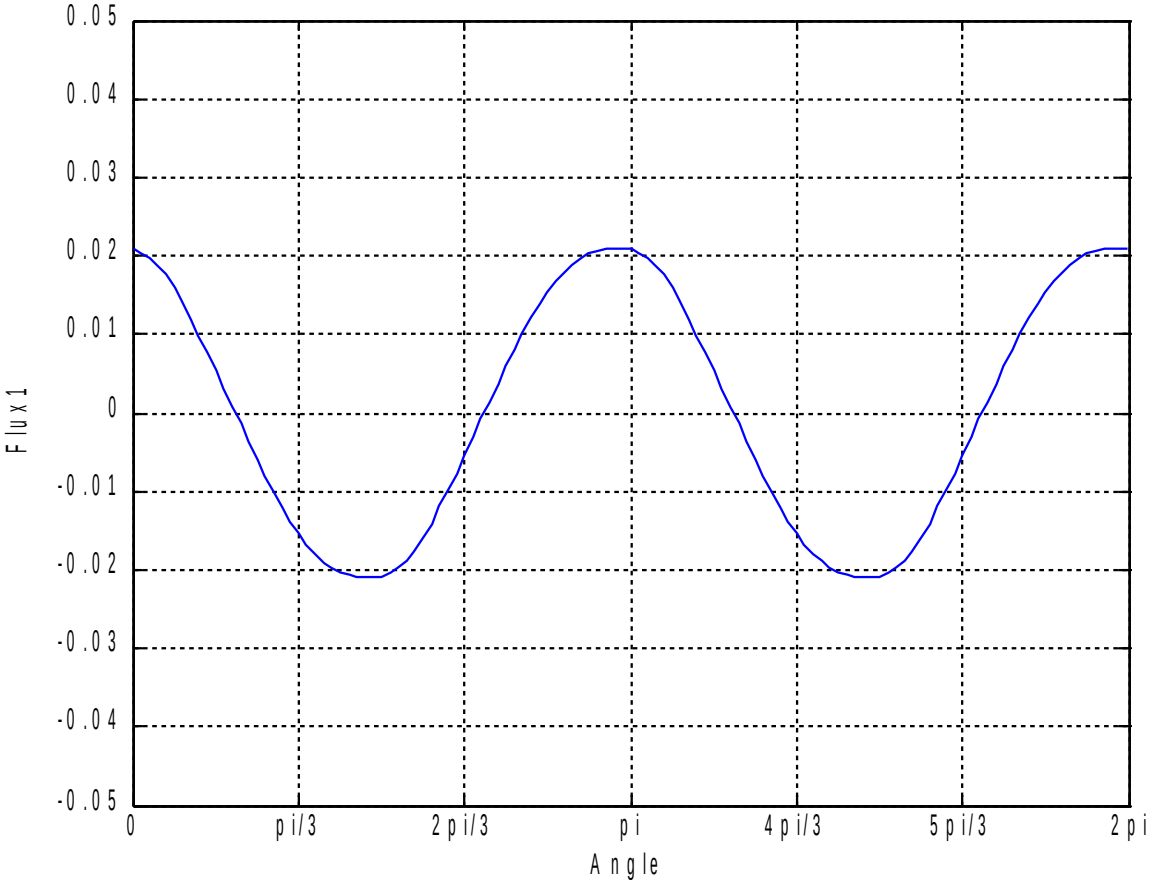

Figure 135

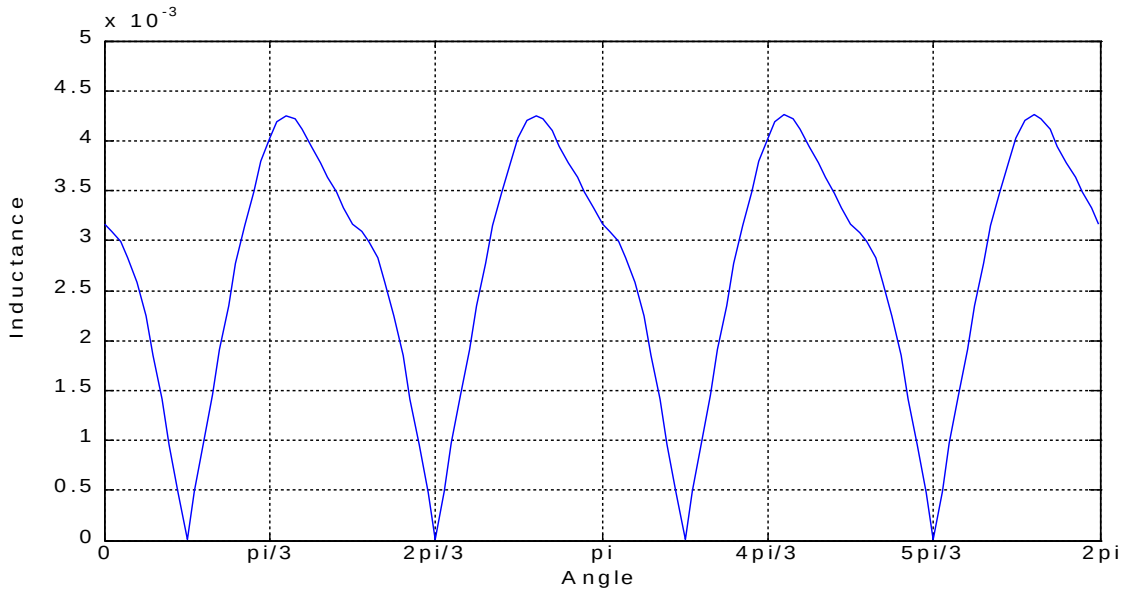

Figure 136

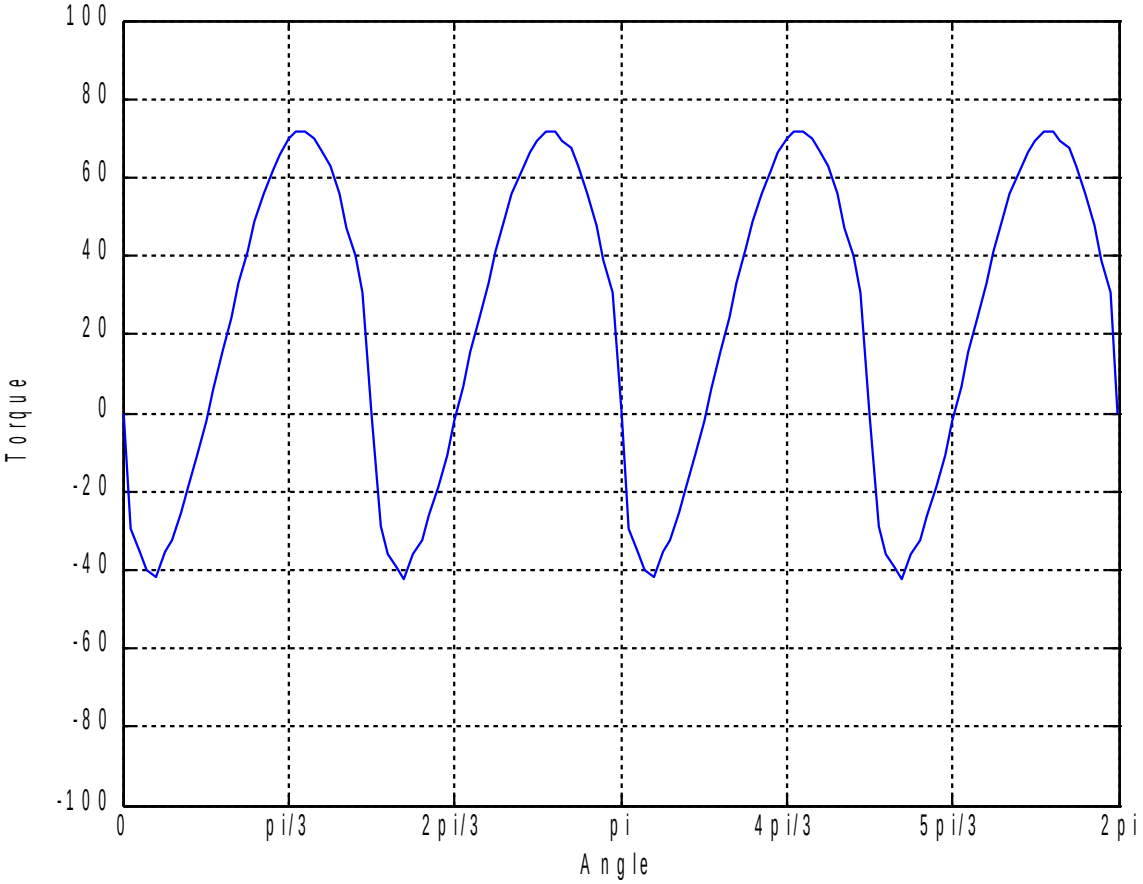

Figure 137

MMF = 1000 At, φ=60°

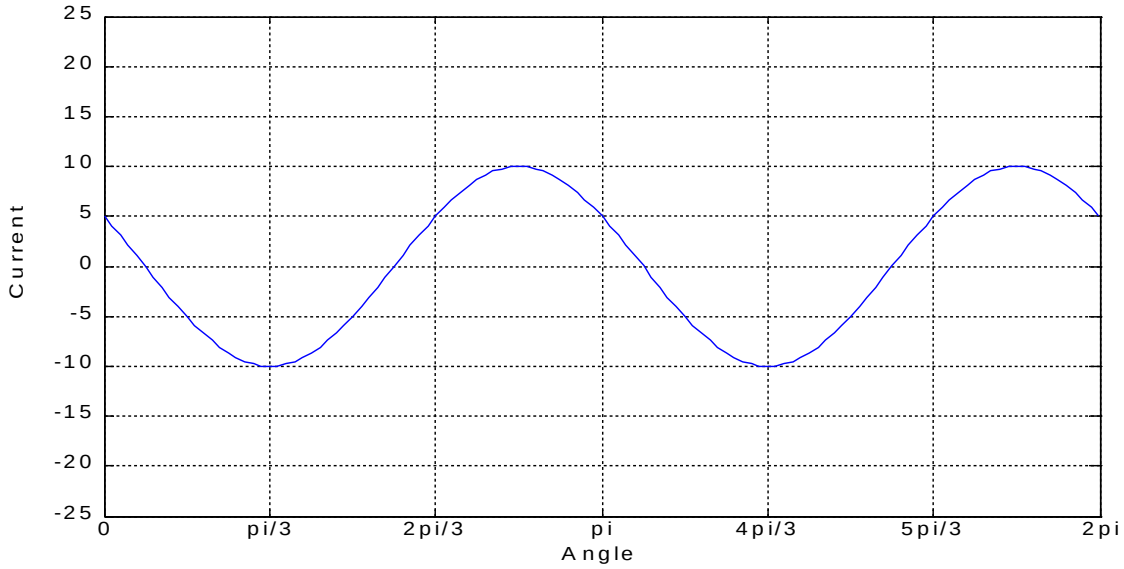

Figure 138

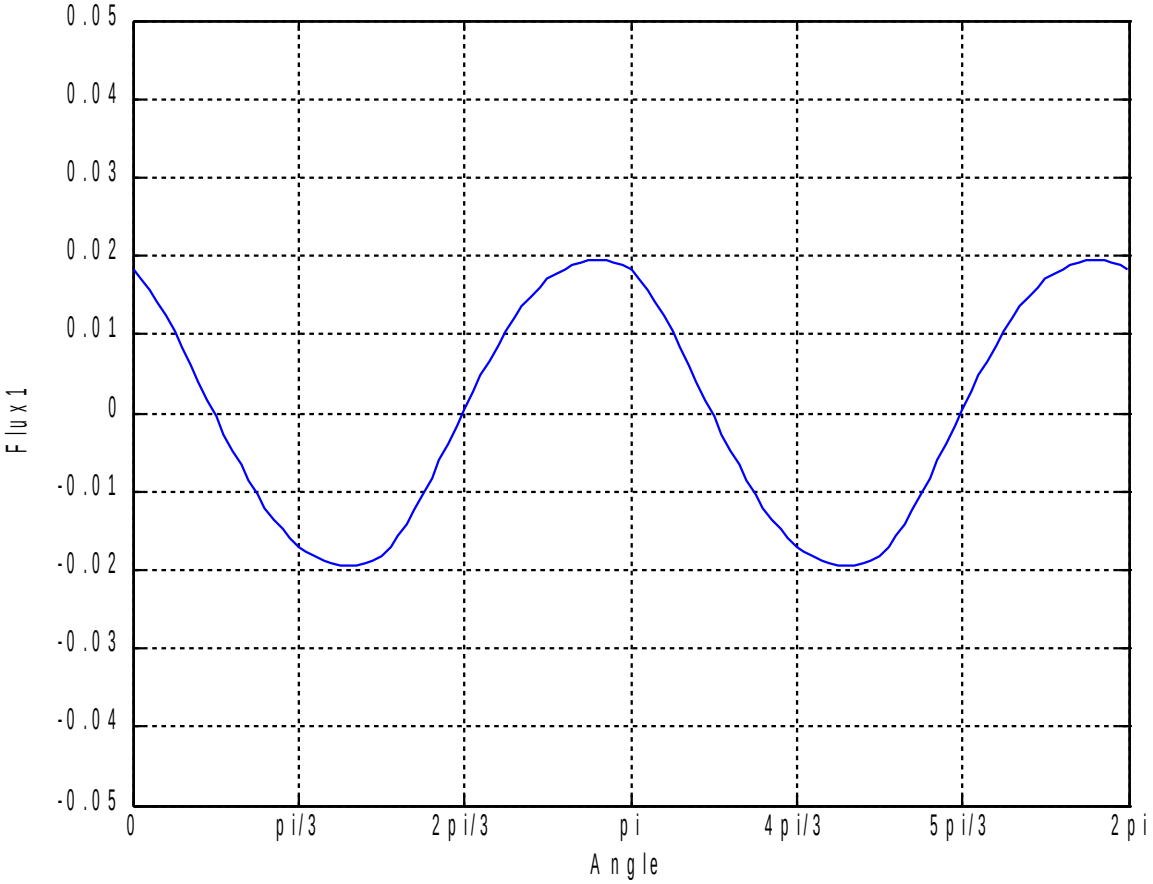

Figure 139

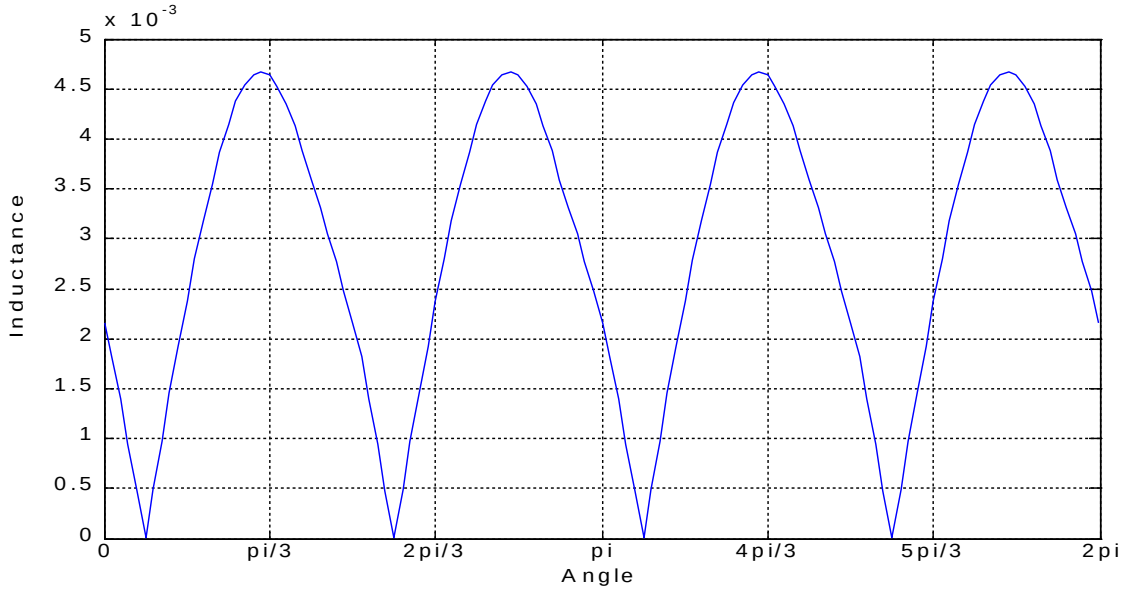

Figure 140

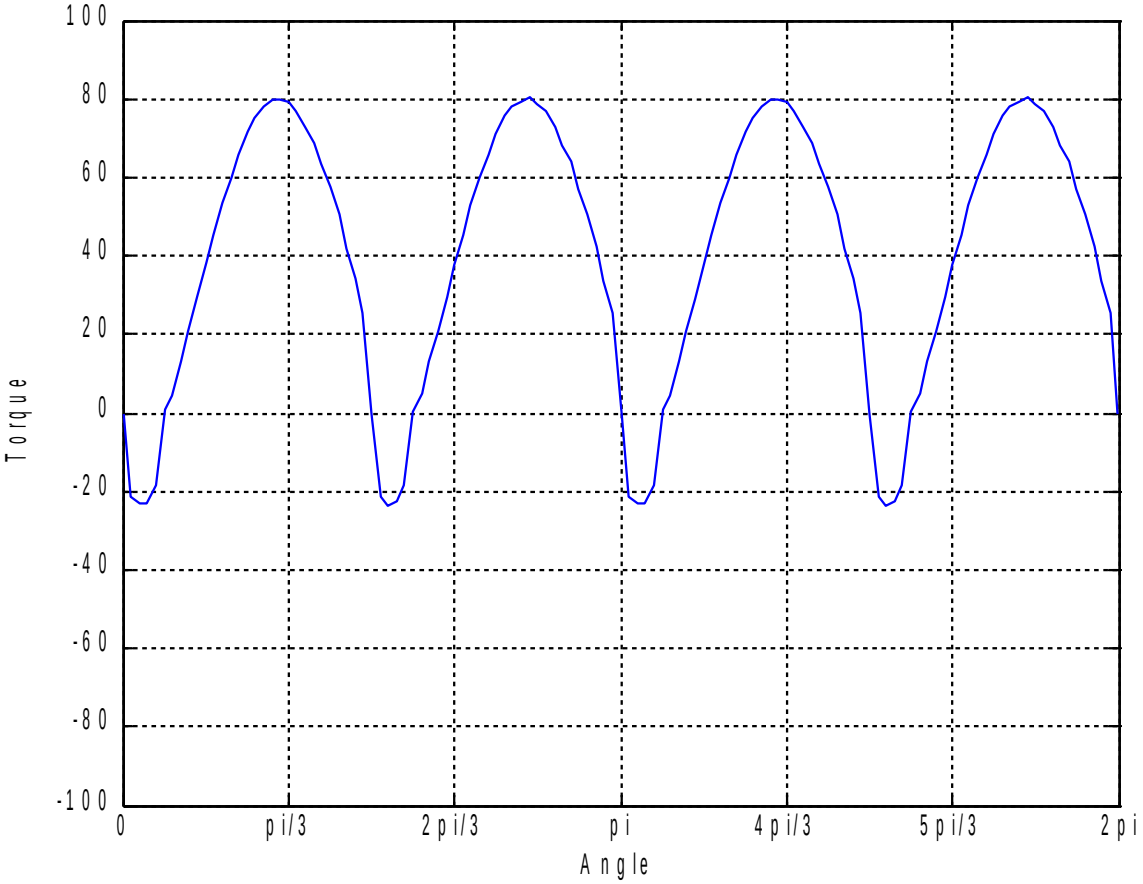

Figure 141

MMF = 1000 At, φ=90°

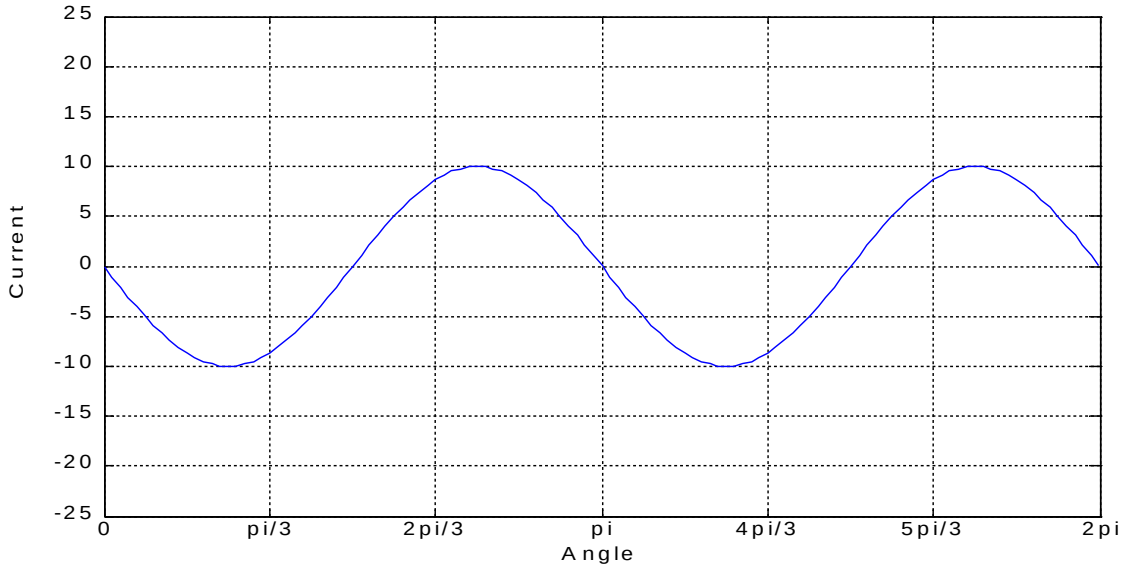

Figure 142

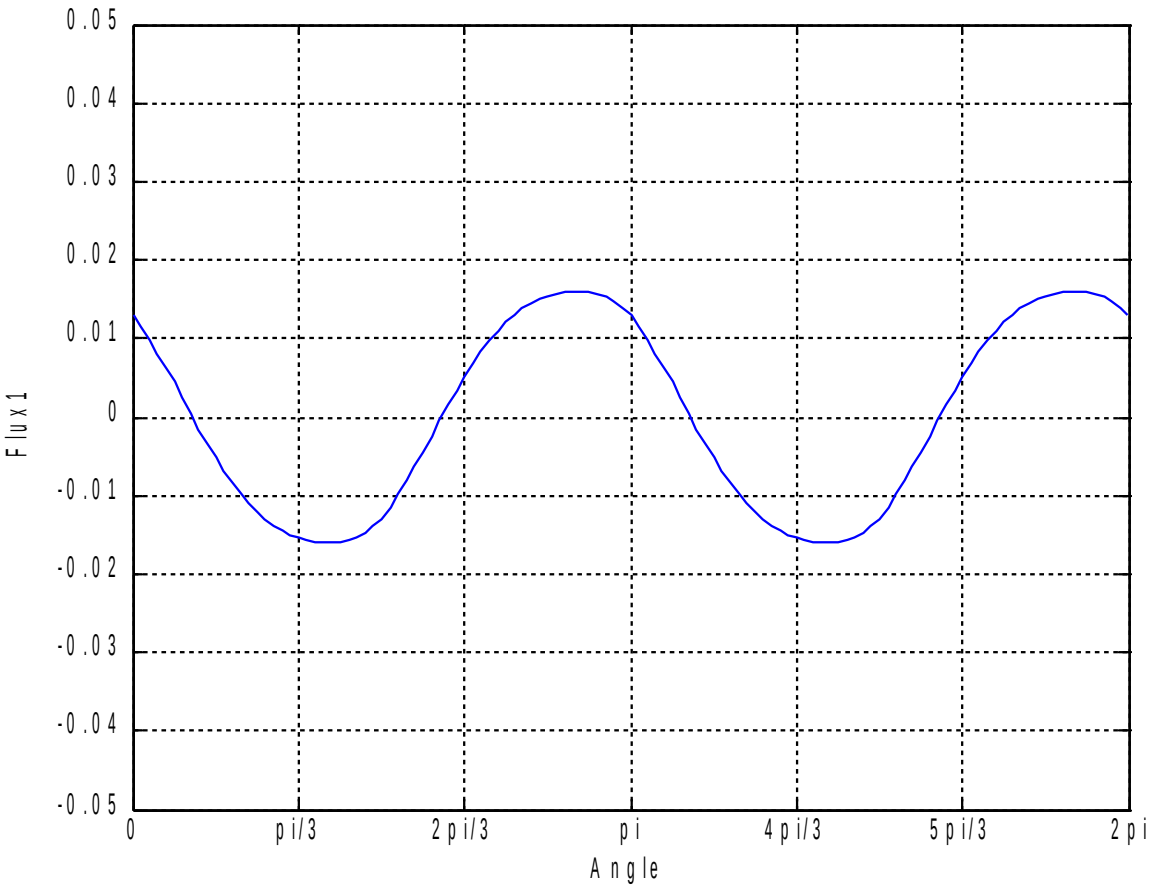

Figure 143

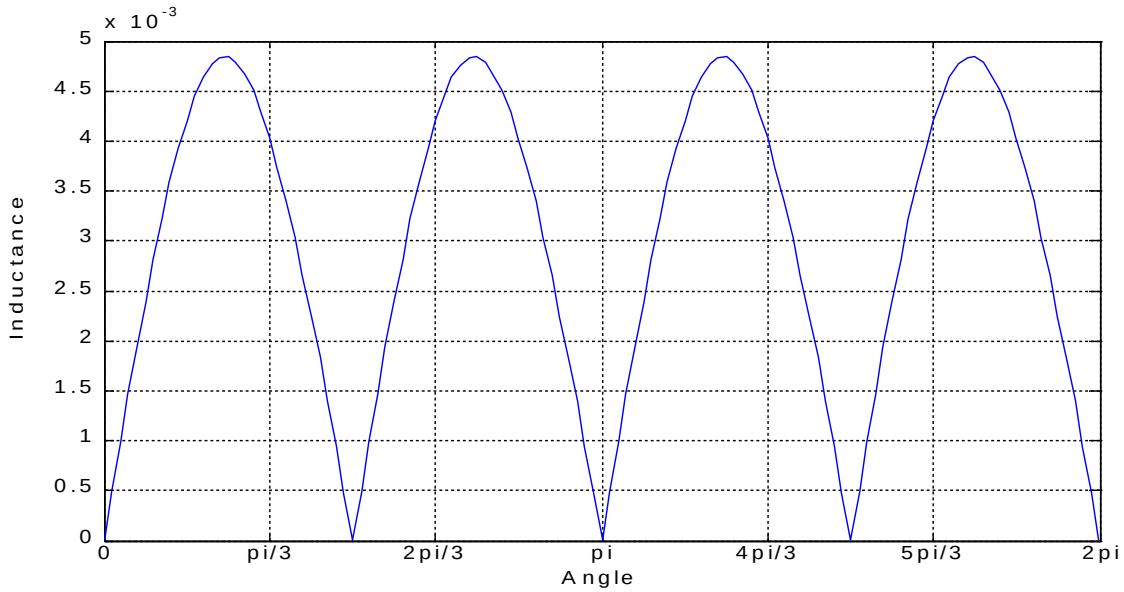

Figure 144

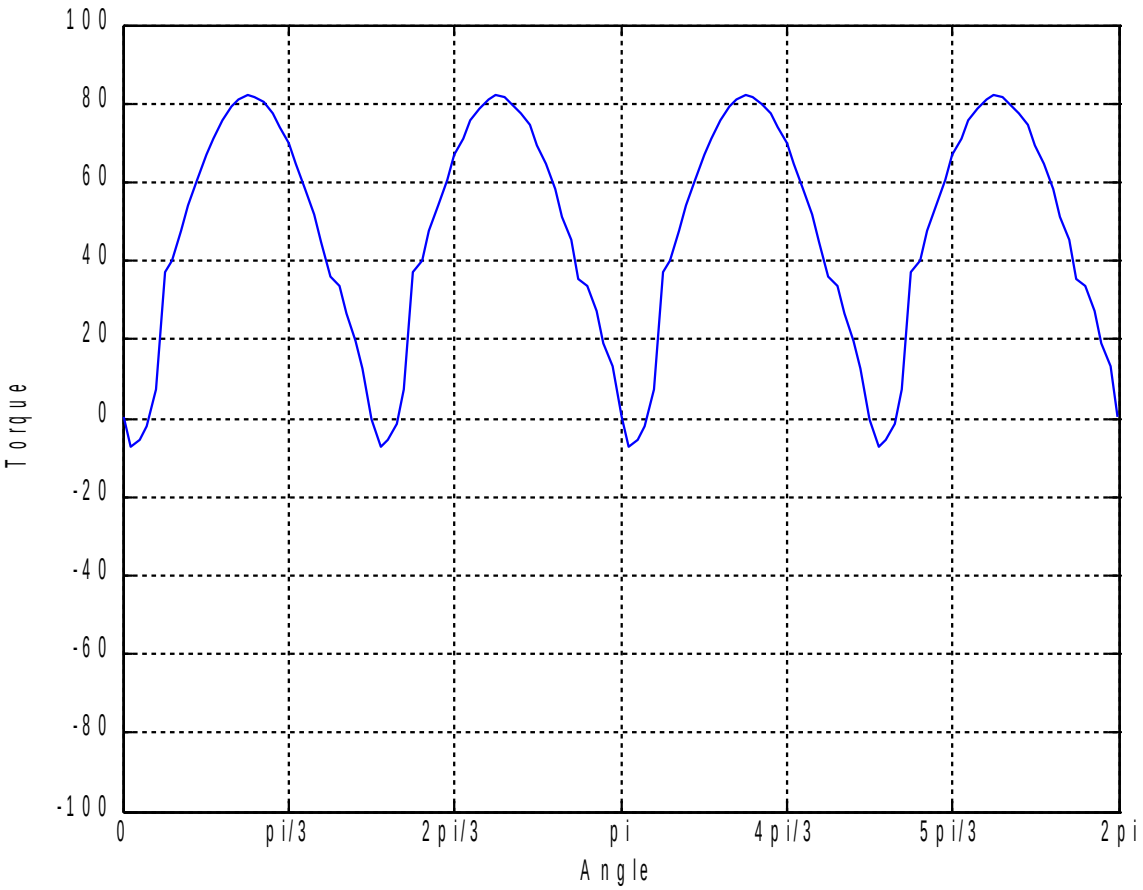
100
80
60
40
20
0
-20
-40
-60
-80
-100
Torque
0
pi/3
2pi/3
pi
4pi/3
5pi/3
2pi
Angle

Figure 145

4. Inductances

As it has been said before, the iron with which the machine is built is not linear, as it can be shown in the figure which reports its B – H characteristic

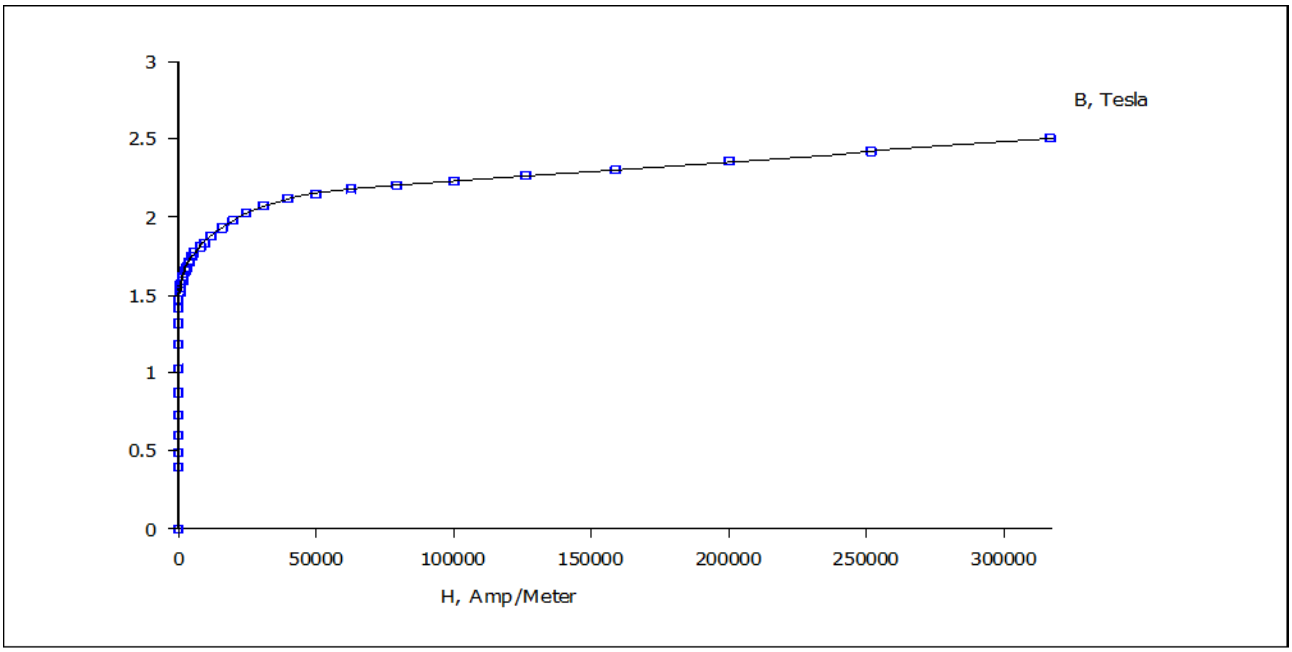

Figure 6

As a consequence, inductances of the two machines are not constant but decreasing with magnetomotive force. As it can be easily understood, the 4-poles configuration has a bigger electric load, due to the higher number of caves.To avoid the saturation phenomenon, and also to keep the value of the current density under certain safety values (J=10 A/mm^2), the MMF with which simulations have been made are different for the two configurations.

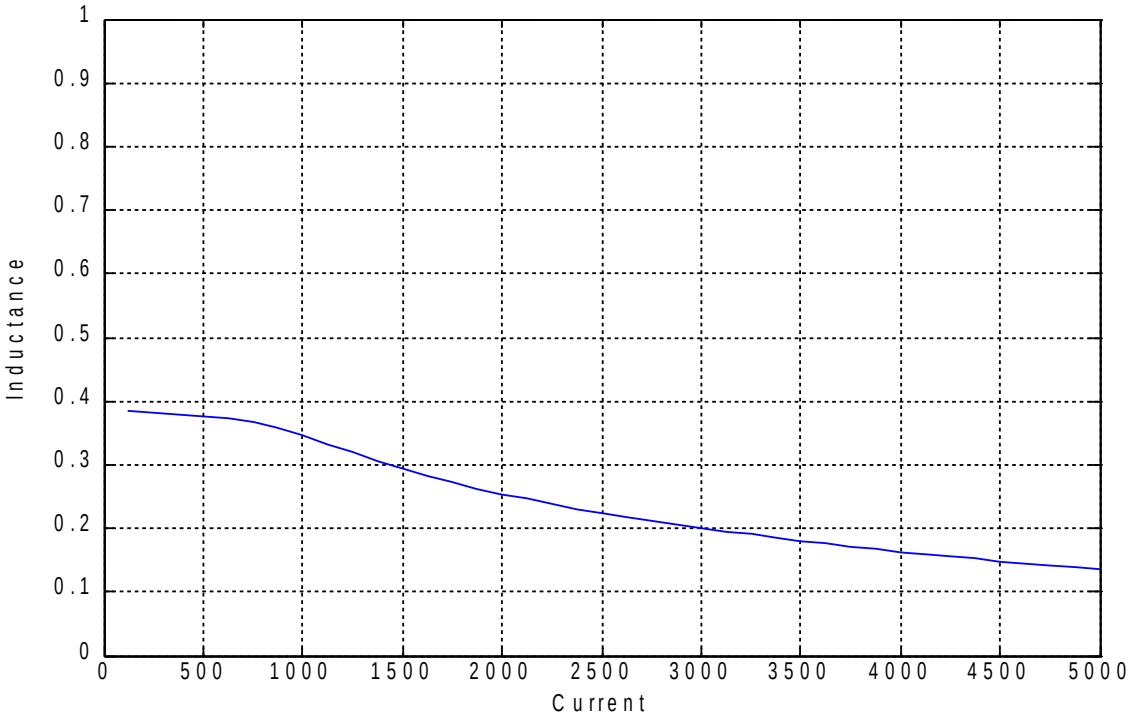

Figure 146

However, the behaviour is very similar in terms of self-inductance – with the parity of electric linear load, as it can be seen in the figures. The first one, Figure , has been obtained for the first configuration, and the second one, the following, for the 4-poles machine

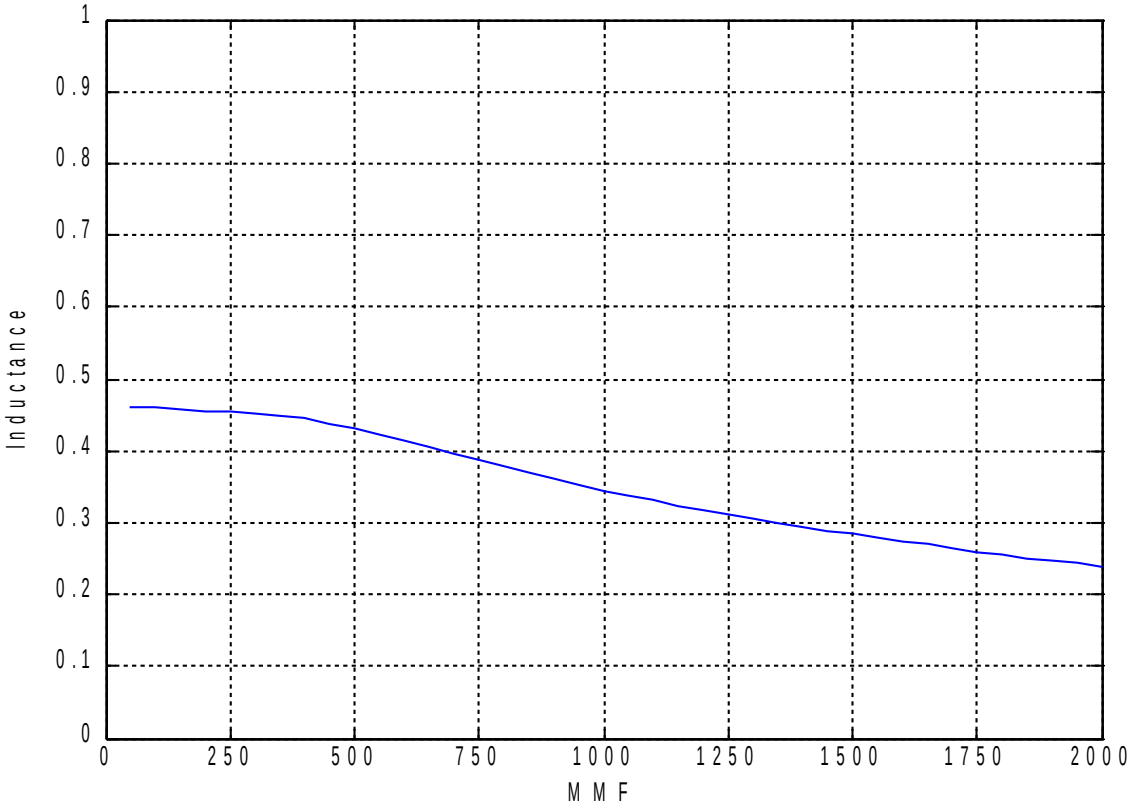

Figure 147

5. Starting Strategy

For many applications needing electromechanical machines the induction motor is chosen instead of other solutions. In fact its working principle is simple, the machine is usually robust and self-starting, with a pre-determined direction of rotation. However, this solution is not always the best, because of some characteristics of it, and in particular its non-constant speed of rotation when the load changes – for environmental reasons, for example. The synchronous permanent magnet-motor has all the advantages of the induction motor, but moreover it has a constant speed, whatever happens to the load.
On the other hand, there are some issues the brushless machine brings, such as: his magnetic field is not rotating but pulsing, so it is not self-starting, and the direction of rotation depends by the initial position of the rotor and by the initial phase of the feeding current. All these problems can be solved through an appropriate design of the machine and an efficient control system.
One way to make the machine become self-starting is to insert a coil which covers only a portion of the pole, making it become a shaded-pole machine. This shading coil makes the magnetic field non-symmetric, because of the opposing current which rises in the coil (short-circuited), and makes the rotor move. The disadvantage of this solution is the low efficiency of the machine.
The problem of the starting can also be solved through a specific geometry of the pole: if the pole is

asymmetric, in fact, the equilibrium position when the machine is not fed is not the aligned one, with the presence of an angle between the rotor direct axis and the stator one in position of rest. This angle is much bigger as bigger is the asymmetry in the geometry of the pole. This kind of shape permits the rotor to move when the current-due flux rises, because the shading coil makes the flux pass through the not shaded part of the pole in the firsts instants, but lets the flux itself pass once that the transient goes lower, making the rotor reach different positions for having the lowest energy: this makes the necessary starting torque take place.

6. Conclusions

The magnetic analysis of the machine has been concluded, and the profiles of reluctance, inductance and torque have been compared with the objective to give the best current feeding the machine.
As it was proposed, the analysed solution permits a reduction of the dimensions with respect to the traditional C-nucleus shape: the torque, in fact, is directly proportional to the volume of the machine in around the air gap. To have the same torque, it is necessary to have the same air-gap volume, but if the stator is outside, all the space necessary for the windings must go to increase the total volume of the machine.
Instead, with the internal stator solution, the windings are already inside the air gap volume, necessary to get the requested torque, and the additional volume outside of it is occupied only by the permanent magnets and by a crown of magnetic steel whose thickness is just the one needed not to saturate with the values of the flux passing through it.
This kind of machine can be an alternative to c-shaped nucleus synchrounous motors, or claw-pole ones.

7. Appendix

In the following chapter MatLab scripts used for simulations will be reported.

Macc1pp.m

```
clc
clear all
close all

turns=250;
u0=4*pi*10^-7;
um=u0*1.43486;
Br=0.4211;
r=0.05;
l=0.3;
beta=5*pi/6;
d=0.005;
Sm=r*l*beta;

addpath('C:\femm42\mfiles');
openfemm

opendocument('Macc1ppSilverio.fem');
mi_saveas('temp.fem');
n=71;
m=4;
zeta=4;
alfa=zeros(n,1);
f1=zeros(n,1);
f2=zeros(n,1);
L=zeros(n,1);
f0=zeros(n,1);
torque=zeros(n,1);
coenergy=zeros(n,1);
i=zeros(n,1);

for k=1:n
    disp(fprintf('iteration %i of %i',k,n));
    mi_analyze;
    mi_loadsolution;
    mo_groupselectblock(1);
    alfa(k)=2*pi*(k-1)/(n-1);
    mo_seteditmode('contour')
    mo_addcontour(-1.6,0)
    mo_addcontour(1.6,0)
    flux=mo_lineintegral(0);
    mo_clearcontour
    f0(k)=flux(1);
    mo_seteditmode('area')
    mo_groupselectblock(1)
    torque(k)=mo_blockintegral(22);
    coenergy(k)=mo_blockintegral(17);
    mi_selectgroup(1);
    mi_moverotate(0, 0, 360/(n-1));
    mi_clearselected
end

figure(101)
plot(alfa,f0)
xlabel('Angle');
ylabel('Flux 0');
```

```
set(gca,'XTick',0:pi/3:2*pi);
set(gca,'XTickLabel',{'0','pi/3','2pi/3','pi','4pi/3','5pi/3','2pi'});
axis([0,2*pi,-0.05,0.05]);
grid on

figure(106)
plot(alfa,torque)
xlabel('Angle');
ylabel('Torque');
set(gca,'XTick',0:pi/3:2*pi);
set(gca,'XTickLabel',{'0','pi/3','2pi/3','pi','4pi/3','5pi/3','2pi'});
axis([0,2*pi,-20,20]);
grid on

figure(107)
plot(alfa,coenergy)
xlabel('Angle');
ylabel('Coenergy');
set(gca,'XTick',0:pi/3:2*pi);
set(gca,'XTickLabel',{'0','pi/3','2pi/3','pi','4pi/3','5pi/3','2pi'});
axis([0,2*pi,0,150]);
grid on

for z=1:zeta
    I=2^(z-1);
    Ieff=I/sqrt(2);
    for j=1:m
        mi_selectgroup(1);
        mi_moverotate(0, 0, -360/(n-1));
        mi_clearselected
        phi=(j-1)*(pi/6);
        for k=1:n
            disp(fprintf('iteration %i of %i',k,n));
            i(k)=I*cos(alfa(k)+phi);
            mi_modifycircprop('Current',1,i(k));
            mi_modifycircprop('-Current',1,-i(k));
            mi_analyze;
            mi_loadsolution;
            mo_groupselectblock(1);
            mo_seteditmode('contour')
            mo_addcontour(-1.6,0)
            mo_addcontour(1.6,0)
            flux=mo_lineintegral(0);
            mo_clearcontour
            f1(k)=flux(1);
            mo_seteditmode('area')
            mo_groupselectblock(1)
            torque(k)=mo_blockintegral(22);
            coenergy(k)=mo_blockintegral(17);
            L(k)=turns*abs((f1(k)-f0(k))./i(k));
            mi_selectgroup(1);
            mi_moverotate(0, 0, 360/(n-1));
            mi_clearselected

        end

    figure(100*z+10*j+1)
    plot (alfa,f1)
    set(gca,'XTick',0:pi/3:2*pi);
    set(gca,'XTickLabel',{'0','pi/3','2pi/3','pi','4pi/3','5pi/3','2pi'});
    xlabel('Angle');
    ylabel('Flux');
    axis([0,2*pi,-0.05,0.05]);
    grid on
```

```
    figure(100*z+10*j+5)
    plot (alfa,L)
    set(gca,'XTick',0:pi/3:2*pi);
    set(gca,'XTickLabel',{'0','pi/3','2pi/3','pi','4pi/3','5pi/3','2pi'});
    xlabel('Angle');
    ylabel('Inductance');
    axis([0,2*pi,0,1]);
    grid on

    figure(100*z+10*j+6)
    plot (alfa,torque)
    set(gca,'XTick',0:pi/3:2*pi);
    set(gca,'XTickLabel',{'0','pi/3','2pi/3','pi','4pi/3','5pi/3','2pi'});
    xlabel('Angle');
    ylabel('Torque');
    axis([0,2*pi,-100,100]);
    grid on

    figure(100*z+10*j+7)
    plot (alfa,coenergy)
    set(gca,'XTick',0:pi/3:2*pi);
    set(gca,'XTickLabel',{'0','pi/3','2pi/3','pi','4pi/3','5pi/3','2pi'});
    xlabel('Angle');
    ylabel('Coenergy');
    axis([0,2*pi,0,150]);
    grid on

    figure(100*z+10*j+8)
    plot (alfa,i)
    set(gca,'XTick',0:pi/3:2*pi);
    set(gca,'XTickLabel',{'0','pi/3','2pi/3','pi','4pi/3','5pi/3','2pi'});
    xlabel('Angle');
    ylabel('Current');
    axis([0,2*pi,-25,25]);
    grid on

    end

end

closefemm
```

Macc2pp.m

```
clc
clear all
close all

turns=100;
u0=4*pi*10^-7;
um=u0*1.43486;
Br=0.4211;
r=0.05;
l=0.3;
beta=5*pi/12;
d=0.005;
Sm=r*l*beta;
omegar=2*pi*50;

addpath('C:\femm42\mfiles');
openfemm
```

```
opendocument('Macc2pp(2).fem');
mi_saveas('temp.fem');
n=71;
m=4;
zeta=4;

x=zeros(n,1);
alfa=zeros(n,1);
f1=zeros(n,1);
f01=zeros(n,1);
L1=zeros(n,1);
torque=zeros(n,1);
coenergy=zeros(n,1);
i=zeros(n,1);

for k=1:n
    disp(fprintf('iteration %i of %i',k,n));
    mi_analyze;
    mi_loadsolution;
    mo_seteditmode('contour')
    mo_addcontour(-3,6)
    mo_addcontour(3,6)
    flux1=mo_lineintegral(0);
    alfa(k)=2*pi*(k-1)/(n-1);
    x(k)=2*pi*(k-1)/(n-1);
    f01(k)=flux1(1);
    mo_seteditmode('area')
    mo_groupselectblock(1)
    torque(k)=mo_blockintegral(22);
    coenergy(k)=mo_blockintegral(17);
    mi_selectgroup(1);
    mi_moverotate(0, 0, 360/(n-1));
    mi_clearselected
end

figure(101)
plot (x,f01)
set(gca,'XTick',0:pi/3:2*pi);
set(gca,'XTickLabel',{'0','pi/3','2pi/3','pi','4pi/3','5pi/3','2pi'});
xlabel('Angle');
ylabel('Flux 01');
axis([0,2*pi,-0.05,0.05]);
grid on

figure (106)
plot (x,torque)
set(gca,'XTick',0:pi/3:2*pi);
set(gca,'XTickLabel',{'0','pi/3','2pi/3','pi','4pi/3','5pi/3','2pi'});
xlabel('Angle');
ylabel('Torque')
axis([0,2*pi,-100,100]);
grid on

figure (1062)
plot (x,torque)
set(gca,'XTick',0:pi/3:2*pi);
set(gca,'XTickLabel',{'0','pi/3','2pi/3','pi','4pi/3','5pi/3','2pi'});
xlabel('Angle');
ylabel('Torque')
axis([0,2*pi,-20,20]);
grid on

figure (107)
plot (x,coenergy)
```

```
set(gca,'XTick',0:pi/3:2*pi);
set(gca,'XTickLabel',{'0','pi/3','2pi/3','pi','4pi/3','5pi/3','2pi'});
xlabel('Angle');
ylabel('Coenergy')
axis([0,2*pi,0,100]);
grid on

figure (1072)
plot (x,coenergy)
set(gca,'XTick',0:pi/3:2*pi);
set(gca,'XTickLabel',{'0','pi/3','2pi/3','pi','4pi/3','5pi/3','2pi'});
xlabel('Angle');
ylabel('Coenergy')
axis([0,2*pi,0,50]);
grid on

figure (1073)
plot (x,coenergy)
set(gca,'XTick',0:pi/3:2*pi);
set(gca,'XTickLabel',{'0','pi/3','2pi/3','pi','4pi/3','5pi/3','2pi'});
xlabel('Angle');
ylabel('Coenergy')
axis([0,2*pi,30,36]);
grid on

for z=1:zeta
    I=(z)*2.5;
    Ieff=I/sqrt(2);
    for j=1:m
        mi_selectgroup(1);
        mi_moverotate(0, 0, -360/(n-1));
        mi_clearselected
        phi=(j-1)*(pi/6);
        for k=1:n
            disp(fprintf('iteration %i of %i',k,j));
            i(k)=I*cos(2*alfa(k)+phi);
            mi_modifycircprop('Current1',1,i(k));
            mi_modifycircprop('-Current1',1,-i(k));
            mi_analyze;
            mi_loadsolution;
            mo_seteditmode('contour')
            mo_addcontour(-3,6)
            mo_addcontour(3,6)
            flux1=mo_lineintegral(0);
            mo_clearcontour
            f1(k)=flux1(1);
            L1(k)=4*turns*abs((f1(k)-f01(k))./I);
            mo_groupselectblock(1)
            torque(k)=mo_blockintegral(22);
            coenergy(k)=mo_blockintegral(17);
            mi_selectgroup(1);
            mi_moverotate(0, 0, 360/(n-1));
            mi_clearselected
        end

        figure(100*z+10*j+1)
        plot (x,f1)
        set(gca,'XTick',0:pi/3:2*pi);
        set(gca,'XTickLabel',{'0','pi/3','2pi/3','pi','4pi/3','5pi/3','2pi'});
        xlabel('Angle');
        ylabel('Flux1');
        axis([0,2*pi,-0.05,0.05]);
        grid on
```

```
        figure(100*z+10*j+5)
        plot (x,L1)
        set(gca,'XTick',0:pi/3:2*pi);
        set(gca,'XTickLabel',{'0','pi/3','2pi/3','pi','4pi/3','5pi/3','2pi'});
        xlabel('Angle');
        ylabel('Inductance');
        axis([0,2*pi,0,1]);
        grid on

        figure(100*z+10*j+6)
        plot (x,torque)
        set(gca,'XTick',0:pi/3:2*pi);
        set(gca,'XTickLabel',{'0','pi/3','2pi/3','pi','4pi/3','5pi/3','2pi'});
        xlabel('Angle');
        ylabel('Torque');
        axis([0,2*pi,-100,100]);
        grid on

        figure(100*z+10*j+7)
        plot (x,coenergy)
        set(gca,'XTick',0:pi/3:2*pi);
        set(gca,'XTickLabel',{'0','pi/3','2pi/3','pi','4pi/3','5pi/3','2pi'});
        xlabel('Angle');
        ylabel('Coenergy');
        axis([0,2*pi,0,100]);
        grid on

        figure(100*z+10*j+8)
        plot (x,i)
        set(gca,'XTick',0:pi/3:2*pi);
        set(gca,'XTickLabel',{'0','pi/3','2pi/3','pi','4pi/3','5pi/3','2pi'});
        xlabel('Angle');
        ylabel('Current');
        axis([0,2*pi,-25,25]);
        grid on

    end

end

closefemm
```

8. Bibliography

[1] M. Andriollo G.Martineli, A.Morini, *Macchine elettriche rotanti,* Libreria Cortina, Padova, 2003.

[2] G.Martineli, A.Morini, *Lezioni di Teoria Unificata delle Macchine Elettriche*, SGEditoriali, Padova, 1999.

[3] Nicola Bianchi, Silverio Bolognani, *Metodologie di Progettazione delle Macchine Elettriche,* Cleup, Padova, 2001.

[4] Nicola Bianchi, *Calcolo delle Macchine Elettriche col Metodo degli Elementi Finiti,* Cleup, Padova, 2001.

9. Acknowledgements

After these years of study, the wish is to thank all the people who gave their contribution, small or big, to the achievement of this result.

As it is impossible to write their names – it will be too much – the simplest way is to remind them in my mind for the years to come, with all the things they taught me.

Special thanks to professors Silverio Bolognani and Paulo Josè da Costa Branco, for their kindness, their advices, and, most of all, for their patience.

Federico Baldo